Protection against Recurrent Ocular Herpes Simplex Virus Type 1 Disease after Therapeutic Vaccination of Latently Infected Mice

C. M. Richards,* R. Case, T. R. Hirst, T. J. Hill, and N. A. Williams

*Department of Pathology and Microbiology, School of Medical Sciences, University of Bristol,
Bristol BS8 1TD, United Kingdom*

The potential of therapeutic vaccination of animals latently infected with herpes simplex virus type 1 (HSV-1) to enhance protective immunity to the virus and thereby reduce the incidence and severity of recurrent ocular disease was assessed in a mouse model. Mice latently infected with HSV-1 were vaccinated intranasally with a mixture of HSV-1 glycoproteins and recombinant *Escherichia coli* heat-labile enterotoxin B subunit (rEtxB) as an adjuvant. The systemic immune response induced was characterized by high levels of virus-specific immunoglobulin G1 (IgG1) in serum and very low levels of IgG2a. Mucosal immunity was demonstrated by high levels of IgA in eye and vaginal secretions. Proliferating T cells from lymph nodes of vaccinated animals produced higher levels of interleukin-10 (IL-10) than were produced by such cells from mock-vaccinated animals. This profile suggests that vaccination of latently infected mice modulates the Th1-dominated proinflammatory response usually induced upon infection. After reactivation of latent virus by UV irradiation, vaccinated mice showed reduced viral shedding in tears as well as a reduction in the incidence of recurrent herpetic corneal epithelial disease and stromal disease compared with mock-vaccinated mice. Moreover, vaccinated mice developing recurrent ocular disease showed less severe signs and a quicker recovery rate. Spread of virus to other areas close to the eye, such as the eyelid, was also significantly reduced. Encephalitis occurred in a small percentage (11%) of mock-vaccinated mice, but vaccinated animals were completely protected from such disease. The possible immune mechanisms involved in protection against recurrent ocular herpetic disease in therapeutically vaccinated animals are discussed.

Ocular herpes simplex virus type 1 (HSV-1) infection is the major cause of nontraumatic blindness in developed countries. Initial infection occurs at the corneal epithelium, where, following replication, the virus enters the sensory nerve endings, travels along axons, and becomes latent in the trigeminal ganglion (TG) (14). The virus remains as a lifelong infection in the TG, probably undetected by the immune system. Under certain conditions, which include stress or exposure to UV light, the virus may reactivate, travel back down the nerve, and cause recurrent infection, most often in the cornea (20). The immune mechanisms involved in protection against HSV-1 infections include the recruitment of proinflammatory immune cells. In the case of the eye, these cells may lead to immunopathological disease by infiltrating the stroma, causing opacity and edema of this tissue. In certain cases, the cornea may become highly vascularized and thickened, particularly after repeated recurrent infections, resulting in severe stromal keratitis and visual impairment (29). Current methods of therapy involve the administration of antiviral drugs and corticosteroids, but these are not always effective and may in some cases exacerbate disease (13). Vaccination to prevent primary infection is problematic, since the virus is often acquired very early in life. Therefore, the development of a therapeutic vaccine for individuals with an established latent infection to prevent recurrent ocular disease or significantly decrease its severity is an attractive approach.

While a number of potential vaccine candidates have been shown to provide protection against primary ocular challenge, the efficacy of the few that have been tested in recurrent models of disease has been disappointing. In one study, a virion host shutoff mutant was tested as a live therapeutic vaccine against recurrent infection in the mouse. Although this live vaccine reduced the incidence of virus shedding following reactivation, the incidence of clinical ocular disease was unaffected (34). The use of subunit vaccines incorporating glycoprotein D in mice (16) and rabbits (21) has been similarly disappointing. These difficulties reflect the complex nature of the immune response in HSV-1 infection and the requirement for vaccination to modulate the protective components of immunity while at the same time limiting immunopathology. In this regard, immunohistochemical studies indicate that the initial response to recurrent infection in the eye involves an influx of neutrophils and macrophages together with CD4$^+$ and CD8$^+$ T cells, indicative of a proinflammatory Th1-type response. While this response is involved in viral clearance, it is also likely to drive the pathological damage to the eye that is associated with herpetic keratitis. At later times, the presence of B cells and anti-inflammatory cytokines (interleukin-10 [IL-10]) corresponds with the resolution of ocular disease (23, 27, 28). A successful therapeutic vaccine for ocular HSV-1 disease may, therefore, be one that can modulate the nature of the immune response, providing a higher degree of protection at the mucosal surface of the eye itself while limiting the proinflammatory effects of the virally induced Th1 response.

We have previously shown that intranasal immunization

_____
* Corresponding author. Mailing address: Department of Pathology and Microbiology, School of Medical Sciences, University of Bristol, University Walk, Bristol BS8 1TD, United Kingdom. Phone: 44 (0) 117 928 7585. Fax: 44 (0) 117 928 7896. E-mail: Claire.M.Richards@bristol.ac.uk

with a mixture of HSV surface glycoproteins in the presence of the recombinant *Escherichia coli* heat-labile enterotoxin B subunit (rEtxB) as adjuvant provided protection against HSV-1 infection. Following primary ocular challenge, immunized mice showed much reduced corneal disease and only limited spread of virus in the nervous system. The latter was evidenced by a reduction in zosteriform lesions and the incidence of latency in regions of the TG not served by the ophthalmic nerve. Immunized mice were also completely protected against the development of encephalitis, even under challenge conditions, in which the mortality in control, mock-vaccinated animals was as high as 95% (22). The immune response induced by our intranasal vaccine was characterized by the presence of strong secretory IgA responses to HSV-1 antigens in mucosal washings and serum neutralizing antibodies. The dominance of IgG1 in the serum antibody response together with the presence of high levels of IL-4 and IL-10 in lymph node cell cultures from immunized mice suggested that the anti-HSV-1 response was Th2 dominated. However, there was also some gamma interferon (IFN-γ) production in such cultures, indicating that Th1 immunity was also present. We hypothesized that the type of immune response generated to our vaccine may be compatible with modulating immunity in the latently infected animal. In order to test this hypothesis, we have utilized a well-characterized mouse model of recurrent herpetic eye disease (24, 25). Mice infected by corneal scarification in the presence of passive antibodies develop mild epithelial disease in 80 to 100% of cases. In our hands, this leads to the establishment of latency in approximately 93% of animals, as determined by inoculation of medium from 5-day TG explant cultures onto Vero cells (26). A slightly modified version of this model used by another laboratory shows that 80 to 100% of mice had latent virus in the TG following ocular infection (16). Reactivation of virus by exposure to UV light occurs in approximately 60% of mice, as determined by viral shedding, incidence of disease, and cell infiltration (24, 28). We describe here the effects of vaccination on the development of recurrent herpetic ocular disease in this mouse model.

MATERIALS AND METHODS

Reactivation model. Female, specific-pathogen-free NIH mice obtained from Harlan Olac, Bicester, United Kingdom, were maintained in the School of Medical Sciences, University of Bristol, Bristol, United Kingdom. At 8 weeks of age, mice were inoculated with HSV in order to establish latent infection in the TG, according to the method described previously (24). Briefly, mice were inoculated intraperitoneally with human serum (Harlan Sera-Lab, Ltd., Loughborough, United Kingdom), containing HSV-1 serum neutralizing antibodies, which was assayed to determine the serum antibody titer required to give 50% virus plaque reduction (50% effective dose [ED$_{50}$]) (25). Serum was diluted in phosphate-buffered saline (PBS) to give an ED$_{50}$ of 8,000 (24). After 24 h, mice were anesthetized (100 mg of ketamine per kg of body weight [Parke-Davis, Pontypool, United Kingdom] mixed with 10 mg of xylazine per kg [Bayer, Bury St. Edmunds, United Kingdom]) and infected with 10^6 PFU of HSV-1 McKrae in a 5-μl drop of medium by ocular scarification of the right cornea with a 26-gauge needle (24). Six weeks after infection, the right eyes of all mice were checked for the presence of any abnormalities, and such mice were discarded. The remaining mice were immunized intranasally three times at 10-day intervals with either 10 μg of HSV-1 glycoproteins, prepared from Vero cells infected with live HSV-1, or mock glycoproteins, prepared from uninfected Vero cells, each mixed with 20 μg of rEtxB to give a final volume of 47 μl (22). Two to 4 weeks after the final immunization, animals were anesthetized and placed with their right eye proptosed below a Hanovia lamp (emitting a peak of 4.02 mJ/cm^2 s at 320 nm), and the right corneas and lids were irradiated for 90 s in order to induce reactivation (25).

Measurement of antibody responses. Individual mice were bled from the tail vein 4 weeks after corneal scarification and 1 week after the final immunization, and the serum was stored at −20°C. Serum from mice infected without passive immunization was collected for use as a positive control. Eye and vaginal washings were collected from mice anesthetized with halothane by pipetting 20 μl of PBS up and down on the surface of each eye 10 times or with 50 μl of PBS pipetted in and out of the vagina 20 times. Samples collected from individual mice over several days were pooled and stored at −20°C.

Sera were analyzed for the presence of HSV-1-specific antibodies, as described previously (7). Briefly, assay plates coated with rabbit anti-HSV-1 (Dako, Ltd., High Wycombe, United Kingdom) were incubated with 1% bovine serum albumin in PBS, followed by HSV-1 antigen, mouse serum, and a rabbit anti-mouse Ig-horseradish peroxidase (HRP) conjugate (Dako Ltd.), with *O*-phenylenediamine (Sigma) as a substrate.

In order to measure the levels of virus-specific IgA in mucosal fluids, the conjugated secondary antibody was replaced with an HRP-conjugated goat anti-mouse IgA (Sigma). The level of IgG1 and IgG2a in the sera was measured with HRP-conjugated rat anti-mouse IgG1 or IgG2a, respectively. The endpoint titers for individual samples were determined by linear regression analysis.

The presence of neutralizing antibodies in sera of infected mice and mice immunized with HSV-1 or mock glycoproteins was determined by pooling aliquots of serum from individual mice in each group, collected as described above, for use in a plaque reduction assay. The ED$_{50}$ was calculated by weighted probit analysis (2), and the titers are given as reciprocals.

Assessment of T-cell responses. Single-cell suspensions of lymphocytes in Hanks' balanced saline solution (HBSS) (Gibco, Paisley, United Kingdom) containing 20 mM HEPES buffer (GIBCO) were prepared from draining lymph nodes, removed from mice either 4 weeks after final immunization or UV irradiation by agitation through wire mesh with a glass rod. Lymphocytes were washed and then cultured at 10^6 cells per ml in minimal essential medium α (α-MEM), supplemented with 20 mM HEPES, 100 U of penicillin per ml, 100 μg of streptomycin per ml, 4 mM L-glutamine (Gibco), 50 μM 2-mercaptoethanol (Sigma), and 0.5% normal autologous mouse serum in 25-cm^2 flasks. Cells were cultured in the presence of UV-inactivated virus (prepared from serum-free supernatant of infected Vero cells) at a predetermined, optimal concentration of 1.5 × 10^5 PFU/ml, an equivalent dilution of mock virus for assessment of nonviral responses, or medium alone (data not shown). Cultures were incubated at 37°C in a humidified atmosphere of 5% CO$_2$. Aliquots of 100 μl were removed on desired days after initiation of the cultures and placed in triplicate into wells of a 96-well plate for assessment of [^{3}H]thymidine incorporation by standard assay techniques (12).

Additional aliquots of cells were removed for assessment of cytokine levels by a previously described method (3). Briefly, cell samples, set up in triplicate, were cultured overnight at 37°C in a humidified atmosphere of 5% CO$_2$ in capture antibody-coated (rat anti-mouse cytokines) enzyme-linked immunosorbent assay (ELISA) plates, before detection with biotinylated rat anti-mouse cytokines (BD Pharmingen, San Diego, Calif.). Thus, cytokine production by cells over a defined period of culture could be assessed under conditions in which the effect of cytokine lability was minimized. Cytokine levels were calculated by regression analysis against standard curves produced with the appropriate recombinant cytokine (BD Pharmingen, San Diego, Calif.).

Analysis of ocular disease and isolation of virus from eye washings following reactivation of latent virus. Following corneal scarification, eyes were examined on days 1, 3, and 7 with a Zeiss 105L slit lamp microscope (Zeiss, Welwyn Garden City, United Kingdom) for development of epithelial ulcers, stromal disease, and uveitis. The eyes were also checked prior to immunization, and any mice with damaged corneas were removed from the experiment. Similarly, mice were analyzed following UV irradiation on days 1, 2, 4, 6, 10, and 14 for ocular disease as well as for spread of virus to other areas, resulting in ulceration and edema of the eyelid as well as zosteriform herpetic lesions in the skin at sites served by the TG (the snout and lower jaw). The severity of each disease parameter was also scored in those mice with disease (1 = mild disease and 5 = most severe disease). Piloerection, loss of weight, hunched posture, and a significant defect in righting reflex were taken as signs of encephalitis, and such animals were killed by cervical dislocation.

Eye washings were collected on day 0 to check for any spontaneous reactivation, as well as on days 2, 3, 4, 5, and 6, from irradiated eyes by pipetting 20 μl of culture medium onto the surface of the proptosed eye 10 times and transferring the washes to Vero cells for isolation of virus (30).

Statistical analysis. Significant differences in the immune response and clinical disease score between groups of mice were determined by Student's *t* test. Incidence data were analyzed with the χ^2 test.
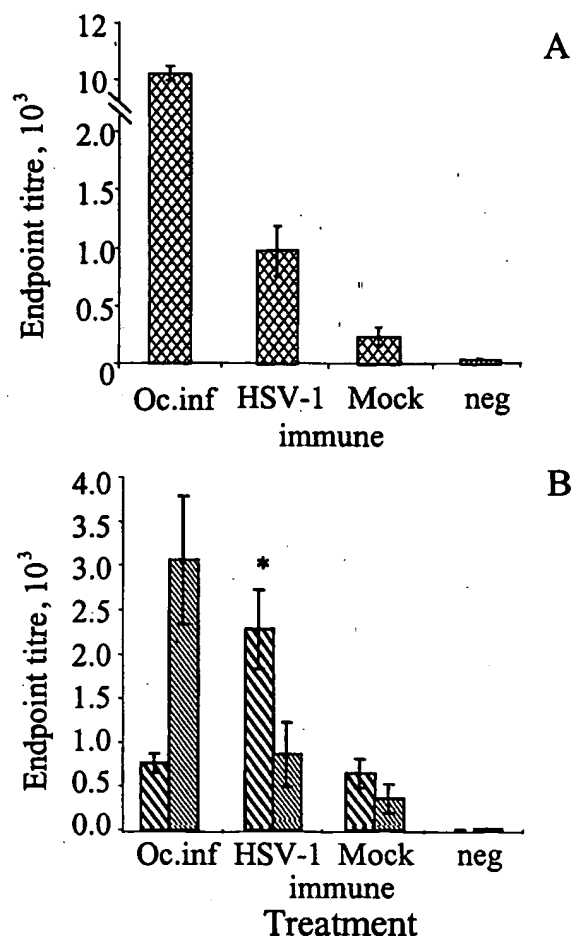
FIG. 1. HSV-1-specific serum responses in mice 4 weeks after corneal scarification with HSV-1 McKrae and 1 week following HSV-1 immunization and mock immunization of latently infected mice as determined by ELISA. The serum Ig responses to HSV-1 antigens were analyzed by regression analysis, and the endpoint titers were determined (A). Endpoint titers were also determined for HSV-1-specific serum IgG1 (bold hatched bars) and IgG2a (light hatched bars) in IgG subclass-specific ELISA (B). Mean values with standard error of the mean were calculated from groups of 20 immunized mice and 5 mice following ocular infection (Oc.inf). Sera from naïve mice were included as the negative control (neg). An asterisk shows a significant difference in response between HSV-1-vaccinated and mock-vaccinated mice as judged by Student's t test ($P < 0.01$). The data presented here are representative of three similar experiments.
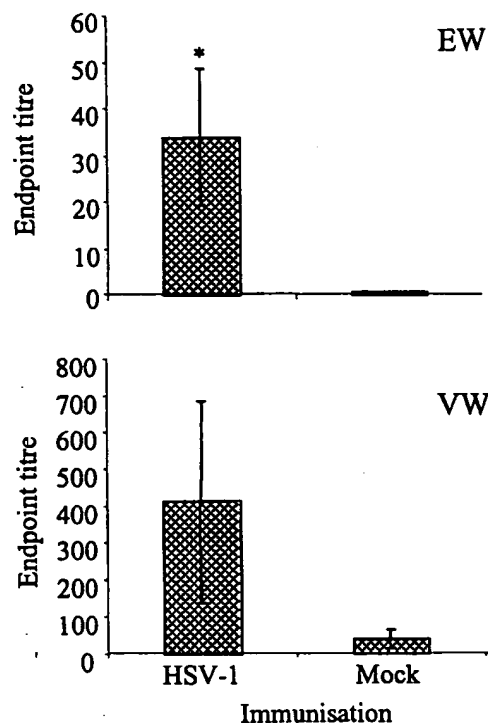

FIG. 2. HSV-1-specific IgA in mucosal washings collected from the eye (EW) and vagina (VW) of HSV-1-vaccinated and mock-vaccinated mice as determined by ELISA. Endpoint titers were calculated by regression analysis for individual mice ($n = 20$), and mean values ± standard errors were determined. An asterisk shows significant difference between HSV-1-vaccinated and mock-vaccinated mice as judged by Student's t test ($P < 0.05$).

RESULTS

Modulation of the anti-HSV-1 antibody response in latently infected mice. High levels of anti-HSV-1 antibodies were detected in the serum of mice that had been infected with HSV-1 by corneal scarification, with endpoint titers in excess of 1:10,000 (Fig. 1A). Serum from passively immunized mice infected by corneal scarification had low levels of anti-HSV-1 antibodies following immunization with mock glycoproteins (prepared from uninfected Vero cells) mixed with rEtxB as adjuvant. In contrast, immunization with glycoproteins from HSV-1-infected Vero cells mixed with rEtxB dramatically enhanced the levels of anti-HSV-1 antibodies in latently infected animals. The mean endpoint titer in mock-immunized mice

was 1:236, compared to 1:971 for the immunized group ($P < 0.01$).

Analysis of the serum IgG subclasses following corneal scarification alone showed that IgG2a was the dominant subclass, resulting in an IgG1/IgG2a ratio of 0.25 (Fig. 1B). In contrast, following HSV-1 immunization of latently infected mice, IgG1 was the dominant subclass, with an endpoint titer of 1:2,276 compared with IgG2a at 1:858. The ratio of IgG1 to IgG2a following immunization in the presence of rEtxB was 2.65. This is a considerable enhancement of the IgG1 and IgG2a responses observed in mock-immunized mice with an IgG1 endpoint titer of 1:640 compared with 1:360 for IgG2a, giving an IgG1/IgG2a ratio of 1.78.

Further characterization of HSV-1-specific antibody responses was undertaken, using pooled serum samples, to assess virus neutralization. Serum from infected only mice gave virus neutralization titers of 1:1,083. Latently infected mice immunized with HSV-1 glycoproteins gave an ED_{50} titer of 1:107, which was in marked contrast to mock-immunized mice, which gave an ED_{50} titer of 1:7 (data not shown).

In addition to the stimulation of serum antibodies to HSV-1, immunization of latently infected mice triggered the production of high levels of secretory IgA, particularly at the ocular surface, local to the site of administration, as well as the vagina, a more distant site (Fig. 2). The mean endpoint titer for eye washings from immunized mice, taken 1 week to 10 days following the final immunization, was 1:34. This is a significant
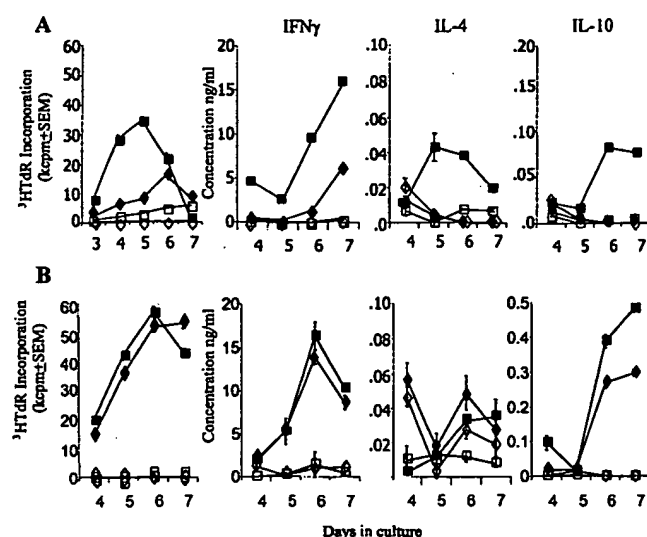
FIG. 3. Draining lymph node cells from HSV-1-vaccinated (squares) and mock-vaccinated (diamonds) mice prior to reactivation (A) or postreactivation (B), cultured in vitro with HSV-1 (solid symbols) or mock antigen (open symbols), were analyzed for proliferative responses by [^{3}H]thymidine (^{3}HTdR) incorporation and secretion of cytokines IFN-γ, IL-4, and IL-10. Mean values ± standard errors of triplicate cultures are shown. The data presented here are representative of three similar experiments.
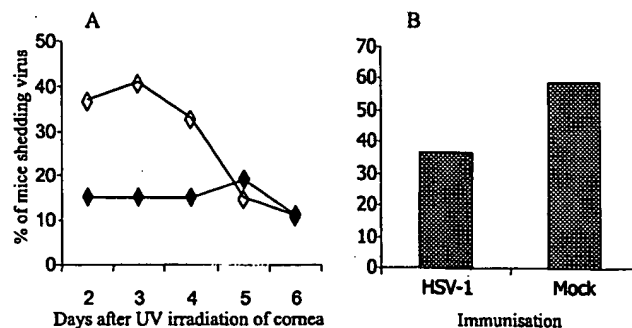

FIG. 4. Percentage of HSV-1-vaccinated (solid symbols) and mock-vaccinated (open symbols) mice shedding virus in eye washings days 2 to 6 after UV-induced reactivation of latent virus (A) and total percentage of mice shedding virus on at least 1 day (B). A significant reduction in viral shedding was observed in HSV-1-vaccinated mice (χ^2 test, $P < 0.01$).

increase compared with that of the mock-immunized controls, which gave a mean endpoint titer of 1:0.5 ($P < 0.05$). The presence of IgA in vaginal washings of immunized mice resulted in a mean endpoint titer of 1:412 compared with 1:40 for the mock-immunized mice. This difference, however, was not significant due to the large variation between individuals within the same group.

Effects of immunization on anti-HSV-1 T-cell responses in latently infected animals. The effect of immunization of latently infected mice on T-cell responses was investigated with lymphocytes isolated from draining lymph nodes either 4 weeks after immunization and prior to reactivation or 4 weeks after subsequent UV-induced reactivation of virus. Cells were cultured in the presence of UV-inactivated HSV-1 or mock antigen, and T-cell proliferation and cytokine production were assessed on days 4 to 7. The results showed strong T-cell proliferative responses to HSV-1 antigens by cells from latently infected, HSV-1-immunized animals (Fig. 3A). A higher and more rapid response indicative of a secondary recall response was observed with cells following reactivation of latent virus in both HSV-1- and mock-immunized animals, with peak incorporation of [^{3}H]thymidine in excess of 50 kcpm on days 6 to 7 (Fig. 3B). The response of these cell cultures to mock antigen was negligible, indicating that proliferation of T cells was specific for viral antigens.

Analysis of the cytokines secreted by proliferating T-cell cultures indicated that following immunization, IFN-γ was the main cytokine secreted, with low levels of IL-10 and IL-4 compared to the results for cells from mock-immunized mice and those cultured with mock antigen. Following reactivation, a more rapid IFN-γ response was seen from cells from both HSV-1-immunized and mock-immunized mice in response to HSV-1 antigen, with peak concentrations of IFN-γ observed

on day 6 of 16 and 14 ng/ml, respectively. Interestingly, the presence of IL-10 was observed in cells cultured following reactivation of virus, but was significantly enhanced in cell cultures from HSV-1-immunized mice compared to mock-immunized mice, with levels of 0.48 ng/ml on day 7 compared with 0.29 ng/ml, respectively. Increased production of IL-10 in cultures from immunized mice following reactivation was observed in each of three similar experiments. While some IL-4 was detected, the levels observed were very low, making the differences between cultures difficult to distinguish.

Clinical disease and viral shedding following reactivation of latent virus. Analysis of the eyes of passively immunized mice infected by corneal scarification revealed that 97.5% of mice developed corneal ulcers by day 3. Of these, 50.5% developed some signs of stromal disease and 25% demonstrated uveitis, although none of these developed severe disease symptoms and thus had recovered by day 7 following infection.

The effect of modulating the immune response to HSV-1 antigens on recurrent herpetic ocular disease was determined following reactivation of latent virus by exposure to UV light. Eye washings were collected immediately prior to UV irradiation to ensure that the presence of virus was not the result of spontaneous shedding; such shedding is rare in this model (21, 22). Indeed, no spontaneous viral shedding was detected in these experiments, indicating that any virus present was most likely due to UV-induced reactivation. The main period for detection of reactivated virus in eye washings taken from mock-immunized mice was represented by days 2, 3, and 4, with a peak incidence on day 3 of 41% (Fig. 4A). In contrast, reactivated virus was only observed in 15% of HSV-1-immunized mice on days 2 to 4, with a peak incidence of 19% occurring on day 5. A significant reduction in the overall incidence of mice shedding virus, over the 10 days following reactivation, was observed between HSV-1-immunized (37%) and mock-immunized (59%) mice (Fig. 4B; χ^2 test, $P < 0.01$).

Reactivation of HSV-1 is partly a consequence of corneal damage caused by exposure to UV light resulting in the development of some corneal abnormalities immediately following UV treatment in both groups of mice. Such abnormalities, however, are short term, and only those mice with HSV-1-associated disease continue to show signs of corneal disease
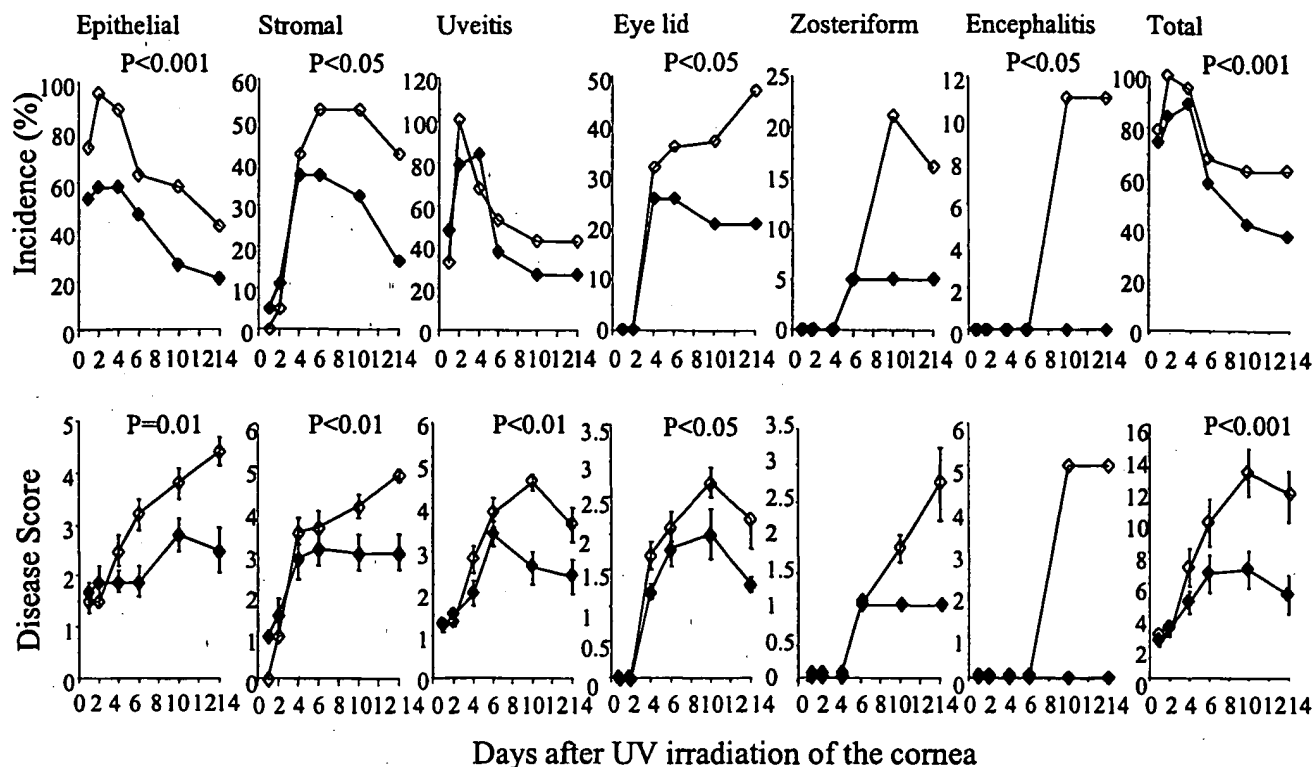
FIG. 5. Incidence and severity of the different clinical parameters following reactivation of latent virus in HSV-1-vaccinated (solid symbols) and mock-vaccinated (open symbols) mice. Disease scores run from 0 (no disease) to 5 (very severe disease). Each group started with 20 mice. Disease scores represent mean values of mice with disease in each group ± standard errors. Significant differences between HSV-1- and mock-vaccinated mice were determined by Student's t test.

and increased severity. Thus, the incidence of epithelial disease in HSV-1-vaccinated mice was significantly reduced over the 14 days analyzed compared with that in the mock-vaccinated mice (χ^2 test, $P < 0.001$), with a maximum of 58% compared with 95%, respectively, on day 2 (Fig. 5). Stromal disease levels were initially similar in both groups of mice, but those vaccinated with HSV-1 peaked at 37% on days 4 to 6 and then declined steadily so that only 16% were affected by day 14. Such disease in mock-immunized mice increased significantly to a peak of 53% by day 6, staying at this level until day 10, before declining to 42% by day 14 (χ^2 test, $P < 0.05\%$). No significant difference in the incidence of uveitis between the two groups was observed, with 84% of HSV-1-immunized mice showing signs of uveitis on day 4 compared with 100% for mock-immunized animals on day 2. Lid disease was first observed in both groups on day 4, with 26% of HSV-1-immunized mice affected compared with 32% of mock-immunized mice. The incidence of lid disease in mock-immunized mice continued to increase significantly to a peak of 47% by day 14. In contrast, a significantly lower incidence of lid disease was observed up to day 14 in HSV-1-immunized mice (χ^2 test, $P < 0.05$), with only 21% affected by day 10. Likewise, zosteriform spread was observed in 5% of mice from both groups on day 6, but no further development of this form of the disease was observed in HSV-1-immunized mice. In contrast, in the mock-immunized mice, the incidence of zosteriform spread increased further to 21%. By day 10, 11% of mock-immunized mice developed encephalitis and were killed by cervical dislo-

cation. Taken together, a significant reduction in the incidence of HSV-1-associated disease was observed in HSV-1-immunized versus mock-immunized mice over the days analyzed following reactivation of virus by UV irradiation (χ^2 test, $P < 0.001$).

In addition to this clear difference in disease incidence, analysis of disease severity in the mice with clinical symptoms further highlighted the protective efficacy of intranasal vaccination of latently infected animals. Although similar levels of ocular disease were observed in both groups of mice in the first few days following reactivation of virus, the mice vaccinated with HSV-1 glycoproteins and rEtxB recovered quickly from UV damage, whereas mock-vaccinated animals continued to develop disease and disease severity increased. In particular, a significant reduction in disease severity was observed for epithelial disease (Student's t test, $P < 0.01$), stromal disease (Student's t test, $P < 0.01$), uveitis (Student's t test, $P < 0.01$), and lid disease (Student's t test, $P < 0.05$). Furthermore, HSV-1-vaccinated mice developed less severe zosteriform lesions, and none showed signs of encephalitis. Thus, there was a significant difference in total incidence and severity of recurrent clinical disease between the two groups (Fig. 5; Student's t test, $P < 0.001$).

DISCUSSION

In this paper, we show that intranasal vaccination of latently infected mice with a mixture of HSV-1 glycoproteins and EtxB

can stimulate protective immunity in a well-characterized mouse model of recurrent ocular herpetic disease. The immune response generated in this way was characterized by increased anti-HSV-1 antibody levels of local IgA and serum IgG, an increased IgG1/IgG2a ratio, and elevated IL-10 production by lymphocytes from local lymph nodes. Vaccination was also associated with a reduction in the percentage of mice shedding virus at the corneal surface, together with reduced incidence of disease induced by UV irradiation. Furthermore, the mice that developed clinical symptoms showed enhanced recovery and limited spread of virus through the nervous system, with only a few vaccinated mice developing lid disease and zosteriform lesions. None showed signs of encephalitis.

Corneal infection in this model results in approximately 90% of mice becoming latently infected with HSV-1 in the ophthalmic region of the TG (16, 26). The presence of latent virus was also shown to correlate well with the development of ocular disease following infection; thus, in this set of experiments, which showed 97.5% of mice developing some signs of ocular disease, the presence of latent virus would be comparable with results of 80 to 100% from previous studies.

UV irradiation itself damages the corneal epithelium and causes uveitis, events that are thought to be necessary for reactivation of virus in the TG (28). Such damage, however, is short lived, so that only those mice with viral reactivation develop the more severe stromal disease associated with herpes stromal keratitis (HSK). Consequently, in this study, a high percentage of both the immunized and mock-immunized mice developed corneal disease following UV irradiation. However, by day 6, most mice had recovered from UV-induced damage, resulting in a fall in the incidence of corneal disease. This was particularly evident in the case of uveitis, from which only 38% of HSV-1-vaccinated mice were affected following initial damage compared with 55% of mock-vaccinated animals, which had uveitis that continued to increase in severity. Similarly, for both epithelial and stromal disease, the severity of disease in the mock-immunized mice with clinical symptoms continued to increase for the duration of the experiment, while HSV-1-vaccinated mice developed less severe disease. Spread of virus from the initial site of infection to other areas within the same dermatome led to lid disease in 48% of mock-immunized mice, whereas only 25% of HSV-1-immunized mice developed the disease, with reduced severity. The further spread of virus causing zosteriform lesions was only observed in 5% of HSV-1-immunized mice, and the severity of these lesions was also low. In addition, none of the HSV-1-immunized mice developed signs of encephalitis. These results indicate that HSV-1 vaccination results in a reduction in the spread of virus through the nervous system when compared with mock-vaccinated mice. Overall, there was a significant reduction in both the incidence and severity of clinical disease in vaccinated mice following reactivation of latent virus, compared with the level in mock-vaccinated animals. Furthermore, in this model, recurrent herpetic eye disease is usually associated with shedding of virus in the tears (25). Therefore, isolation of virus from eye washings provided an indicator of the presence of reactivating virus. In previous studies, approximately 60% of mice shed virus in the tears following UV irradiation of the cornea (17, 24, 25, 34), which is comparable with the incidence in the mock-immunized mice in the present experiments. In contrast,

this incidence was only 37% in HSV-1-immunized mice. A similar reduction in viral shedding was also observed in mice vaccinated with the virion host shutoff (vhs)-defective mutant of HSV-1 (17). At present, it is not clear whether this lower incidence is due to antibody-mediated neutralization of virus at the surface of the eye or a reduction in the number of reactivating events in the TG.

In the present study, the immune response induced by vaccination of latently infected mice was similar to that obtained by vaccination of naïve mice (22). High levels of virus-specific serum Ig, comparable to that obtained following corneal scarification of mice with live HSV-1, were detected by enzyme-linked immunosorbent assay (ELISA) and by neutralization in plaque reduction assays. Of particular importance for protective immunity at the corneal surface was the induction of virus-specific IgA in eye washings, the site of infection and recurrent disease. While some mice also developed high levels of IgA at the more distant mucosal site, the vagina, this was highly variable, which may be a consequence of the transient nature of IgA in mucosal washings. However, the presence of virus-specific IgA at the ocular surface, the site of infection and recurrence, has been shown to play a part in protection against ocular disease and corneal scarring (9). Analysis of the spread of virus in in vitro cultures has shown that virus-specific antibodies prevent spread between epidermal cells by neutralization during transmission across the intercellular gap (19). Similar mechanisms may also limit the spread of virus between epidermal cells and axonal termini in vivo (11). Thus, following reactivation, virus-specific antibody is likely to play an important role in limiting viral shedding from the nerve endings in the cornea and the spread of virus between neighboring corneal cells once they are infected.

Other mechanisms that may be involved in reduced corneal disease include the switch from the Th1-dominated, proinflammatory immune response observed in mice after a primary infection to a more balanced Th1/Th2-type response associated with anti-inflammatory cytokines observed following immunization. This approach contrasts with that aimed at providing protection against vaginal challenge with the closely related HSV-2. In these studies, induction of strong Th1-type responses enhanced viral clearance, resulting in reduced incidence and severity of genital lesions (10). However, following infection of the eye, the persistence of proinflammatory cytokines following viral clearance results in continued influx of Th1 immune cells, leading to opacity and vascularization of this highly specialized, normally transparent organ (6). Thus, the potential to modify the immune response to reactivating virus by immunization with rEtxB toward a more balanced Th1/Th2-type anti-inflammatory response, as observed in previous studies after immunization of naïve mice (22), was considered to be advantageous. It is also possible, however, that the major factor that affects the protection from disease observed in the present studies is the increase in levels of IL-10. This may reflect the activation of a T regulatory population following immunization that is able to suppress the immunopathological processes associated with ocular disease.

Accordingly, a switch in the dominance of IgG1 and IgG2a was observed, with the change in the IgG1/IgG2a ratio from 0.25 following ocular infection to 2.65 following HSV-1 immunization of latently infected animals indicating the potency of

rEtxB to modulate the immune response. Interestingly, serum from mock-immunized mice also showed higher levels of IgG1 than IgG2a, resulting in a ratio of 1.78, suggesting that the use of rEtxB alone is capable of influencing the balance of the IgG subclasses. This is consistent with our observations that show rEtxB can, when given alone, modulate Th1 responses to autoantigens mediating protection in animal models of autoimmune disease (18). Several studies have also shown the importance of the anti-inflammatory cytokines IL-4 and IL-10 in the resolution of stromal keratitis (4, 5). The involvement of IL-4 in the resolution of corneal disease, however, is contradictory, the presence of IL-4 also being associated with development of HSK (1) and increased mortality (15). Recent studies have indicated that the mode of action of IL-4 is dependent on the other cell types present, such as CD4$^+$ or CD8$^+$ T cells (8). While we have not yet assessed the effects of immunization on the activation of HSV-specific cytotoxic T lymphocytes, the clear association with increased IL-4 and IL-10 levels suggests that such responses are unlikely to be a key feature of vaccination in this way. Further investigations will be required to determine this. Different roles for IL-4 and IL-10 have also been demonstrated following administration of either IL-4 or IL-10 DNA by different routes prior to ocular infection. The use of IL-4 DNA resulted in a significant switch toward a Th2 subset balance, whereas IL-10 did not (4). The involvement of IL-4 in this study is not clear; the level of IL-4 seen following immunization of these latently infected animals is comparable to that seen with previous studies involving immunization of naïve mice (22). Analysis of the cytokines following reactivation of virus showed similar levels of IL-4 in both HSV-1- and mock-immunized mice. Whereas, although only low levels of IL-10 were observed following immunization, this was greatly enhanced upon reactivation, in excess of that seen in the mock-immunized controls. The induction of IL-10 has been shown to be of primary importance in regulation of inflammatory responses and the resolution of HSK (1, 4, 5). The presence of IL-10 following HSV-1 corneal infection has been reported to be associated with suppression of certain chemokines, such as macrophage inflammatory protein 2 (MIP-2) and MIP-1α, resulting in a reduction in the migration of inflammatory cells to the cornea (31, 35). In addition, IL-10 has been shown to down-regulate expression of proinflammatory cytokines such as IL-2 and IL-6 (32). Further studies are required to determine the mechanism involved in IL-10 secretion. The observation that only local administration of IL-10 was effective led to the conclusion that either corneal epithelial cells or infiltrating immune cells may be able to secrete IL-10 (35). However, the cytokine profile observed here was similar to that following exposure of human monocytes to rEtxB, with high IFN-γ and IL-10 levels (33). This cytokine profile was consistent with that described for a subset of IL-10-secreting lymphocytes that possess regulatory properties (Tr1 cells) and that have been shown to be capable of preventing or treating Th1-mediated autoimmune diseases. This suggests that the ability of EtxB to trigger activation of T-regulatory cells (18) may be an important feature in modulating the immune-mediated damage associated with herpetic ocular disease.

In conclusion, we have demonstrated the potential of therapeutic vaccination to protect against recurrent ocular HSV-1 infection. Mucosal administration of viral antigens, together with the use of the potent immunomodulator rEtxB, induced an immune response that protected against corneal damage and blindness. The possible mechanisms involved include a rapid IgA antibody response at the corneal surface, enabling neutralization of virus. The presence of high levels of the IgG1 subclass of HSV-1-specific antibody helped give a more balanced Th1/Th2 and anti-inflammatory response. The induction of IL-10 is involved in the regulation of inflammatory responses, possibly due to the induction of Tr1 cells by rEtxB. Taken together, the modulation of both humoral and cell-mediated immune responses resulted in a significant reduction in the incidence and severity of this immunopathological disease.

REFERENCES

1. Babu, J. S., S. Kanangat, and B. T. Rouse. 1995. T cell cytokine mRNA expression during the course of the immunopathologic ocular disease herpetic stromal keratitis. J. Immunol. 154:4822–4829.
2. Bailey, M., N. A. Williams, A. D. Wilson, and C. R. Stokes. 1992. Probit: weighted probit regression analysis. J. Immunol. Methods 153:261–262.
3. Beech, J. T., T. Bainbridge, and S. J. Thompson. 1997. Incorporation of cells into an ELISA system enhances antigen-driven lymphokine detection. J. Immunol. Methods 205:163–168.
4. Chun, S., M. Daheshia, N. A. Kuklin, and B. T. Rouse. 1998. Modulation of viral immunoinflammatory responses with cytokine DNA administered by different routes. J. Virol. 72:5545–5551.
5. Daheshia, M., N. Kuklin, E. Manickan, S. Chun, and B. T. Rouse. 1998. Immune induction and modulation by topical ocular administration of plasmid DNA encoding antigens and cytokines. Vaccine 16:1103–1110.
6. Deshpande, S. P., M. Zheng, S. Lee, and B. T. Rouse. 2002. Mechanisms of pathogenesis in herpetic immunoinflammatory ocular lesions. Vet. Microbiol. 86:17–26.
7. Erturk, M., T. J. Hill, C. Shimeld, and R. Jennings. 1992. Acute and latent infection of mice immunised with HSV-1 ISCOM vaccine. Arch. Virol. 125:87–101.
8. Ghiasi, H., Y. Osorio, G.-C. Perng, A. B. Nesburn, and S. L. Wechsler. 2001. Recombinant herpes simplex virus type 1 expressing murine interleukin-4 is less virulent than wild-type virus in mice. J. Virol. 75:9029–9036.
9. Ghiasi, H., S. L. Wechsler, S. Cai, A. B. Nesburn, and F. M. Hofman. 1998. The role of neutralizing antibody and T-helper subtypes in protection and pathogenesis of vaccinated mice following ocular HSV-1 challenge. Immunology 95:352–359.
10. Gyotoku, T., F. Ono, and L. Aurelian. 2002. Development of HSV-specific CD4+ Th1 responses and CD8+ cytotoxic T lymphocytes with antiviral activity by vaccination with the HSV-2 mutant ICP10ΔPK. Vaccine 20:2796–2807.
11. Halford, W. P., L. A. Veress, B. M. Gebhardt, and D. J. Carr. 1997. Innate and acquired immunity to herpes simplex virus type 1. Virology 236:328–337.
12. Harper, H. M., L. Cochrane, and N. A. Williams. 1996. The role of small intestinal antigen-presenting cells in the induction of T-cell reactivity to soluble protein antigens: association between aberrant presentation in the lamina propria and oral tolerance. Immunology 89:449–456.
13. Hendricks, R. L. 1997. An immunologist's view of herpes simplex keratitis: Thygeson Lecture 1996, presented at the Ocular Microbiology and Immunology Group meeting, October 26, 1996. Cornea 16:503–506.
14. Hill, T. J. 1987. Ocular pathogenicity of herpes simplex virus. Curr. Eye Res. 6:1–7.
15. Ikemoto, K., R. B. Pollard, T. Fukumoto, M. Morimatsu, and F. Suzuki. 1995. Small amounts of exogenous IL-4 increase the severity of encephalitis induced in mice by the intranasal infection of herpes simplex virus type 1. J. Immunol. 155:1326–1333.
16. Keadle, T. L., K. A. Laycock, J. K. Miller, K. K. Hook, E. D. Fenoglio, M. Francotte, M. Slaoui, P. M. Stuart, and J. S. Pepose. 1997. Efficacy of a recombinant glycoprotein D subunit vaccine on the development of primary and recurrent ocular infection with herpes simplex virus type 1 in mice. J. Infect. Dis. 176:331–338.
17. Keadle, T. L., L. A. Morrison, J. L. Morris, J. S. Pepose, and P. M. Stuart. 2002. Therapeutic immunization with a virion host shutoff-defective, replication-incompetent herpes simplex virus type 1 strain limits recurrent herpetic ocular infection. J. Virol. 76:3615–3625.

18. Luross, J. A., T. Heaton, T. R. Hirst, M. J. Day, and N. A. Williams. 2002. *Escherichia coli* heat-labile enterotoxin B subunit prevents autoimmune arthritis through induction of regulatory CD4+ T cells. Arthritis Rheum. 46:1671–1682.

19. Mikloska, Z., P. P. Sanna, and A. L. Cunningham. 1999. Neutralizing antibodies inhibit axonal spread of herpes simplex virus type 1 to epidermal cells in vitro. J. Virol. 73:5934–5944.

20. Nash, A. A., and P. Cambouropoulos. 1993. The immune response to herpes simplex virus. Semin. Virol. 4:181–186.

21. Nesburn, A. B., R. L. Burke, H. Ghiasi, S. M. Slanina, and S. L. Wechsler. 1998. A therapeutic vaccine that reduces recurrent herpes simplex virus type 1 corneal disease. Investig. Ophthalmol. Vis. Sci. 39:1163–1170.

22. Richards, C. M., A. T. Aman, T. R. Hirst, T. J. Hill, and N. A. Williams. 2001. Protective mucosal immunity to ocular herpes simplex virus type 1 infection in mice by using *Escherichia coli* heat-labile enterotoxin B subunit as an adjuvant. J. Virol. 75:1664–1671.

23. Shimeld, C., J. L. Whiteland, S. M. Nicholls, D. L. Easty, and T. J. Hill. 1996. Immune cell infiltration in corneas of mice with recurrent herpes simplex virus disease. J. Gen. Virol. 77:977–985.

24. Shimeld, C., D. L. Easty, and T. J. Hill. 1999. Reactivation of herpes simplex virus type 1 in the mouse trigeminal ganglion: an in vivo study of virus antigen and cytokines. J. Virol. 73:1767–1773.

25. Shimeld, C., T. Hill, B. Blyth, and D. Easty. 1989. An improved model of recurrent herpetic eye disease in mice. Curr. Eye Res. 8:1193–1205.

26. Shimeld, C., T. J Hill, W. A. Blyth, and D. L. Easty. 1990. Passive immunization protects the mouse eye from damage after herpes simplex virus infection by limiting spread of virus in the nervous system. J. Gen. Virol. 71:681–687.

27. Stumpf, T. H., R. Case, C. Shimeld, D. L. Easty, and T. J. Hill. 2002. Primary herpes simplex virus type 1 infection of the eye triggers similar immune responses in the cornea and the skin of the eyelids. J. Gen. Virol. 83:1579–1590.

28. Stumpf, T. H., C. Shimeld, D. L. Easty, and T. J. Hill. 2001. Cytokine production in a murine model of recurrent herpetic stromal keratitis. Investig. Ophthalmol. Vis. Sci. 42:372–378.

29. Thomas, J., and B. T. Rouse. 1997. Immunopathogenesis of herpetic ocular disease. Immunol. Res. 16:375–386.

30. Tullo, A. B., C. Shimeld, W. A. Blyth, T. J. Hill, and D. L. Easty. 1983. Ocular infection with herpes simplex virus in nonimmune and immune mice. Arch. Ophthalmol. 101:961–964.

31. Tumpey, T. M., H. Cheng, X. T. Yan, J. E. Oakes, and R. N. Lausch. 1998. Chemokine synthesis in the HSV-1-infected cornea and its suppression by interleukin-10. J. Leukoc. Biol. 63:486–492.

32. Tumpey, T. M., V. M. Elner, S. H. Chen, J. E. Oakes, and R. N. Lausch. 1994. Interleukin-10 treatment can suppress stromal keratitis induced by herpes simplex virus type 1. J. Immunol. 153:2258–2265.

33. Turcanu, V., T. R. Hirst, and N. A. Williams. 2002. Modulation of human monocytes by *Escherichia coli* heat-labile enterotoxin B-subunit; altered cytokine production and its functional consequences. Immunology 106:316–325.

34. Walker, J., K. A. Laycock, J. S. Pepose, and D. A. Leib. 1998. Postexposure vaccination with a virion host shutoff defective mutant reduces UV-B radiation-induced ocular herpes simplex virus shedding in mice. Vaccine 16:6–8.

35. Yan, X. T., M. Zhuang, J. E. Oakes, and R. N. Lausch. 2001. Autocrine action of IL-10 suppresses proinflammatory mediators and inflammation in the HSV-1-infected cornea. J. Leukoc. Biol. 69:149–157.

Escherichia coli Heat-Labile Enterotoxin B Subunit Is a More Potent Mucosal Adjuvant than Its Closely Related Homologue, the B Subunit of Cholera Toxin

DOUGLAS G. MILLAR,[1]* TIMOTHY R. HIRST,[2] AND DENIS P. SNIDER[1]

Department of Pathology and Molecular Medicine, McMaster University, Hamilton, Ontario, Canada L8N 3Z5,[1] and Department of Pathology and Microbiology, University of Bristol, Bristol, United Kingdom[2]

Although cholera toxin (Ctx) and *Escherichia coli* heat-labile enterotoxin (Etx) are known to be potent mucosal adjuvants, it remains controversial whether the adjuvanticity of the holotoxins extends to their nontoxic, receptor-binding B subunits. Here, we have systematically evaluated the comparative adjuvant properties of highly purified recombinant EtxB and CtxB. EtxB was found to be a more potent adjuvant than CtxB, stimulating responses to hen egg lysozyme when the two were coadministered to mice intranasally, as assessed by enhanced serum and secretory antibody titers as well as by stimulation of lymphocyte proliferation in spleen and draining lymph nodes. These results indicate that, although structurally very similar, EtxB and CtxB have strikingly different immunostimulatory properties and should not be considered equivalent as prospective vaccine adjuvants.

Oral or nasal mucosal administration of protein antigen is thought to favor a state of immunological unresponsiveness by a process of peripheral tolerance, in order to avoid activation of detrimental immune responses to innocuous dietary and airborne environmental antigens (11, 23). Cholera toxin (Ctx) and heat-labile enterotoxin (Etx) from enterotoxinogenic strains of *Escherichia coli*, however, are strongly immunogenic by both parenteral and mucosal routes and elicit strong antitoxin antibody responses when administered either orally or nasally (reviewed in reference 21). Ctx and Etx are also recognized as two of the most potent mucosal adjuvants yet identified, able to greatly enhance antibody responses to coadministered antigens (for recent reviews, see references 17 and 25). However, their toxicity is likely to preclude usage in human vaccines.

The toxins are hetero-oligomeric complexes each composed of an enzymatic A subunit and five identical B subunits (9). The A subunit is responsible for toxicity, catalyzing ADP ribosylation of $G_{s\alpha}$, increasing cyclic AMP (cAMP) levels, and producing chloride efflux and fluid loss. The B subunits are arranged in a pentameric ring and contain five receptor-binding pockets for high-avidity association with cellular membranes containing GM_1 ganglioside. The nontoxic B subunits, CtxB and EtxB, are also potent immunogens, avoiding tolerance induction when administered mucosally and generating strong secretory and systemic antibody responses (reviewed in references 17, 21, and 25).

While early studies suggested that the adjuvant activities of Ctx and Etx were completely dependent on the ability of the catalytic A subunit to raise intracellular cAMP levels and that nontoxic derivatives were devoid of adjuvanticity, it is now well established that this is not the case. Dickinson and Clements

(2) constructed a single point mutation in EtxA which led to reduced ADP ribosylation activity, cAMP elevation, and cellular toxicity, though adjuvanticity was retained (5). Other completely nontoxic point mutants in both CtxA (8, 26–28) and EtxA (4, 6) are now being extensively characterized for their utility in promoting immune responses to mucosally administered antigens.

The possibility that GM_1 binding itself may trigger altered responses to mucosally encountered antigens has been a recurrent subject of investigation. Recombinant B subunits have now been shown to possess distinct immunomodulatory activities. These activities include elevation of both Th1- and Th2-type cytokines (14), $CD8^+$ and $CD4^+$ T-cell apoptosis (24, 29), B-cell activation of major histocompatibility complex II, intracellular adhesion molecule 1 (ICAM-1), CD25, CD40, and B7 expression (15), and modulation of antigen presentation by B cells (10) and macrophages (12, 13). While often overshadowed by more potent holotoxin activity, recombinant B subunit has been found to stimulate antibody responses to coadministered protein antigens, and the GM_1-binding function of the B subunit was found to be essential for both immunogenicity and adjuvant activity (1, 3, 7, 16). Because of the close structural similarity of CtxB and EtxB, which exhibit more than 80% sequence identity, most studies have not sought to carefully discriminate whether these molecules might exhibit differential activities.

In this paper we have directly compared the induction of mucosal and systemic antibody responses and examined antigen-specific lymphocyte proliferation, following intranasal (i.n.) administration of a model protein antigen together with purified recombinant CtxB or EtxB to identify their relative adjuvant and immunostimulatory activities. Contrary to what was expected, we observed striking differences in the immunomodulatory properties of these closely related molecules.

Preparation of toxin B subunits. Recombinant EtxB and CtxB were purified from culture supernatants of *Vibrio* sp. 60

---

* Corresponding author. Present address: Department of Medical Biophysics, Ontario Cancer Institute, 610 University Ave., Room 8-318, Toronto, Ontario, Canada M5G 2M9. Phone: (416) 946-4501, ext. 5471. Fax: (416) 946-2086. E-mail: dmillar@uhnres.utoronto.ca.
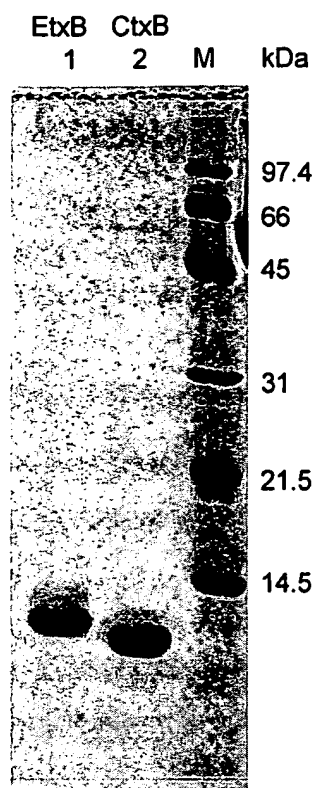
EtxB CtxB
1   2   M   kDa

97.4
66
45
31
21.5
14.5

FIG. 1. SDS-PAGE analysis of purified, recombinant ExtB and CtxB. The adjuvants (30 μg) were boiled in SDS sample buffer, separated by SDS–15% PAGE, and visualized using Coomassie Blue R-250 staining. Lane 1, EtxB; lane 2, CtxB; lane M, molecular size standards.

harboring plasmids pMMB68 or pATA13, respectively, by the method previously described (18). Sodium dodecyl sulfate-polyacrylamide gel electrophoresis (SDS-PAGE) analysis of the purified proteins revealed, for each, a single band at the expected molecular weight and demonstrated more than 98% purity (Fig. 1). The preparations of EtxB and CtxB contained equivalent, low levels of lipopolysaccharide ($\leq$ 0.06 endotoxin unit (EU)/μg [data not shown]) as assessed by the *Limulus* amebocyte lysate endotoxin assay according to the manufacturer's protocol (E-Toxate; Sigma, Oakville, Ontario, Canada).

Stimulation of systemic and mucosal antibody responses by the B subunit. Hen egg lysozyme (HEL) (three times crystallized, dialyzed, and lyophilized; catalog number L-6876; Sigma) was used as a model vaccine antigen with either EtxB or CtxB as an adjuvant. Proteins were aseptically prepared in sterile phosphate-buffered saline (PBS) at the appropriate concentration for i.n. administration in a total volume of 14 μl (7 μl per nare). To identify whether CtxB and EtxB had similar abilities to enhance systemic and mucosal antibody responses, groups of three to five female C3H/HeN ($H-2^k$) mice (Charles River Laboratories, Montreal, Quebec, Canada) were immunized i.n. with HEL alone, HEL plus CtxB (HEL+CtxB), HEL plus EtxB (HEL+EtxB), or HEL plus Ctx (HEL+Ctx) (Fig. 2). Mice were given two immunizations, 7 days apart. Three weeks following immunization, mice were bled from the retro-orbital plexus, and the serum was collected by centrifugation after 1 h of clotting at room temperature. Sodium azide was
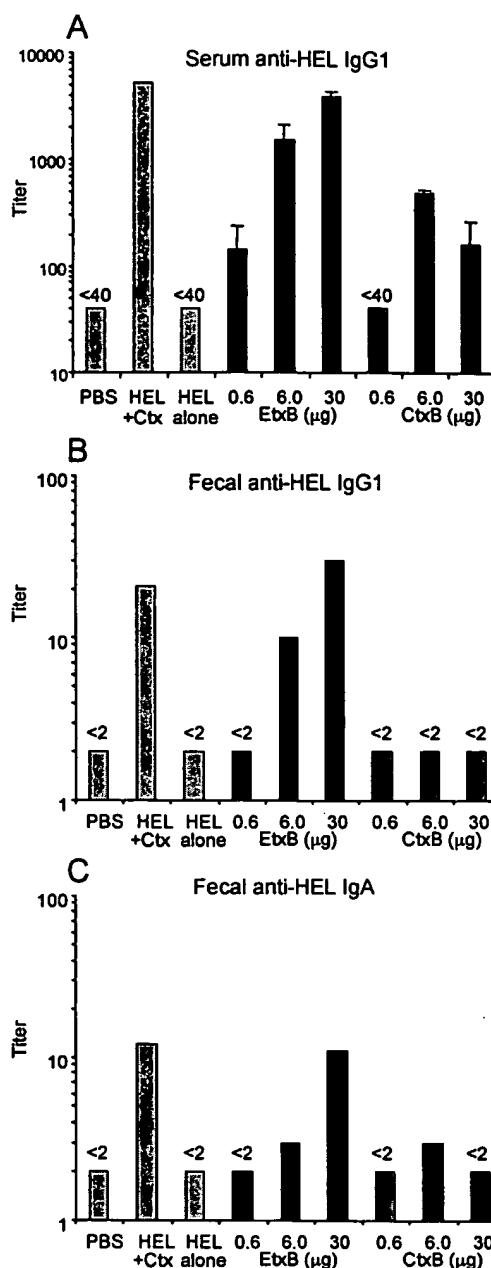
A
Serum anti-HEL IgG1

B
Fecal anti-HEL IgG1

C
Fecal anti-HEL IgA

FIG. 2. Serum and fecal antibody responses following i.n. immunization with HEL+EtxB or HEL+CtxB. C3H/HeN ($H-2^k$) mice were immunized i.n. on two occasions, 7 days apart, with 1 μg of HEL either alone or mixed with different amounts of EtxB or CtxB. Controls received PBS alone or 1 μg of HEL plus 1 μg of Ctx holotoxin. Samples were collected 21 days following the first immunization and assayed for HEL-specific antibody by ELISA. Data bars, mean antibody titers (error bars, standard errors of the means [SEM]) (n = 3 mice per group). Fecal samples from all mice in each group were pooled to determine fecal antibody titers. (A) Serum anti-HEL IgG1; (B) fecal anti-HEL IgG1; (C) fecal anti-HEL IgA.

added to a final concentration of 0.1%, and the serum samples were stored at −20°C until use. Fresh fecal samples were obtained from each mouse, and the individual samples within each experimental group were pooled and extracted overnight at 4°C in PBS containing 2 mM phenylmethylsulfonyl fluoride
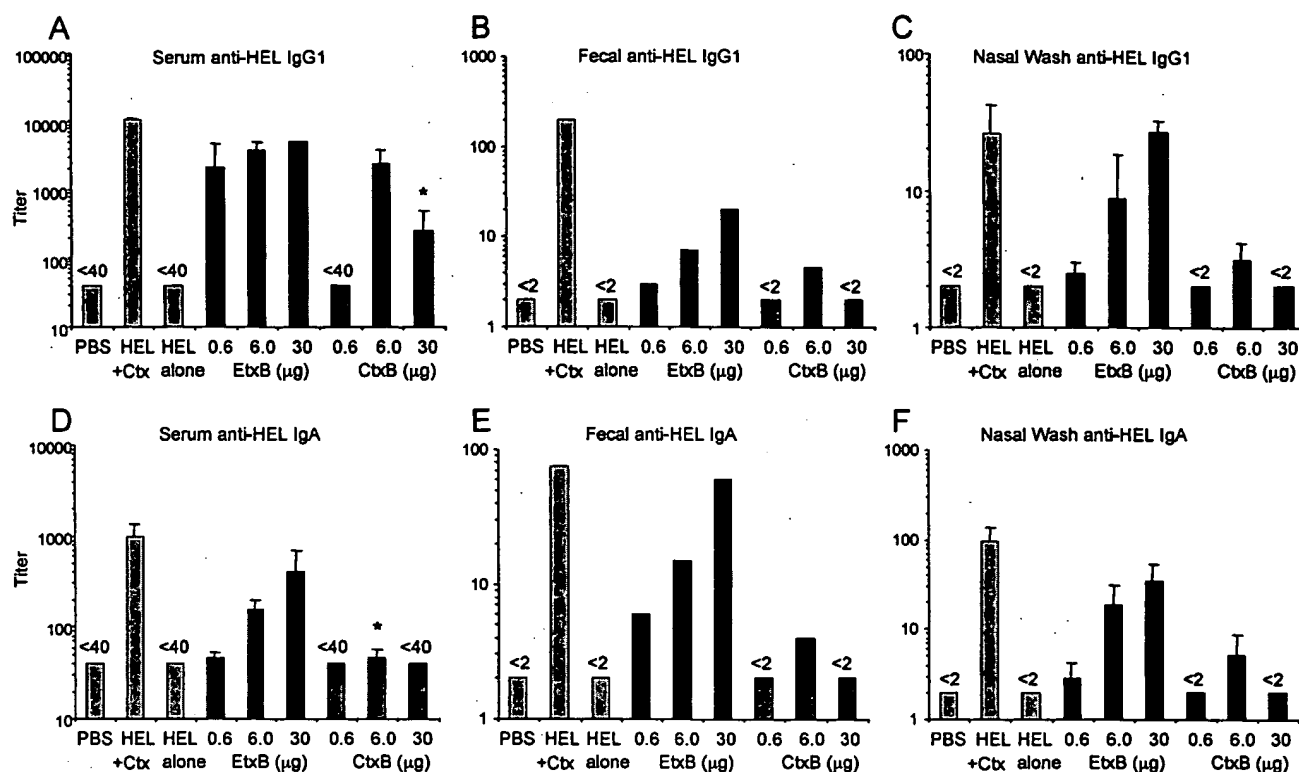
FIG. 3. Recall antibody responses to i.n. priming with HEL+EtxB or HEL+CtxB. Mice were given two i.n. immunizations, 7 days apart, as described for Fig. 2. On day 22 after the first immunization, all mice were challenged i.n. with 1 μg of HEL plus 1 μg of Ctx. Ten days later, the mice were sacrificed and samples were obtained. Samples were assayed for HEL-specific antibody by ELISA. Data bars, mean antibody titers (error bars, SEM) ($n = 3$ mice per group). Fecal samples from all mice in each group were pooled to determine fecal antibody titers. *, $P < 0.05$ compared to equivalent dose of EtxB. (A) Serum anti-HEL IgG1; (B) fecal anti-HEL IgG1; (C) nasal anti-HEL IgG1; (D) serum anti-HEL IgA; (E) fecal anti-HEL IgA; (F) nasal anti-HEL IgA.

(PMSF), 200 μg of aprotinin per ml, 10 mM EDTA, and 0.1% NaN$_3$. Insoluble fecal material was removed by centrifugation, and the supernatants were stored at $-20°C$ until use. Antibody titers were determined by standard end-point enzyme-linked immunosorbent assay (ELISA). ELISA plates (Maxisorb; Nunc) were coated with 100 μg of HEL per ml overnight at 4°C, washed, and incubated with diluted serum, fecal, or nasal wash samples overnight at 4°C. Biotinylated goat anti-mouse immunoglobulin G1 (IgG1) or biotinylated goat anti-mouse IgA (Jackson Immunotech) was used to detect specific HEL-bound antibody isotypes, which were then detected with alkaline phosphatase-conjugated avidin (Extra-Avidin; Sigma), using p-nitrophenyl phosphate as the substrate in 10% ethanolamine–1 mM MgCl$_2$ buffer [pH 9.8], and the intensity was measured spectrophotometrically at 405 nm. Titers were obtained from the highest dilution yielding an intensity twofold above that observed with samples taken from nonimmunized mice. Statistical significance was determined using Student's t test at the 95% confidence level.

Antibody responses against HEL were undetectable in mice given saline or HEL alone (Fig. 2) but were significantly stimulated in mice immunized with various doses of HEL+EtxB (Fig. 2). IgG1 titers were 5- to 15-fold higher in feces and 4- to 100-fold higher in serum, and IgA titers were 2- to 5-fold higher than those observed after immunization with HEL alone, depending on the dose of EtxB. As little as 6 μg of EtxB

stimulated anti-HEL IgG1 and IgA titers in feces, while even the lowest dose (0.6 μg) was able to elicit an anti-HEL IgG1 response in serum. CtxB admixed with HEL was unable to stimulate an anti-HEL IgG1 response in feces and elicited only a weak fecal IgA response. CtxB did stimulate a serum anti-HEL IgG1 response (Fig. 2A), though at titers consistently lower than those elicited by equivalent doses of EtxB. CtxB lost all stimulatory ability at the lowest dose used (0.6 μg). Serum anti-HEL IgA was undetectable following immunization with either B subunit (data not shown). Interestingly, increasing the dose of CtxB to 30 μg decreased the anti-HEL antibody responses (Fig. 2A and C), in contrast to the increased-dose response stimulated by EtxB. Antibody titers elicited by the highest dose of HEL+EtxB were similar to those produced by immunization with HEL plus 1 μg of Ctx holotoxin.

Next, the effect of admixed B subunit on the recall antibody responses of mice primed i.n. with HEL+EtxB or HEL+CtxB was examined following a secondary antigen challenge with Ctx holotoxin. Mice were primed with no antigen (PBS), HEL alone, HEL+EtxB, or HEL+CtxB and then challenged 3 weeks later with HEL+Ctx administered i.n., and anti-HEL antibody responses were measured (Fig. 3). Serum and fecal samples were obtained as described above, and the mice were sacrificed for nasal wash sampling as previously described (22). Briefly, the trachea was ligated with surgical thread and 60 G polyethylene tubing was inserted, aside the trachea, into the

nasal cavity. PBS containing 2 mM PMSF, 200 μg of aprotinin per ml, 10 mM EDTA, and 0.1% NaN_3 was injected into the nasal cavity via a syringe attached to the tubing and collected as it emerged from the nares into a 1.5-ml centrifuge tube placed below the nose. A total wash volume of 1 ml was injected and collected by this procedure. Nasal wash samples were clarified by centrifugation, and the supernatants were stored at −20°C until use.

Priming i.n. with HEL alone yielded no antibody responses 10 days following a secondary challenge with HEL+Ctx (Fig. 3). By contrast, when EtxB was included with HEL during the initial priming (Fig. 3), high titers of serum and secretory anti-HEL-specific antibody were induced following the secondary challenge. Priming with HEL+CtxB, however, yielded much weaker antibody titers in feces and nasal secretions and low IgA responses in serum, following challenge. The titers of HEL-specific IgG1 and IgA in feces and nasal secretions, as well as those of anti-HEL IgG1 and IgA in serum, were significantly greater in mice primed with HEL+EtxB than in those given equivalent doses of HEL+CtxB. Only at an intermediate dose of B subunit (6 μg) were CtxB and EtxB able to induce similar, high titers of anti-HEL IgG1 in serum. A high dose of CtxB (30 μg) was less effective at stimulating anti-HEL antibody responses, even after Ctx challenge. Priming with HEL+Ctx holotoxin produced the highest titers of both systemic and secreted antibody observed (Fig. 3).

Parallel studies using an alternative model antigen, ovalbumin (OVA), were also undertaken. Mice immunized i.n. with OVA plus EtxB or OVA plus CtxB exhibited a similarly differential response, with EtxB triggering potent anti-OVA antibody responses, while CtxB elicited either meager or no anti-OVA response (data not shown).

Kinetics of antibody stimulation by recombinant B subunits. To determine whether CtxB was simply slower acting than EtxB and if its adjuvant effects might approach those of EtxB at later time points, the kinetics of anti-HEL antibody stimulation were examined over the course of 5 weeks using two doses of B subunit, 6 and 30 μg (Fig. 4). Following i.n. immunization with HEL+EtxB, elevated serum and fecal anti-HEL antibody titers were detectable 13 days after the primary administration (Fig. 4A, C, and E). Antibody titers in both serum and feces increased over the next 3 weeks. The serum anti-HEL IgG1 response when CtxB was used as the adjuvant (Fig. 4B, D, and F) lagged 1 week behind that observed for EtxB used as the adjuvant, appearing at 20 days postimmunization, and remained significantly lower over the next 3 weeks. Again, no detectable titers of fecal IgG1 were stimulated by CtxB. Fecal anti-HEL IgA induced by CtxB appeared between weeks 2 and 4 and decreased by week 5. Again, a high dose of CtxB yielded lower anti-HEL antibody titers in serum and feces than a low dose, in contrast to the dose response to EtxB.

HEL-specific lymphocyte priming following B subunit immunization. The presence of T cells primed to respond to HEL following i.n. immunization with HEL+CtxB or HEL+EtxB was determined by measuring the proliferation of lymphocytes restimulated in vitro with HEL (Fig. 5). The spleen, mesenteric lymph nodes (MLN), cervical lymph nodes (CLN), and inguinal lymph nodes (ILN) were removed from immunized mice and placed in sterile Hank's balanced salt solution at 4°C. Tissues were homogenized by grinding between frosted glass

slides followed by gentle pipeting. A single cell suspension was obtained by passing the homogenate though 60 μm-opening nylon mesh, and the lymphocytes were recovered by centrifugation. Red blood cells were removed using osmotic lysis by resuspending the cells in 1 ml of cold erythrocyte lysis solution (0.15 M NH_4Cl, 10 mM $KHCO_3$, 0.1 mM EDTA) and incubating the suspension for 1 min before dilution with 10 volumes of Hank's balanced salt solution. Membrane debris and adipocytes were then removed by further centrifugation, the supernatant was discarded, and the lymphocyte pellet was resuspended in complete RPMI medium containing 10% fetal bovine serum, 50 μM 2-mercaptoethanol, 100 μg of penicillin-streptomycin per ml, 100 μg of amphotericin B (Fungizone; GIBCO BRL) per ml. Total lymphocytes from each tissue were cultured at 5×10^5 cells in a 96-well flat-bottomed tissue culture plate (Nunc), in complete RPMI medium with or without 200 μg of HEL per ml. Cells were incubated for 72 h at 37°C in 5% CO_2, and [^{3}H]thymidine was added for the final 15 h to assess proliferation. Cells were harvested onto glass-fiber filter paper using a PHD (Cambridge, Mass.) harvester, and incorporated counts were measured by liquid scintillation counting in a Beckman beta counter. Optimum proliferation was observed during 72 h of incubation in culture medium containing 200 μg of HEL per ml (reference 20 and data not shown). Proliferative responses were detected 7 days following i.n. immunization with HEL+Ctx in all the tissues examined (Fig. 5). When EtxB was used as the adjuvant, similar cell proliferation was also seen in all locations examined (Fig. 5). However, when CtxB was used as adjuvant (Fig. 5), the cell proliferation level was not significantly above the background (nonimmune) level in either the CLN or spleen, and the response in MLN was significantly lower than that observed for HEL+EtxB or HEL+Ctx. Surprisingly, the proliferation of ILN lymphocytes following HEL+CtxB administration was equivalent to that stimulated by HEL+Ctx or HEL+EtxB. The restricted localization of HEL-primed lymphocytes to distal, peripheral lymph nodes, and their absence from spleen and local CLN, following immunization with HEL+CtxB correlated with the lack of systemic humoral responses and weak mucosal antibody responses. In contrast, HEL+EtxB immunization lead to primed lymphocytes in spleen, as well as in both local and distal lymph nodes, and stimulated both systemic and mucosally secreted antibody production.

Additionally, limiting dilution analysis revealed frequencies of HEL-specific lymphocytes in the peripheral lymph nodes (MLN and ILN) following immunization with HEL+CtxB that were lower than those observed following immunization with HEL+EtxB or HEL+Ctx (data not shown). This suggests that EtxB treatment produces a greater expansion of the antigen-specific T-cell population than CtxB, which may then lead to the enhanced immune responses observed.

Concluding remarks. These findings demonstrate that although EtxB and CtxB are close homologs, their capacity to function as mucosal adjuvants is markedly different. Using recombinant EtxB and CtxB, we found EtxB to be more potent than CtxB at inducing high-titer antibody responses both systemically and at distant mucosal sites when coadministered i.n. with antigen. Moreover, it was recently reported that i.n. immunization with EtxB stimulated protective mucosal immunity to ocular herpesvirus infection, while CtxB did not (18). Why

EtxB + HEL

A
Serum anti-HEL IgG1

B
CtxB + HEL

Serum anti-HEL IgG1

C
Fecal anti-HEL IgG1

D
Fecal anti-HEL IgG1

E
Fecal anti-HEL IgA

F
Fecal anti-HEL IgA

Days post i.n. immunization
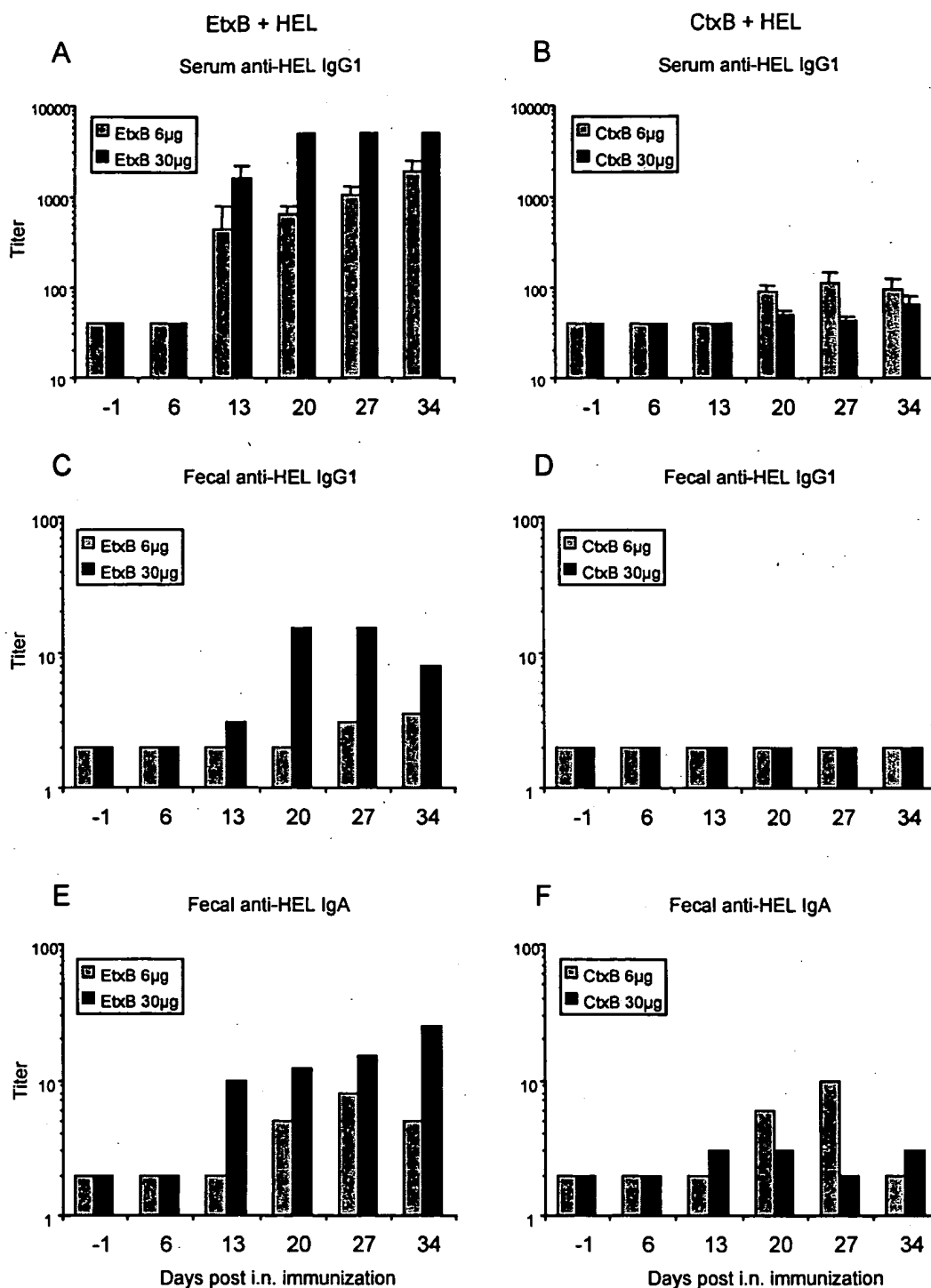
Days post i.n. immunization

FIG. 4. Kinetics of antibody responses to i.n. immunization with HEL+EtxB or HEL+CtxB. Mice were immunized with 1 μg of HEL either alone or with the indicated amount of EtxB or CtxB exactly as described for Fig. 2. Samples were taken at the indicated time points before and after the first immunization and were then assayed for HEL-specific antibody by ELISA. Data bars, mean antibody titers in serum (error bars, SEM) ($n = 3$ mice per group). Fecal samples from all mice in each group were pooled to determine fecal antibody titers. (A and B) Serum anti-HEL IgG1; (C and D) fecal anti-HEL IgG1; (E and F) fecal anti-HEL IgA.

EtxB is such a potent adjuvant whereas CtxB exhibits such poor adjuvanticity remains to be fully explained. Since it is thought that EtxB is more promiscuous than CtxB in binding to a range of cell surface receptors in addition to GM_1 ganglio-side, it is possible that the enhanced adjuvanticity of EtxB stems from its ability to interact with non-GM_1 receptors. The observation by Ruddock et al. (19) that the intrinsic stability of EtxB is much greater than that of CtxB, as measured by its

A   Cervical LN

B   Mesenteric LN

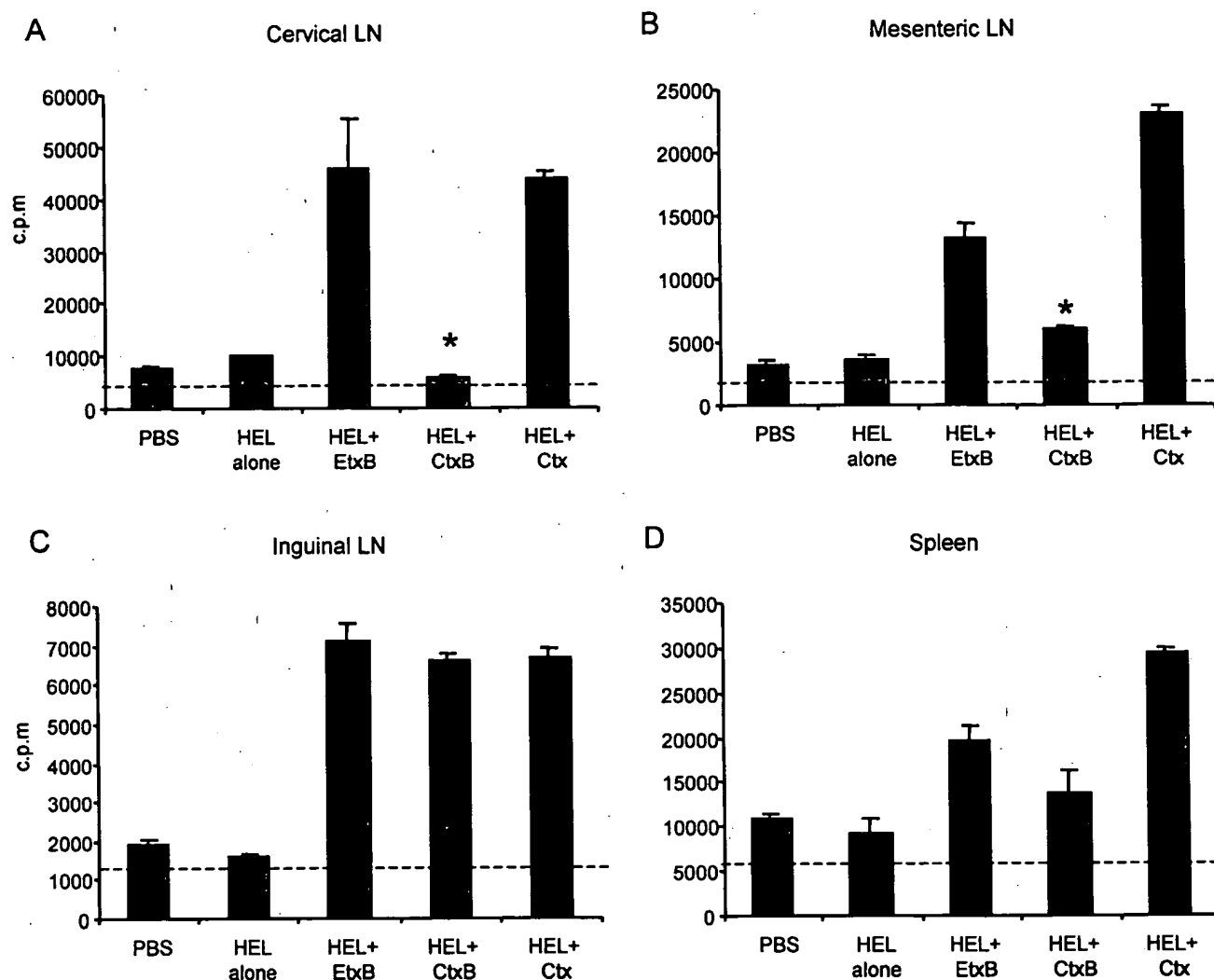C   Inguinal LN

D   Spleen

FIG. 5. HEL-specific lymphocyte proliferation following i.n. immunization with HEL+EtxB or HEL+CtxB. Mice were immunized once i.n. with either 1 μg of HEL alone, 1 μg of HEL plus 30 μg of EtxB, 1 μg of HEL plus 30 μg of CtxB, or 1 μg HEL plus 1 μg of Ctx, as indicated. Controls received PBS. Seven days later, cell suspensions were isolated from CLN (A), MLN (B), ILN (C), and spleen (D). The cells were cultured in the presence or absence of 200 μg of HEL per ml for 72 h. Proliferation was measured by incorporation of [^{3}H]thymidine during the final 15 h of culture, and data are mean counts per minute ± SEM from triplicate cultures. Dashed line, background proliferation from cultures without HEL. *, $P < 0.05$ compared to HEL+EtxB.

resistance to pH-induced denaturation, thermostability, and susceptibility to detergents, may provide an alternative explanation for their differential adjuvanticity. It is conceivable that it is this differential ability to maintain a pentameric structure that permits EtxB to sustain its effects on the immune system while CtxB easily disassembles into a less active form. Interestingly, neither B subunit is a very effective adjuvant by the oral route (4), perhaps reflecting the ability of the harsh environment of the gut to denature both proteins. Furthermore, the presence of the A subunit, including nontoxic variants, may enable the stabilization of the CtxB pentamer structure and thereby account for the reported enhanced adjuvanticity of such molecules (3, 8, 26–28). However, because of concern about the safety of attenuated Ctx and Etx holotoxins, it is encouraging that EtxB (devoid of any A subunit) demonstrates such a potent adjuvant activity. In so doing, it should be suit-

ably applicable as an immunoadjuvant for inclusion in mucosal vaccines.

REFERENCES

1. de Haan, L., I. K. Feil, W. R. Verweij, M. Holtrop, W. G. Hol, E. Agsteribbe, and J. Wilschut. 1998. Mutational analysis of the role of ADP-ribosylation activity and GM1-binding activity in the adjuvant properties of the Escherichia coli heat-labile enterotoxin towards intranasally administered keyhole limpet hemocyanin. Eur. J. Immunol. 28:1243–1250.
2. Dickinson, B. L., and J. D. Clements. 1995. Dissociation of Escherichia coli heat-labile enterotoxin adjuvanticity from ADP-ribosyltransferase activity. Infect. Immun. 63:1617–1623.
3. Douce, G., M. Fontana, M. Pizza, R. Rappuoli, and G. Dougan. 1997. Intra-

nasal immunogenicity and adjuvanticity of site-directed mutant derivatives of cholera toxin. Infect. Immun. 65:2821–2828.

4. Douce, G., V. Giannelli, M. Pizza, D. Lewis, P. Everest, R. Rappuoli, and G. Dougan. 1999. Genetically detoxified mutants of heat-labile toxin from *Escherichia coli* are able to act as oral adjuvants. Infect. Immun. 67:4400–4406.

5. Giannelli, V., M. R. Fontana, M. M. Giuliani, D. Guangcai, R. Rappuoli, and M. Pizza. 1997. Protease susceptibility and toxicity of heat-labile enterotoxins with a mutation in the active site or in the protease-sensitive loop. Infect. Immun. 65:331–334.

6. Giuliani, M. M., G. Del Giudice, V. Giannelli, G. Dougan, G. Douce, R. Rappuoli, and M. Pizza. 1998. Mucosal adjuvanticity and immunogenicity of LTR72, a novel mutant of Escherichia coli heat-labile enterotoxin with partial knockout of ADP-ribosyltransferase activity. J. Exp. Med. 187:1123–1132.

7. Guidry, J. J., L. Cardenas, E. Cheng, and J. D. Clements. 1997. Role of receptor binding in toxicity, immunogenicity, and adjuvanticity of *Escherichia coli* heat-labile enterotoxin. Infect. Immun. 65:4943–4950.

8. Hagiwara, Y., K. Komase, Z. Chen, K. Matsuo, Y. Suzuki, C. Aizawa, T. Kurata, and S. Tamura. 1999. Mutants of cholera toxin as an effective and safe adjuvant for nasal influenza vaccine. Vaccine 17:2918–2926.

9. Hirst, T. R. 1995. Biogenesis of cholera toxin and related oligomeric enterotoxins, p. 123–184. *In* J. Moss, M. Vaughan, B. Iglewski, and A. T. Tu (ed.), Bacterial toxins and virulence factors in disease, vol. 8. Marcel Dekker Inc., New York, N.Y.

10. Li, T. K., and B. S. Fox. 1996. Cholera toxin B subunit binding to an antigen-presenting cell directly co-stimulates cytokine production from a T cell clone. Int. Immunol. 8:1849–1856.

11. Lowrey, J. L., N. D. Savage, D. Palliser, M. Corsin-Jimenez, L. M. Forsyth, G. Hall, S. Lindey, G. A. Stewart, K. A. Tan, G. F. Hoyne, and J. R. Lamb. 1998. Induction of tolerance via the respiratory mucosa. Int. Arch. Allergy Immunol. 116:93–102.

12. Matousek, M. P., J. G. Nedrud, W. Cieplak, Jr., and C. V. Harding. 1998. Inhibition of class II major histocompatibility complex antigen processing by *Escherichia coli* heat-labile enterotoxin requires an enzymatically active A subunit. Infect. Immun. 66:3480–3484.

13. Matousek, M. P., J. G. Nedrud, and C. V. Harding. 1996. Distinct effects of recombinant cholera toxin B subunit and holotoxin on different stages of class II MHC antigen processing and presentation by macrophages. J. Immunol. 156:4137–4145.

14. Nakagawa, I., I. Takahashi, H. Kiyono, J. R. McGhee, and S. Hamada. 1996. Oral immunization with the B subunit of the heat-labile enterotoxin of Escherichia coli induces early Th1 and late Th2 cytokine expression in Peyer's patches. J. Infect. Dis. 173:1428–1436.

15. Nashar, T. O., T. R. Hirst, and N. A. Williams. 1997. Modulation of B-cell activation by the B subunit of Escherichia coli enterotoxin: receptor interaction up-regulates MHC class II; B7, CD40, CD25 and ICAM-1. Immunology 91:572–578.

16. Nashar, T. O., H. M. Webb, S. Eaglestone, N. A. Williams, and T. R. Hirst. 1996. Potent immunogenicity of the B subunits of Escherichia coli heat-labile enterotoxin: receptor binding is essential and induces differential modulation of lymphocyte subsets. Proc. Natl. Acad. Sci. USA 93:226–230.

17. Rappuoli, R., M. Pizza, G. Douce, and G. Dougan. 1999. Structure and mucosal adjuvanticity of cholera and Escherichia coli heat-labile enterotoxins. Immunol. Today 20:493–500.

18. Richards, C. M., A. T. Aman, T. R. Hirst, T. J. Hill, and N. A. Williams. 2001. Protective mucosal immunity to ocular herpes simplex virus type 1 infection in mice by using *Escherichia coli* heat-labile enterotoxin B subunit as an adjuvant. J. Virol. 75:1664–1671.

19. Ruddock, L. W., S. P. Ruston, S. M. Kelly, N. C. Price, R. B. Freedman, and T. R. Hirst. 1995. Kinetics of acid-mediated disassembly of the B subunit pentamer of Escherichia coli heat-labile enterotoxin. Molecular basis of pH stability. J. Biol. Chem. 270:29953–29958.

20. Schaffeler, M. P., J. S. Brokenshire, and D. P. Snider. 1997. Detection of precursor Th cells in mesenteric lymph nodes after oral immunization with protein antigen and cholera toxin. Int. Immunol. 9:1555–1562.

21. Snider, D. P. 1995. The mucosal adjuvant activities of ADP-ribosylating bacterial enterotoxins. Crit. Rev. Immunol. 15:317–348.

22. Snider, D. P., B. J. Underdown, and M. R. McDermott. 1997. Intranasal antigen targeting to MHC class II molecules primes local IgA and serum IgG antibody responses in mice. Immunology 90:323–329.

23. Strobel, S., and A. M. Mowat. 1998. Immune responses to dietary antigens: oral tolerance. Immunol. Today 19:173–181.

24. Truitt, R. L., C. Hanke, J. Radke, R. Mueller, and J. T. Barbieri. 1998. Glycosphingolipids as novel targets for T-cell suppression by the B subunit of recombinant heat-labile enterotoxin. Infect. Immun. 66:1299–1308.

25. Williams, N. A., T. R. Hirst, and T. O. Nashar. 1999. Immune modulation by the cholera-like enterotoxins: from adjuvant to therapeutic. Immunol. Today 20:95–101.

26. Yamamoto, S., H. Kiyono, M. Yamamoto, K. Imaoka, K. Fujihashi, F. W. Van Ginkel, M. Noda, Y. Takeda, and J. R. McGhee. 1997. A nontoxic mutant of cholera toxin elicits Th2-type responses for enhanced mucosal immunity. Proc. Natl. Acad. Sci. USA 94:5267–5272.

27. Yamamoto, S., Y. Takeda, M. Yamamoto, H. Kurazono, K. Imaoka, K. Fujihashi, M. Noda, H. Kiyono, and J. R. McGhee. 1997. Mutants in the ADP-ribosyltransferase cleft of cholera toxin lack diarrheagenicity but retain adjuvanticity. J. Exp. Med. 185:1203–1210.

28. Yamamoto, S., M. Yamamoto, K. Imaoka, M. Yamamoto, K. Fujihashi, H. Kiyono, Y. Takeda, and J. R. McGhee. 1997. A nontoxic mutant of cholera toxin elicits mucosal immunity to vaccines given intranasally. J. Allergy Clin. Immunol. 99:146.

29. Yankelevich, B., V. A. Soldatenkov, J. Hodgson, A. J. Polotsky, K. Creswell, and A. Mazumder. 1996. Differential induction of programmed cell death in CD8+ and CD4+ T cells by the B subunit of cholera toxin. Cell. Immunol. 168:229–234.

16.01.2004

Recombinant *Streptococcus equi* proteins protect mice in challenge experiments and induce immune response in horses.

Margareta Flock,[a] Karin Jacobsson,[b] Lars Frykberg, [b] , Timothy R. Hirst,[c,e] Anders Franklin,[d] Bengt Guss,[b] and Jan-Ingmar Flock[a*]

Department of Laboratory Medicine, Karolinska Institutet, Stockholm, Sweden[a]; Department of Microbiology, Swedish University of Agricultural Sciences, Uppsala, Sweden[b]; Department of Pathology & Microbiology, University of Bristol, Bristol, United Kingdom[c]; National Veterinary Institute, Uppsala, Sweden [d].

Running title: vaccination against equine strangles

*Corresponding author. Mailing address: Department of Laboratory medicine, Division of Clinical Bacteriology, Karolinska Institutet, Huddinge University Hosptial, F 82, S-141 86 Stockholm, Sweden. Phone +46858581169. Fax: +4687113918. E-mail: jan-ingmar.flock@labmed.ki.se

[e]Present address: The Quadrangle, The University of Sydney, Sydney

Horses that have undergone infection caused by *Streptococcus equi* subspecies *equi* (strangles) were found to have significantly increased serum titers against three previously characterized proteins, FNZ (cell surface bound fibronectin binding protein), SFS (secreted fibronectin binding protein) and EAG (α_2-macroglobulin, albumin and IgG binding protein) from *S. equi*. To assess the protective efficacy of vaccination with these three proteins, a mouse model of equine strangles was utilized. Parts of the three recombinant proteins were used to immunize mice, either subcutaneously or intranasally, prior to nasal challenge with subsp. *equi*. The adjuvant used was EtxB, a recombinant form of the B subunit of *Escherichia coli* heat labile enterotoxin. It was shown that nasal colonization of subsp. *equi* and weight loss due to infection were significantly reduced after vaccination as compared with a mock vaccinated control group. This effect was more pronounced after intranasal vaccination than after subcutaneous vaccination; nearly complete eradication of nasal colonization was obtained after intranasal vaccination ($p < 0.001$). When the same antigens were administered both intranasally and subcutaneously to healthy horses significant mucosal IgA and serum IgG antibody responses against FNZ and EAG were obtained. The antibody response was enhanced when EtxB was used as adjuvant. No adverse effects of the antigens or EtxB were observed. Thus, FNZ and EAG in conjunction with EtxB are promising candidates for an efficacious and safe vaccine against strangles.

Streptococcus equi, subsp. *equi,* is the causative agent of strangles, one of the most widespread and costly horse diseases worldwide (4, 5). The disease is highly contagious and common symptoms are fever, lymphadenitis and abscesses mainly in the head and neck regions. Also more generalized symptoms such as endocarditis, rheumatic fever, glomerulonephritis and fatal outcomes occur (1). The disease is characterized by a long convalescence period and diseased horses are isolated for at least four weeks in order to prevent further spread of the disease (1). Affected animals may harbor the bacteria, among other places in the guttoral pouches for several months and thus shed and act as reservoirs of subsp. *equi* (17, 25). Although subsp. *equi* is quite sensitive to penicillin and other antibiotics, antibiotic treatment is for various reasons mostly ineffective (4). In order to combat the disease and mitigate the serious clinical complications, research has mainly aimed at developing efficient vaccines. Vaccines against strangles such as bacterins or adjuvanted extracts have been used since the 80s. Bacterins or adjuvanted extracts do however not confer efficient protection against infection with subsp. *equi* (8, 23). During recovery and convalescence, horses develop a protective immune response, indicating that efficient vaccines might be developed (3). The antibody response is strong predominantly against the antiphagocytic cell-wall associated M-like protein SeM. Convalescent horses have antibodies of IgG and IgA types against SeM both in serum and in nasal secretions and because of the strong antibody response, SeM has attracted much interest as a vaccine component (16, 21). Vaccination of horses with SeM, using different adjuvants and different routes, gave no significant protection against infection with subs. *equi* (20, 21).

Many different pathogenic bacteria have evolved extra-cellular proteins that bind host proteins. These proteins are considered as potential virulence factors and are candidate components for vaccine development. Many bacterial species have been reported to express extra-cellular proteins that bind the serum proteins fibronectin (Fn) or IgG, indicating that that these interactions are of particular importance for the virulence. The Fn-binding is considered to be of importance for bacterial adherence and internalization into mammalian cells (15), whereas binding of IgG can affect antibody-mediated complement activation and phagocytosis (9, 19). Two different Fn-binding proteins have been identified in subsp. *equi*, FNE and SFS. FNE was first identified in subsp. *zooepidemicus* and named FNZ (11, 13), later a homologous gene was found in subsp. *equi*. However, there is one major difference between *fne* and *fnz*, in that the *fne* gene contains a base pair deletion, which results in a truncated Fn-binding protein of ~30 kDa. The *sfs*-gene encodes a 40-kDa extra-cellular protein and the gene is found in all tested strains of subsp. *equi* and 41 of 48 *zooepidemicus* strains (10). Furthermore, an IgG, serum albumin and α_2-macroglobulin-binding surface protein called ZAG first isolated from subsp. *zooepidemicus* has attracted interest as a virulence factor (6, 7). Using Southern blot analysis, the *zag* gene was detected in both subspecies (12). The *zag* gene in subsp. *equi* has in this study been named *eag,* encoding the protein EAG.

The aim of the present study was to evaluate the extra-cellular antigens FNZ, EAG and SFS as components in a vaccine against strangles using a mouse strangles model. The antibody responses to these antigens were also studied in convalescent horses, in horses without a history of strangles and in experimentally immunized horses.

MATERIALS AND METHODS

Bacterial strains, plasmids, and growth conditions. *S. equi* subsp. *equi* strain 1866 was obtained from NordVacc Läkemedel, Stockholm. The *E. coli* strain ER2566 and plasmid vector pTYB4 were obtained from New England Biolabs MA, USA (NEB). Streptococcal strains were grown on horse blood agar plates (BG plates) or in Todd-Hewitt broth (THB) (Oxoid, Basingstoke, Hampshire, UK) supplemented with 0.5% yeast extract. *E. coli* was cultured in Luria-Bertani (LB) broth, supplemented with ampicillin (100μg/ml) or on LAA-plates (LB broth with ampicillin and agar (15g/l))

Adjuvant preparation. Recombinant *E. coli* heat-labile enterotoxin B-subunit (EtxB) was expressed in *Vibrio sp60* (pMMB68) and purified from the culture supernatant as reported previously by Richards et al. (18). Briefly, EtxB was recovered from the culture medium by diafiltration and then subjected to ammonium sulfate precipitation (30% saturation) and hydrophobic interaction and anion exchange chromatography using phenyl superose HR5/5 (Amersham Biosciences) and Resource Q (Amersham) columns, respectively. The single peak eluting from the Resource Q column was desalted using a NAP-10 column equilibrated in phosphate buffered saline (PBS, 0.15M NaCl, sodium phosphate pH7.2). Purified preparations of EtxB were depleted of residual lipopolysaccharide using Detoxi-Gel columns (Pierce, Rockford, Ill), followed by dialysis against PBS. The purified protein was stored at −80° C prior to use.

Construction of clones and preparation of antigens. The SFS protein (GeneBank accession number AF136451) from subsp. *equi* has previously been described by Lindmark and Guss (10). A clone expressing the C-terminal fragment of this protein was produced as follows: The 3′ end of the *sfs* gene was PCR amplified using chromosomal DNA from subsp. *equi* strain 1866 as template and the synthetic oligonucleotides OSFS25; 5′-GGTCCCATGGCAACTCCGAATTTAGAAGGA, and OSFS23; 5′-CAGACTCGAGGTCGGGATTGTAAGAATAG. After amplification the PCR product was digested with *Nco*I and *Xho*I, and ligated into plasmid vector pTYB4, which previously had been digested with the same enzymes. After electro-transformation of the ligation mix into *E. coli* strain ER2566, clones harboring the correct insert were identified by sequence analysis. One clone called pSFSC1, encoding the truncated SFS protein (SFSC1) was chosen for preparation of antigen according to manufacturing procedure provided by NEB.

Protein FNZ from subsp. *zooepidemicus* (EMBL accession number X99995) has previously been described by Lindmark et al. (11-13). A similar protein called FNE (GeneBank accession number is AF360373) is also expressed by strains of subsp. *equi* (13). The construction of a clone called pT2fnzN encoding the N-terminal part of FNZ, called FNZN, has previously been described by Lindmark et al (13).

In Lindmark et al (12) a gene similar to *zag* (GenBank accession number for the *zag* gene is U25852) from subsp. *zooepidemicus* was also described in subsp. *equi*. The gene present in subsp. *equi* is hereafter called *eag*. A part of this gene was cloned and expressed essentially as described above using the primers OZAG43B 5′-TTT TCT CGA GCT ACG GTA GAG CTG ATA AAA TCT C-3′ and OZAG15 5′-TCA GCC

ATG GCT CTA GAT GCT ACA ACG GTG TT-3′. The PCR-amplified DNA-fragment corresponds to amino acids 34-262 in protein ZAG. Correct transformants were identified by colony screening using Horse Radish Peroxidase (HRP) labeled human serum albumin. The insert of the clone, pEAG4B chosen for further work was sequenced to verify the correct insertion into the vector and the presence of a stop codon between EAG and the intein affinity tag. The stop codon between the albumin binding domain and the intein tag was introduced since a previous intein fusion construct was not cleaved in the presence of DTT. To purify the truncated EAG protein (EAG4B) human serum albumin was immobilized on a HiTrap NHS-activated column (Amersham) according to the manufacturer's instructions. The column was washed with 20 mM Na-phosphate pH 7.0 (binding buffer) before the lysed cell sample was loaded onto the column. The column was washed with binding buffer and the bound EAG4B protein was eluted in 0.1 M glycine-HCl pH 3.0. After elution, the pH of the sample was neutralized with 2M Tris buffer, pH 8, and dialyzed against PBS.

For simplicity, the recombinant proteins SFSC1, FNZN, and EAG4B will in this study be called SFS, FNZ and EAG, respectively (Fig.1).

Immunization of mice. Seven mice were immunized on four occasions at one week intervals with a combination of FNZ, SFS and EAG, four with EtxB adjuvant and three without adjuvant. Mice were immunized either subcutaneously (s.c) or intranasally (i.n). For each antigen (FNZ, SFS and EAG), 12 µg was mixed with an equal amount of EtxB, all components at a final concentration of 300 µg/ml. In the

case of immunization i.n., the total volume was kept to less than 40µl and applied into the nostrils of mice anaesthetized with Hypnorm (Janssen Pharmaceutica, Beerse, Belgium). For both s.c and i.n. immunizations, four doses were given with one-week intervals. Challenge intranasally with subsp. *equi* was given one week after the last booster dose. Control mice were given only EtxB in the same volume. Animals were divided into groups of four in each cage in all experiments.

Immunization of horses. Horses with no previous history of strangles and with low antibody titers against FNZ, SFS and EAG were selected. An experimental design with four groups (A-D) of horses with three horses in each group was used. The horses were randomly allocated into four groups and were immunized as follows: A) EAG, FNZ and SFS with EtxB as adjuvant, given both i.n. and s.c; B) EAG, FNZ and SFS with EtxB as adjuvant but given only i.n.; C) EAG, FNZ and SFS but without EtxB as adjuvant, given both i.n. and s.c; and D) Only EtxB and no antigens, given both i.n. and s.c.

Each dose consisted of 35 µg of each antigen and 100 µg of EtxB in a volume of 2 ml for i.n. and/or s.c. immunization. Immunizations were given on days 0, 14, 28 and 42. Immunizations of horses were performed at the Centre for Preventative Medicine, Animal Health Trust, Newmarket, UK. Blood samples for determination of IgG serum antibody titers and nasal washings for determination of mucosal IgA were collected immediately prior to the first immunization and on day 56 after the first immunization. The experimental horses were inspected daily during the whole study period for possible signs of adverse side effects. The rectal temperature of each horse was checked once daily.

Determination of antibody titers from horses in ELISA. Serum samples were taken from horses without any previous or present sign of strangles (n=16), as well as from horses with clinical signs of strangles and positive cultivation of subsp. *equi* (n=10). Microtiter wells (Costar) were coated overnight with 100μl FNZ, SFS or EAG at 10 μg per ml overnight in phosphate buffered saline (PBS). The plates were then blocked with 2% (w/v) bovine serum albumin (BSA) for 1 hour at 37°C. After washing, horse sera were added to wells at a 20-fold dilution in PBS with 0.05% Tween (PBST), followed by 2-fold serial dilutions. The plates were washed after 1 hour incubation at 37°C. After washing, detection of antibody binding was done, with antibodies, diluted 1000x, against horse IgG, raised in rabbit and conjugated with HRP (Sigma Chemical Co). Development of colorimetric reaction was done with OPD tablets (Dako, Denmark). Absorbance was determined spectrophotometrically at 492 nm.

Antigen-specific IgA in nasal wash samples from immunized horses were determined by an indirect ELISA. Plates (Immulon 4, Dynatech Laboratories) were coated with 50μl of the antigens at 4μg/ml at 4°C for 16-18 hours and blocked with 5% Marvel skimmed milk in PBST at 37°C for 1 hour. Samples (50μl) containing IgA was added and incubated at 37°C for 1 hour. Mouse monoclonal antibody K129-3E7 (50μl; 2μg/ml) to equine IgA was used to detect bound IgA in the samples by incubation at 37°C for 1 hour, followed by a goat anti-mouse immunoglobulin HRP conjugate (2μg/ml) (Dako) (incubation at 37°C for 1 hour). HRP was detected by incubation with 100μl TMB microwell peroxidase substrate (3,3',5,5'-tetramethylbenzidine; Kirkegaard & Perry Laboratories) at room temperature for 10

minutes. The reaction was stopped by the addition of 100µl 0.18M H_2SO_4 and absorbance was read at 450nm. Background values (plates without antigens) were subtracted from the result and all samples were analyzed in triplicate. ELISA data of antigen-specific IgA is expressed relative to the total IgA in order to correct for nasal secretion dilution during the nasal wash procedure. Total IgA in nasal wash samples was determined by a capture ELISA using two different monoclonal antibodies specific to equine IgA. One (K129-2G5) was used to coat wells at 10µg/ml (100µl/well). IgA samples (100µl) were added and incubated at 37 ° C for 1 hour. After washing, the second biotinylated monoclonal antibody (K129-3E7) was used to detect IgA. K129-3E7 was biotinylated using a biotinylation kit (Amersham) according to the manufacturer's instructions. The biotinylated monoclonal antibody was detected using a streptavidin-HRP conjugate at 0.25µg/ml (Amersham). Monoclonal antibody and streptavidin-HRP concentrations were optimised such that none were limiting in the assay. Samples were analysed in triplicate. Monoclonal antibodies against horse IgA have been described (14, 21).

Analysis of IgA in immunized horses was performed at Centre for Preventive Medicine, Animal Health Trust, Newmarket, UK.

Serum samples were also taken from the immunized horses and analyzed for IgG as described above for convalescent and non-infected horses.

Determination of antibody titers in mouse with ELISA. Serum samples were taken from mice (NMRI), which had undergone experimental subsp. *equi* infection for two weeks. Control samples were taken before infection. The samples were analyzed in ELISA as described above for horses; detection of mice immunoglobulins was done

using HRP conjugated antibodies from rabbit (Dako) detecting all classes of immunoglobulins. The broncheolar lavage (BAL) procedure was performed as described in (22). IgA in BAL was determined in a similar way but using specific anti mouse IgA antibodies from goat conjugated with HRP (Sigma).

Experimental infection of mice with subsp. *equi*. The model described by Chanter was followed (2). The strain 1866 was first passaged through an animal by inoculating ca 10^6 CFU in each nostril of an anaesthetized mouse (NMRI), although the necessity to do this has not been assessed. Bacteria were recovered after 6 days from the submandibular glands and grown on BG plates at $37^{\circ}C$ in 10% CO_2. A single colony was grown in THB overnight at $37^{\circ}C$. The culture was kept at -80 $^{\circ}C$ in vials and a new vial was used for each experiment. To infect mice, bacteria were grown on BG plates at $37^{\circ}C$ in 10% CO_2 overnight, followed by inoculation into THB supplemented with 1% Yeast extract and grown without shaking over night. The cultures was then diluted 10 times into THB with 1% Yeast extract and 10% horse serum (Sigma) and grown for 4 hours at $37^{\circ}C$. The culture was centrifuged and resuspended in THB. To determine an optimal inoculation dose, 20 mice were divided into 4 groups which were given $5x10^7$, $1.3x10^7$, $3x10^6$ and $8x10^5$ CFU of strain 1866 in 10 µl in the nostrils, respectively. After 5 days, the mice were killed and presence of bacteria was determined in submandibular glands, trachea, kidneys, blood, and liver. Daily during the infection, and without killing the mice, growth was also determined quantitatively in nostrils by gently touching the nostrils to BG-plates. A dose containing $1x10^6$ CFU in 10µl was used for infections of mice. Bacterial growth was scored on a four-graded scale from 0 to +++ where 0 means no growth or

<8 colonies, 1 means 9 to ca. 100 colonies, 2 means > ca. 100, and 3 means confluent growth. The weight was determined every day and animals loosing >15% weight were killed, here defined as the clinical end point.However, in the experiment shown in Figure 5A and B, some animals lost more than 15% but were included.

Statistical methods. The serum dilutions required to achieve an absorbance value of A=1.0 were calculated in ELISA of sera from horses with or without strangles. The $\log_{10}$ of these dilutions were compared using non-paired students' t-test. For ELISA of sera from mice taken before and after experimental infection, a cut off value of A=0.5 was taken, due to lower absorbance values as compared with the horses, and the $\log_{10}$ of dilutions were calculated. In this case, paired t-test was used for comparison. For comparison of weight changes and nasal growth in mice, non-paired t-test was used. Fischer's exact test was used for comparison of proportions of mice that lost more than 15% weight or died.

RESULTS

Antibody responses against FNZ, SFS and EAG in horses with strangles. Sera were collected from 10 horses with a recent history of strangles and from 16 healthy horses without strangles. These sera were tested in an ELISA for IgG recognizing FNZ, SFS and EAG. For each sample, the dilution was determined which was required to give an absorbance value of 1.0, which is on the linear part of the titration curves (data not shown)., The log_{10} values of these dilutions are shown in Figure 2. It is clear that the sera from horses with strangles had elevated antibody levels to all three antigens compared to horses without strangles. The differences were significant with p-values for the two groups for FNZ, SFS, and EAG of <0.001, 0.02 and <0.0001, respectively. These findings indicate that all three antigens are expressed during natural infection with strangles and that they are able to elicit a serum antibody response.

Evaluation of experimental infection in mice with subsp. *equi.* Preliminary studies using different doses of bacteria revealed that 1×10^6 CFU per 10μl, administered intranasally was sufficient to infect 80-100% of mice. Clinical symptoms, bacterial growth in submandibular glands, trachea, kidneys and blood were followed and used as criteria for infection. It was also noted that loss of weight and growth of bacteria in the nostrils correlated perfectly ($p < 10^{-4}$) with the other signs of infection. Consequently, in the following experiments only those two latter parameters were followed as a correlate of infection.

A time study was performed by infecting 20 mice which were followed for 23 days. Eight animals that lost more than ca 15% weight were killed. In some animals, bacterial growth in the nostrils peaked between days 4 to 8. After 8 days bacterial growth in nostrils declined. In other animals, a high level of bacterial growth was evident from day 1. Weight loss was also highest on day 6-8 (mean value 12%). Some mice slowly regained weight after that time in an apparent spontaneous recovery. Three randomly chosen animals were analyzed for bacterial growth in lung, trachea, heart and brain. The median CFU values of subsp. *equi* per gram of tissue were 8.9×10^6, 3×10^5, 4.6×10^3 and 2.4×10^5, respectively.

Antibody response in mice infected with subsp. *equi*. Serum samples were taken before and 13 days after infection of 15 mice that had been experimentally infected with subsp. *equi* . The serum antibody responses to FNZ, SFS and EAG are shown in Figure 3. where the the $\log_{10}$ dilution values required to give an absorbance value of 0.5 are shown. Infection with subsp. *equi* led to highly significant ($p = <0.0001$) rises in antibody titers to all three antigens. Although, generally lower titers were obtained in mice than in horses, these findings indicate that FNZ, SFS and EAG are all expressed during experimental subsp. *equi* infection of mice.

Immunization of mice with FNZ, SFS and EAG. Seventeen mice were immunized i.n. on four occasions at one week intervals with a combination of FNZ, SFS and EAG, eleven with EtxB adjuvant and six without adjuvant. An analysis of the broncheiolar lavage taken after the last immunization revealed significant IgA levels to EAG in those animals immunized with the three antigens and the EtxB adjuvant (Fig 4A). By contrast, mice immunized with the three *S. equi* antigens in the absence

of EtxB gave a significantly lower IgA response (p=0.02) (Fig 4A). IgA levels against the other antigens was more variable and not significantly different with or without EtxB (data not shown). The total serum Ig and IgA responses to the three antigens following i.n. immunization are shown in Figs 4B and 4C. Although serum Ig responses to the three *S. equi* antigens tended to be slightly higher in animals immunized with the EtxB adjuvant, these differences were not statistically significant (Fig 4B). Likewise there was no apparent difference in serum IgA levels in mice given *S. equi* antigens with or without the adjuvant.

Protection against subsp. *equi* infection in vaccinated mice.

When mice (n=12) were immunized i.n, as above, with FNZ, SFS and EAG together with EtxB, and then challenged with subsp. *equi* one week after the last booster immunization, a highly significant difference in the course of the infection was observed compared with a control group (n =12) that received only EtxB. Figs. 5A and 5B show nasal growth and weight loss, respectively. Subsp. *equi* failed to colonize or grow to any significant levels in animals that had been immunized with *S. equi* antigens and EtxB, and there was virtually no weight loss in the animals over the 8 days following experimental infection. This contrasted with the control group that showed an increase in bacterial growth in the nose, which peaked on day 4, and a striking loss in weight. The difference in bacterial growth and weight loss between the immunized and control groups was highly significant; with p-values of <0.001 and <0.005 respectively, from day 4 and onwards. We therefore conclude that i.n. immunization of mice with FNZ, SFS, EAG and EtxB affords significant protection against nasal challenge with subsp. *equi*.

In addition to i.n. immunization, an alternative route of s.c. immunization was also evaluated. Mice (n=12) were immunized s.c. with FNZ, SFS, EAG and EtxB and then infected with subsp. *equi* one week later, as above. The control group (n=12) was given only EtxB. Figure 5 C shows that nasal growth was significantly different in vaccinated mice as compared with control mice. For example on days 2, 3, and 7 the p-values were 0.03, 0.02 and 0.01, respectively. Fig. 5 D shows that the weight loss in mice was higher in the non-vaccinated group, although this was not statistically significant. However, the number of animals that did not survive or lost more than 15% of their weight (which was the clinical end point in this experiment) was significantly higher in the control group (p<0.05 using Fischer's exact test). These findings demonstrate that s.c. immunization with *S. equi* antigens together with EtxB, affords protection against experimental challenge with *S. equi* A difference between the control groups in Figures 5 B and D can be seen; a faster progression of the infection in Figure 5 D is due to natural variability between challenge experiments. Therefore, one cannot unambiguously say that i.n. immunisation is better than s.c. immunisation after comparing Figures 5A/C and B/D.

Since strangles is a highly contagious disease, we also analyzed the rate of spread of the infection between animals. Two non-infected mice were introduced into one cage each with three infected mice. Importantly, no signs of infection in these newcomers were observed (data not shown) implying that the extent of infection in the mice used in the vaccination studies can be regarded as independent cases, with infection not being the result of a few animals contaminating the others.

To explore whether the combination vaccine comprising all three *S. equi* antigens afforded better protection than immunization with a single antigen (EAG) and whether or not inclusion of the EtxB adjuvant enhanced the protective efficacy of the vaccine, an additional vaccination experiment was carried out. Animals were immunized i.n. with FNZ, SFS and EAG either with EtxB (Group A; n =8) or without EtxB (Group B; n = 10), or with EAG together with EtxB (Group C; n = 10) or with EtxB alone (Group D control; n = 9). One week after the final booster immunization, animals were challenged by nasal inoculation with subsp. *equi* as above. Table 1 shows the weight loss and nasal growth of bacteria in each of groups A, B, and C on day 14 after challenge. Weight loss for Group D is not included since only two out of nine mice were left. Nasal growth in group D, as shown in Table 1, is calculated at the time of clinical end point; 15% weight loss or death.

By day seven after challenge, seven mice in the control group (D) had lost >15% of their body weight and were sacrificed. By contrast in the three immunized groups (A+B+C) only 9 of the 28 animals had died, (p=0.02, Fischer's exact test). Also nasal growth differs between the control group (D) and the vaccinated group (A) (p=0.004) thus confirming the protective effect of the immunizations.

At day 14 after challenge, the mean body weight of the vaccinated mice in group A had increased compared to their initial weight and the numbers of CFU of subsp. *equi* recovered from the nostrils were very low (Table 1). An analysis of whether or not inclusion of EtxB altered the level of protection in the two groups (A & B) revealed that protection on day 14, measured as nasal growth, was more prominent when EtxB was included in the vaccination (p<0.05). This is in line with the observation (Figure 4A) that including EtxB results in better mucosal IgA response against EAG.

The vaccination of mice with EAG as a single antigen and EtxB (Group C) was less effective at affording protection, than immunization with FNZ, SFS, EAG and EtxB (Group A) (Table 1), although not statistically significant, (p=0.08 for nasal growth). This implies that inclusion of several different antigens from *S. equi* in a strangles vaccine is likely to be beneficial.

Immune responses of horses. The promising findings on the induction of mucosal IgA antibodies to FNZ, SFS, and EAG, as well as the protective efficacy to challenge following immunization of mice with the three *S. equi* antigens and EtxB prompted us to test whether a similar regime of vaccination might enhance antigen-specific immune responses in horses. Twelve horses were used in the study and divided into four groups, A-D (n=4x3). A) both i.n. and s.c. with FNZ, SFS and EAG with EtxB; B) as group A but only i.n. immunization; C) both i.n. and s.c. with FNZ, SFS and EAG but omitting EtxB; D) both i.n. and s.c. with EtxB alone . Serum samples were taken before each immunization on days 0 and 56, and nasal washings were taken on day 0 and day 56. As can be seen in Fig. 6 only those horses immunized both i.n. and s.c. with the three *S. equi* antigens and EtxB (group A) exhibited high mucosal antigen-specific IgA responses against FNZ and EAG. For horses vaccinated i.n. only, whether immunized with or without EtxB, (groups B and C) the levels of mucosal IgA responses to FNZ and EAG were modest, and not significantly different from the control group. It was also found that the IgA responses to SFS were very low in all of the animals, irrespective of the route of administration or inclusion of EtxB (data not shown).

An analysis of the serum IgG levels revealed that the antigen specific responses to

FNZ and EAG were most pronounced in Groups A and C (Fig 7). This was expected

for Group A, since the horses were immunized both i.n. and s.c.; but the high titers in

Group C indicate that i.n. vaccination alone is sufficient to trigger seroconversion in

horses. As with IgA, it was also found that the serum IgG responses to SFS were very

low in all of the animals, irrespective of the route of administration or inclusion of

EtxB (data not shown).

DISCUSSION

Horses that have undergone infection with subsp. *equi* (strangles) do not acquire strangles soon afterwards. This suggests that strangles triggers an immune response that affords protection. The nature of such protection is however not elucidated but is generally thought to involve induction of neutralizing antibodies.

Apparently the cell bound antigen SeM, in spite of high serum and mucosal antibody titers following various administration routes, does not afford protection against challenge with subsp. *equi* (16, 20). Vaccination with live attenuated strains of subsp. *equi* may induce protection against infection with subsp. *equi*. Since 1998, Pinnacle, a live mutant attenuated non-encapsulated subsp. *equi* strain administered intranasally has been widely used in North America as a strangles vaccine, however not without complications. It causes abscesses and other adverse effects probably due to revertant mutations (24). Recently a non-encapsulated deletion mutant of the Pinnacle strain lacking two of the genes encoding hyaluronate synthase was constructed. However, this strain has not yet been reported as a strangles vaccine (24). Another attenuated deletion mutant of subsp. *equi* was recently used as a vaccine in challenge experiments (5). This strain was reported to protect horses against challenge with a heterologous subsp. *equi* strain. However, various adverse effects in the form of local reactions were observed. Thus, live attenuated strains, to date, seem to be inadequate for the use as vaccine. It would therefore be of particular interest to further study the antibody response after vaccination with recombinant sub-unit vaccines, since such vaccines may elicit a protective effect and minimal adverse effects.

Horses with a recent history of subs. *equi* infection had significantly increased levels of antibodies against the three antigens used here. Little is known about the exact role of FNZ, SFS and EAG during infection, but it can be assumed that they influence the pathogenicity of *S. equi*. The raise in antibody titers against the three antigens after both natural infection in horses and after induced infection in mice demonstrates that the genes encoding these proteins are expressed during infection. Thus antibodies against these proteins may neutralize their function.

The individual variation in antibody levels between the horses was large. Some horses without a known history of strangles had antibody titers near the level of convalescent horses. This may be due to cross-reactivity between antigens from subsp. *equi* and subsp. *zooepidemicus*, of which the latter commonly colonizes horses. It is also possible that some of the investigated horses have had a previous un-diagnosed subclinical infection with subsp. *equi*.

The infection model mimicking strangles in mouse, used in this study, has been described earlier (2). We have here confirmed these findings and observations. In horses, systemic infection is observed in about 5-10 % of cases of strangles, whereas in the mouse this seems to be much more common. The mucosal route of infection and the ability of the bacteria to disseminate from the upper respiratory tract in mice resembles the events during a clinical case of equine strangles. We therefore conclude that this murine model of stangles is the best model at hand for testing of vaccine components. As with most experimental infection models in animals, the individual response to bacterial challenge is varying. Likewise, the average severity of infection

was found to vary between experiments. Systemic infection correlated very well with weight loss, which was an easy method for evaluation of infection and also for recovery. A systemic infection leading to a weight loss exceeding ca 15% was found eventually to be fatal, and such animals were killed for ethical reasons.

Because of the antibody response observed against FNZ, SFS and EAG after infection, we decided to investigate the protective effect of all antigens in combination in vaccination trials. A significant protection against subsp. *equi* infection was found upon vaccination. A s.c. immunization route led to less nasal colonization and fewer animals loosing more than 15% in weight. After nasal vaccination, the protective effect appeared more pronounced although comparison between experiments may be uncertain.

An IgA response was found after nasal vaccination, particularly against SFS, which seemed to be the most immunogenic of the three antigens in mice. A nasal immunization giving a better IgA response is presumably important to prevent early establishment of infection in the nasal mucosa. Inclusion of EtxB resulted in better protection (Table 1), and also higher mucosal IgA levels (Figure 4A). Dissemination of bacteria from this site via the blood stream to peripheral sites is prevented by circulating IgG. Therefore, it is likely that both IgA and IgG are required for an effective protective effect.

It has not been the main focus in these studies to pinpoint which is the best of the three antigens. However, the results imply a synergistic effect, since a better protection was obtained with all three antigens than with EAG alone.

When horses were vaccinated a poor response against SFS was obtained, contrary to the mice (Figures 4B and C). From the data obtained here, it seems as if i.n. immunization is more important for a good response in mice than in horses. The combination of s,c. and i.n. immunization in the horse gave far better response than i.n. alone. It was also seen that addition of EtxB increased the IgA antibody titer in the nasal mucosa (Figure 6). The difference in immunological behavior between the mouse and the horse, strongly implies that route of immunization and choice of adjuvant should be best assessed in the target animal. The mouse model, however, serves well to select target antigens for a vaccine.

In conclusion, we found that vaccination with FNZ, SFS and EAG together gives an antibody response, which is highly protective in the mouse.. When administered both intranasally and subcutaneously in horses significant mucosal IgA and serum IgG antibody responses against FNZ and EAG were obtained. The antibody titers tended to be higher when EtxB was used as an adjuvant. These antigens had no adverse effects on horses and neither had the adjuvant, EtxB. Thus, these antigens are promising candidates for an effective and safe vaccine against strangles.

ACKNOWLEDGEMENTS

Figure legends

Figure 1

Figure. 1. Schematic presentation of the three *S. equi* proteins EAG, SFS and FNZ. Abbreviations, (S) the signal sequence, (W) the cell wall associated domain, (M) the membrane-spanning region. For protein EAG the albumin-binding region (Alb) are indicated. For protein FNZ and SFS different repetitive regions are indicated by (R). Arrows indicate the part of the respective protein that was used for antigen preparation. The deduced molecular mass for proteins EAG4B, SFSC1 and FNZN are indicated.

Figure 2

Antibody titers in sera from horses. The $\log_{10}$ dilution of sera required to give an absorbance at a cut off value of 1.0 was calculated for each individual serum sample. Mean values with standard errors are shown. P-values for comparing normal (n=16) vs. strangles sera (n=10) against FNZ, SFS and EAG are <0.001, 0.02 and <0.0001, respectively.

Figure 3

Antibody titers in sera from mice The $\log_{10}$ dilution of sera required to give an absorbance at a cut off value of 0.5 was calculated for each individual serum sample. Mean values with standard errors are shown. Samples taken before challenge, which at lowest dilution (20x), gave an absorbance <0.5 were assigned a value of 1.30. P-values for comparing sera taken before challenge and during infection against all three antigens are <10^{-4}.

Figure 4

Antibodies in immunized mice. Seventeen mice were immunized intra nasally with FNZ, SFS and EAG; eleven with EtxB six without EtxB. Panel A shows mean values and SE of IgA levels against EAG in bronchiolar lavage (p=0.02). Panel B shows the mean values and SE of serum dilutions giving an absorbance of 1.0 for the three antigens in ELISA detecting all classes of antibodies (n=4 for animals where EtxB was included and n=3 for animals without EtxB). Panel C shows IgA levels in sera (same animals as in 4B) at 40x dilution; symbols: white: preimmune; gray: after immunization.

Figure 5

Protection against infection by subsp. *equi* Mice (n=12) were immunized with FNZ, SFS and EAG with EtxB (filled symbols) and control groups (n=12) were given only EtxB (open symbols). Mean values with standard errors are shown.

Panels A and B show results after intranasal (i.n.) route of immunization; C and D after subcutaneous (s.c.) immunization.

Panels A and C show growth of subsp. *equi* in noses. The nasal growth of subsp. *equi* was determined by placing the noses against BG plates and the bacteria were streaked out to single colonies. The number of bacteria were given a value from 0 to 3 where 0 means no growth or <8 colonies, 1 means 9 to ca. 100 colonies, 2 means > ca. 100, and 3 means confluent growth.

Panels B and D show the daily percentage weight loss. Significance values are given in the text.

Figure 6

IgA antibodies in nasal washings of immunized horses. Mean absorbance values (n=3) in ELISA are shown from groups A-D. The horses were divided into four groups; A) antigens + EtxB given both s.c. and i.n.; B) as group A but immunization only i.n.; C) as in group A but omitting EtxB; D) control group given only EtxB both i.n. and s.c. Light gray bars: samples from day 0 and dark gray bars from day 56.

Figure 7

IgG antibodies in sera of immunized horses. The log dilution of sera required to give an absorbance at a cut off value of 1.0 was calculated for each individual serum sample. Mean values (n=3) with standard errors are shown. Samples taken before (day 0) and after (day 56) immunizations are shown. The horses, the same as in Figure 6, were divided into four groups A) (white bars): antigens + EtxB given both

s.c. and i.n.; B) (striped bars): as group A but immunization only i.n.; C) (gray bars): As in group A but omitting EtxB; D) (black bars): control group given only EtxB both i.n. and s.c.

Table 1

		Weight change[a]		Nasal growth[b]		Number of mice loosing >15% on day seven	
Group (n)	Vaccinated with	Mean	SE	Mean	SE		
A (8)	FNZ,SFS,EAG+ +EtxB	0,7	1,9	0,83	0,17	2	
B (10)	FNZ,SFS,EAG	-6,8	6,8	1,5	0,23	3	
C (10)	EAG+EtxB	-8,11	5,24	1,44	0,26	4	
D (9)	EtxB	-	-	1.78[c]	0.22	7	

[a] Weight change on day 14 in per cent of initial weight.

[b] Growth on a scale from 0 to 3+ on day 14.

[c] Nasal growth at death or at 15% weight loss.

REFERENCES

1. Chanter, N. 2002. Bacterial infections including mycoplasmas. *In* P. Lekeux (ed.), Equine Respiratory Diseases. International Veterinary Informations Services, Ithaca, NY.

2. Chanter, N., K. C. Smith, and J. A. Mumford. 1995. Equine strangles modelled in mice. Vet. Microbiol. 43:209-218.

3. Hamlen, H. J., J. F. Timoney, and R. J. Bell. 1994. Epidemiologic and immunologic characteristics of Streptococcus equi infection in foals. JAVMA 204:768-775.

4. Harrington, D. J., I. C. Sutcliffe, and N. Chanter. 2002. The molecular basis of *Streptococcus equi* infection and disease. Microbes Infect. 4:501-510.

5. Jacobs, A. A., D. Goovaerts, P. J. Nuijten, R. P. Theelen, O. M. Hartford, and T. J. Foster. 2000. Investigations towards an efficacious and safe strangles vaccine: submucosal vaccination with a live attenuated Streptococcus equi. Vet Rec 147(20):563-7.

6. Jacobsson, K., H. Jonsson, H. Lindmark, B. Guss, M. Lindberg, and L. Frykberg. 1997. Shot-gun phage display mapping of two streptococcal cell-surface proteins. Microbiol. Res. 152:1-8.

7. Jonsson, H., H. Lindmark, and B. Guss. 1995. A protein G-related cell surface protein in Streptococcus zooepidemicus. Infect Immun 63(8):2968-75.

8. Jorm, L. R. 1990. Strangles in horse studs: incidence, risk factors and effect of vaccination. Aust Vet J 67(12):436-9.

9. Kihlberg, B.-M., M. Collin, A. Olsén, and L. Björck. 1999. Protein H, an antiphagocytic surface protein in *Streptococcus pyogenes*. Infect. Immun. 67:1708-1714.

10. Lindmark, H., and B. Guss. 1999. SFS, a novel fibronectin-binding protein from Streptococcus equi, inhibits the binding between fibronectin and collagen. Infect Immun 67(5):2383-8.

11. Lindmark, H., K. Jacobsson, L. Frykberg, and B. Guss. 1996. Fibronectin-binding protein of Streptococcus equi subsp. zooepidemicus. Infect Immun 64(10):3993-9.

12. Lindmark, H., H. Jonsson, E. Olsson Engvall, and B. Guss. 1999. Pulsed-field gel electrophoresis and distribution of the genes zag and fnz in isolates of *Streptococcus equi*. Research in Veterinary Science 66:93-99.

13. Lindmark, H., M. Nilsson, and B. Guss. 2001. Comparison of the fibronectin-binding protein FNE from Streptococcus equi subspecies equi with FNZ from S. equi subspecies zooepidemicus reveals a major and conserved difference. Infect Immun 69(5):3159-63.

14. Lunn, D. P., M. A. Holmes, D. F. Antczak, N. Agerwal, J. Baker, S. Bwendali-Ahcene, M. Blanchard-Chanelle, K. M. Byrne, K. Cannizz, W. Davis, M. J. Hamilton, D. Hannan, T. Kondo, J. H. Kydd, M. C. Monier, P. F. Moore, P. F. O'Neil, B. R. Schram, A. S. Sheoran, J. L. Stotte, T. Sugiura, and K. E. Vagnonia. 1998. Report of the Second Equine Leucocyte Antigen Workshop, Squaw Valley, California, July 1995. Vet. Immunol. Immunopath. 62:101-143.

15. Molinari, G., M. Rhode, C. A. Guzman, and G. S. Chhatwal. 2000. Two distinct pathways for the invasion of *Streptococcus pyogenes* in non-phagocytic cells. Cell Microbiol. 2:145-154.

16. Nally, J. E., S. Artiushin, A. S. Sheoran, P. J. Burns, B. Simon, R. M. Gilley, J. Gibson, S. Sullivan, and J. F. Timoney. 2001. Induction of mucosal and systemic antibody specific for SeMF3 of Streptococcus equi by intranasal vaccination using a sucrose acetate isobutyrate based delivery system. Vaccine 19(4-5):492-7.

17. Newton, J. R., N. Dunn, M. N. de Brauwere, and N. Chanter. 1997. Naturally occurring persistent and asymptomatic infection of the guttoral pouches of horses with Streptococcus equi,. Vet. Rec. 140:84-90.

18. Richards, C. M., A. T. Aman, T. R. Hirst, T. J. Hill, and N. A. Williams. 2001. Protective mucosal immunity to ocular herpes simplex virus type 1 infection in mice by using Escherichia coli heat-labile enterotoxin B subunit as an adjuvant. J. Virol. 75:1664-71.

19. Schalen, C., L. Truedsson, K. K. Christensen, and P. Christensen. 1985. Blocking of antibody complement-dependent effector functions by streptococcal IgG Fc-receptor and staphylococcal protein A. Acta Pathol Microbiol Immunol Scand 93:395-400.

20. Sheoran, A. S., S. Artiushin, and J. F. Timoney. 2002. Nasal mucosal immunogenicity for the horse of a SeM peptide of Streptococcus equi genetically coupled to cholera toxin. Vaccine 20(11-12):1653-9.

21. Sheoran, A. S., B. T. Sponseller, M. A. Holmes, and J. F. Timoney. 1997. Serum and mucosal antibody isotype responses to M-like protein (SeM) of Streptococcus equi in convalescent and vaccinated horses. Vet Immunol Immunopathol 59(3-4):239-51.

22. Takao, S.-I., K. Kiyotani, T. Sakaguchi, Y. Fujii, M. Seno, and T. Yoshida. 1997. Protection of mice from respiratory sendai virus infections by recombinant vaccinia virus. J Virol. 71:823-38.

23. Timoney, J. F., and D. Eggers. 1985. Serum bactericidal responses to Streptococcus equi of horses following infection or vaccination. Equine Vet J 17(4):306-10.

24. Walker, J. A., and J. F. Timoney. 2002. Construction of a stable non-mucoid deletion mutant of the Streptococcus equi Pinnacle vaccine strain. Vet Microbiol 89(4):311-21.

25. Wood, J. L., N. Dunn, N. Chanter, and M. N. de Brauwere. 1993. Persistent infection with Streptococcus equi and the epidemiology of strangle. Vet. Rec 133:375-375.

Protein EAG

S			Alb			W	M

→ Protein EAG4B 19 kDa

Protein SFS

S		R1	R2	

→ Protein SFSC1 14 kDa

Protein FNZ

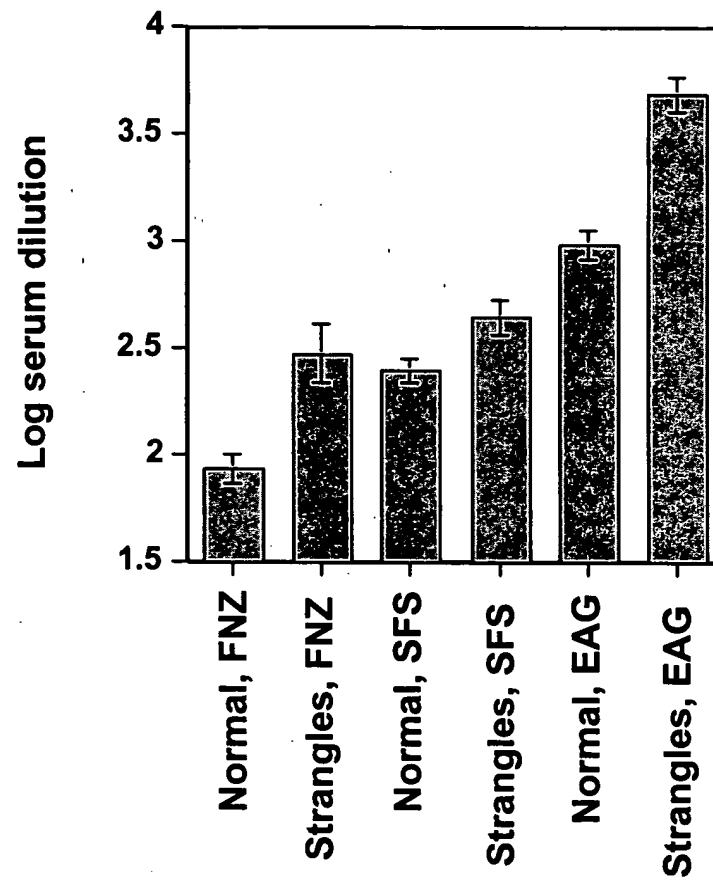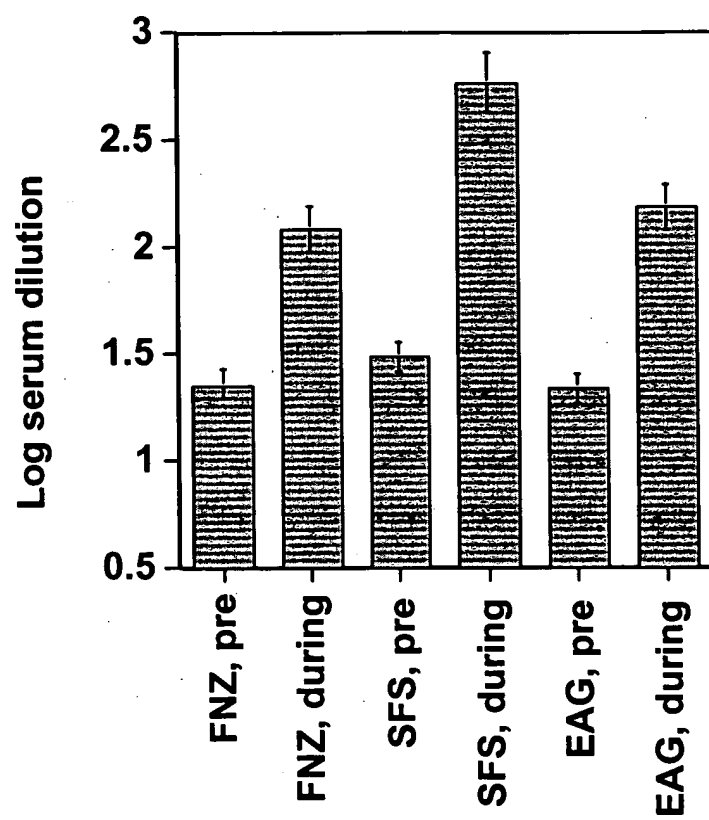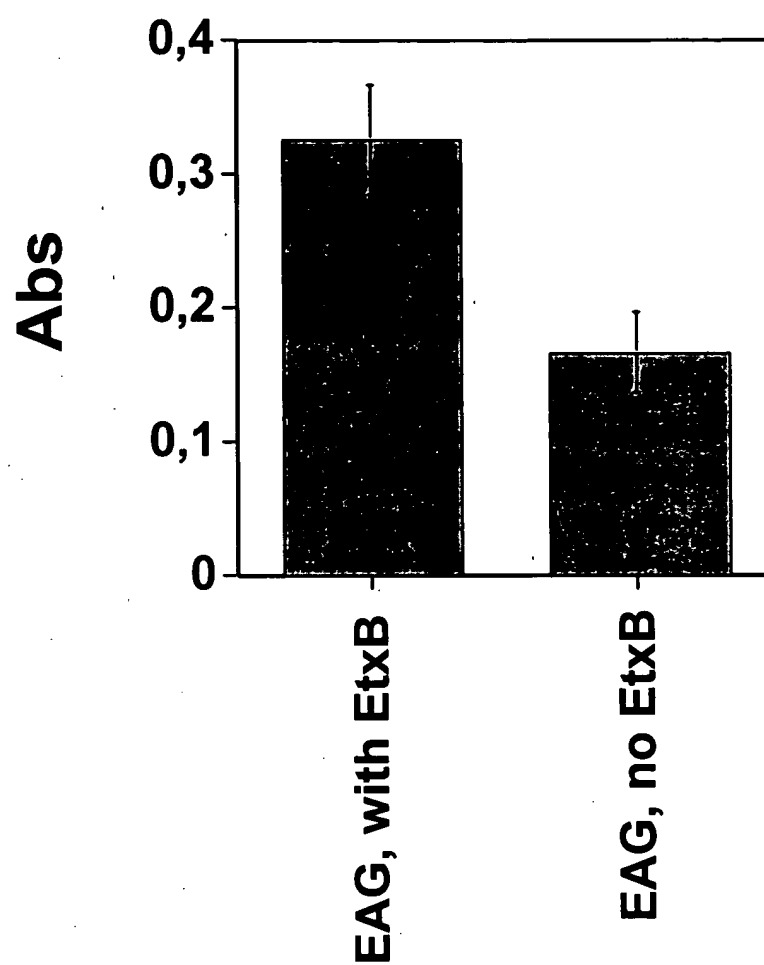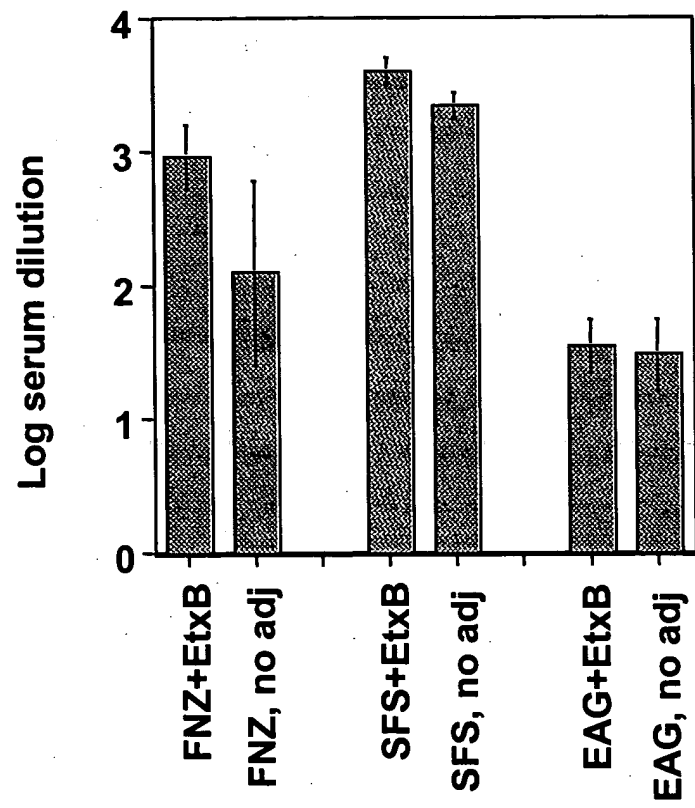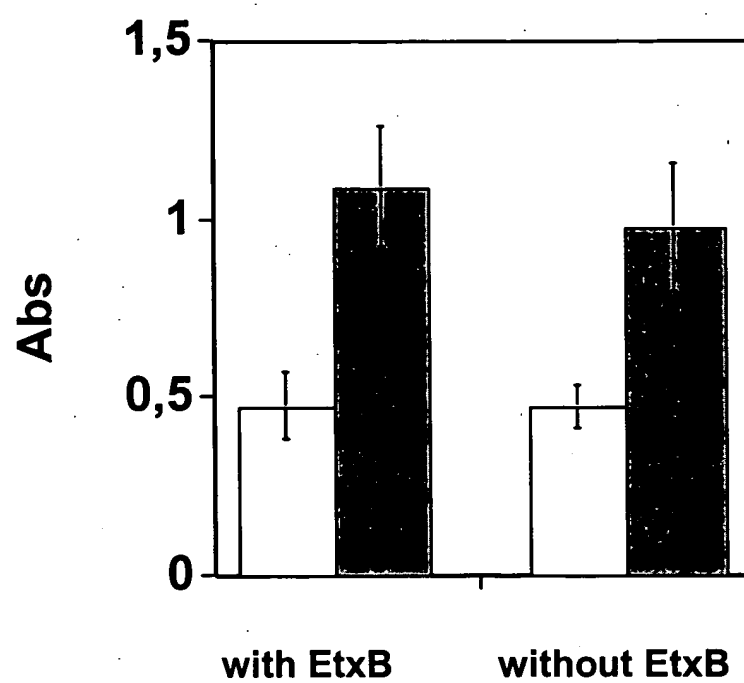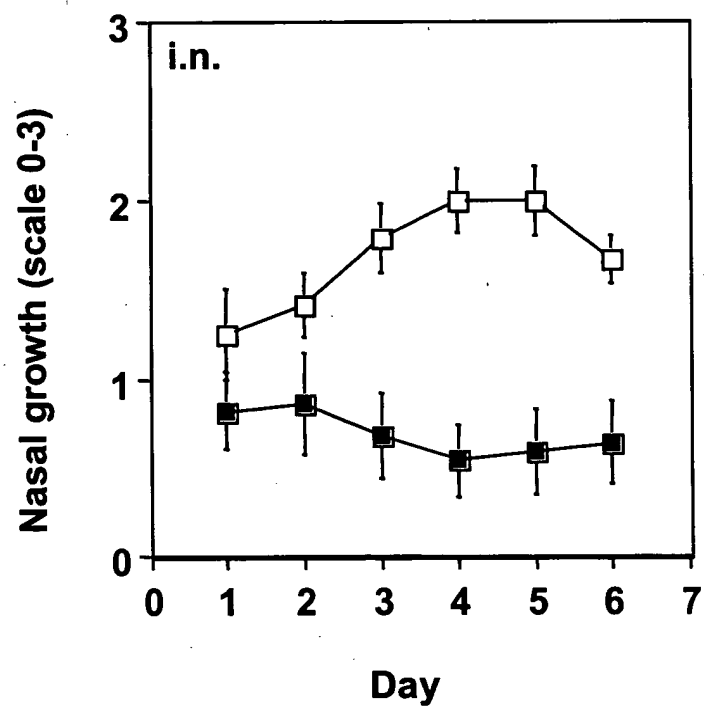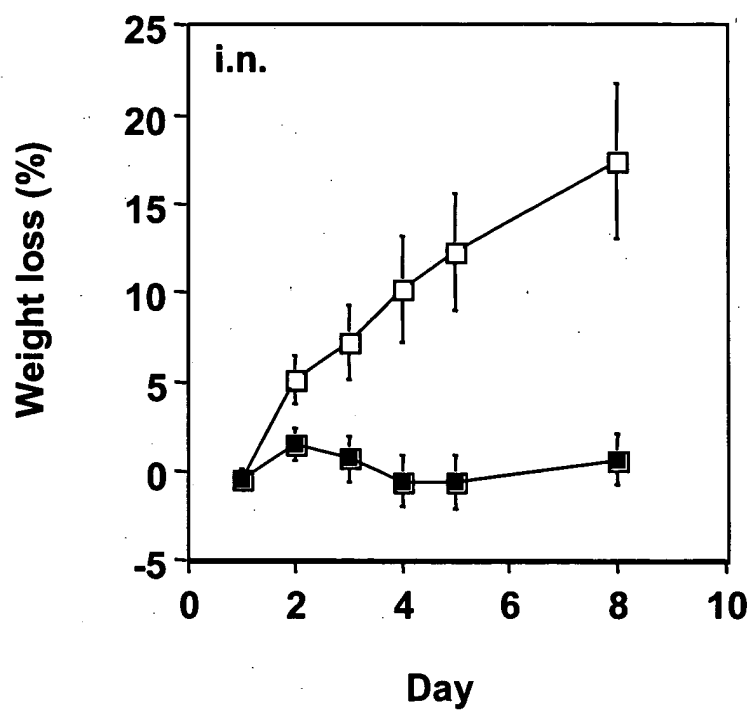| S			R1	R2	R3	R4	R5	W	M

→ Protein FNZN 34 kDa

Figure 2

Figure 3

Fig 4A

Figure 4B

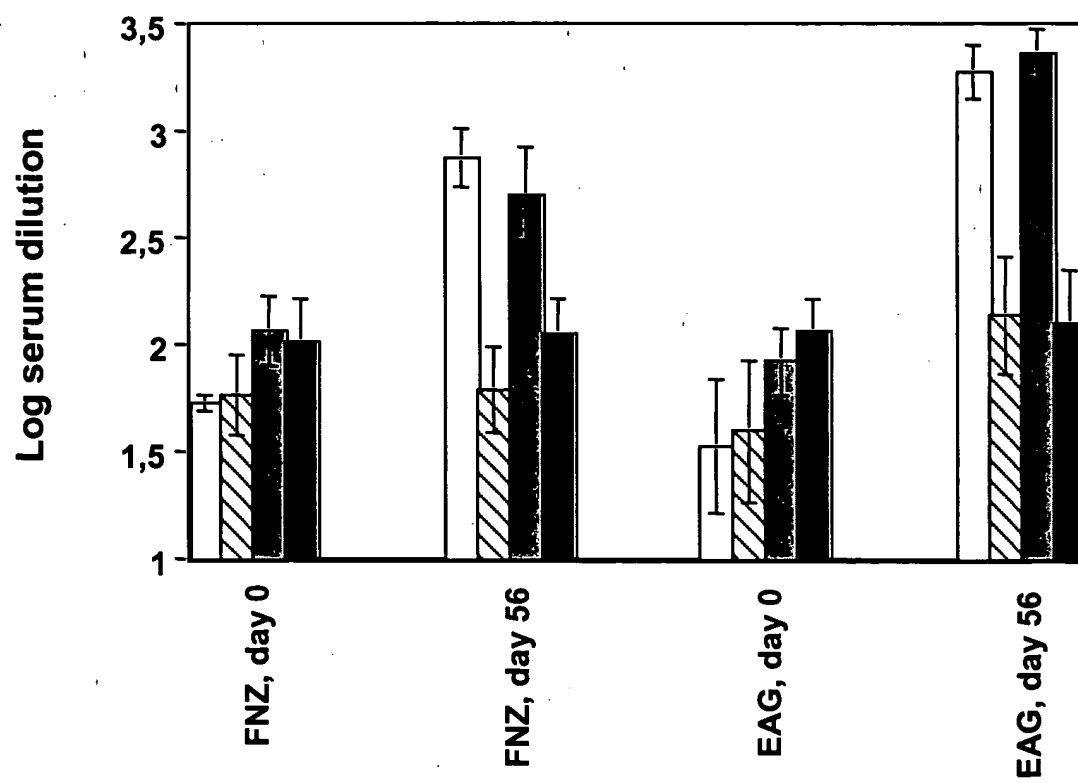Figure 4C

Figure 5A

Figure 5B

Figure 5C

Figure 5D

Figure 6

Figure 7

Enhanced Delivery of Exogenous Peptides into the Class I Antigen Processing and Presentation Pathway

Lolke de Haan,[1] Arron R. Hearn,[2] A. Jennifer Rivett,[2] and Timothy R. Hirst[1]*

Departments of Pathology & Microbiology[1] and Biochemistry,[2] School of Medical Sciences, University of Bristol,
Bristol BS8 1TD, United Kingdom

Current immunization strategies, using peptide or protein antigens, generally fail to elicit cytotoxic-T-lymphocyte responses, since these antigens are unable to access intracellular compartments where loading of major histocompatibility complex class I (MHC-I) molecules occurs. In an attempt to circumvent this, we investigated whether the GM1 receptor-binding B subunit of Escherichia coli heat-labile toxin (EtxB) could be used to deliver class I epitopes. When a class I epitope was conjugated to EtxB, it was delivered into the MHC-I presentation pathway in a GM1-binding-dependent fashion and resulted in the appearance of MHC-I–epitope complexes at the cell surface. Importantly, we show that the efficiency of EtxB-mediated epitope delivery could be strikingly enhanced by incorporating, adjacent to the class I epitope, a 10-amino-acid segment from the C terminus of the DNA polymerase (Pol) of herpes simplex virus. The replacement of this 10-amino-acid segment by a heterologous sequence or the introduction of specific amino acid substitutions within this segment either abolished or markedly reduced the efficiency of class I epitope delivery. If the epitope was extended at its C terminus, EtxB-mediated delivery into the class I presentation pathway was found to be completely dependent on proteasome activity. Thus, by combining the GM1-targeting function of EtxB with the 10-amino-acid Pol segment, highly efficient delivery of exogenous epitopes into the endogenous pathway of class I antigen processing and presentation can be achieved.

Cytotoxic CD8^{+} T lymphocytes (CTLs) represent an important component of the protective and therapeutic immune response to intracellular bacteria, viruses, and tumors via their capacity to recognize foreign peptides that have bound to major histocompatibility complex class I (MHC-I) molecules (17, 32). The majority of the peptides presented are derived from endogenously synthesized proteins that are cleaved into small peptide fragments by the proteasome (reviewed in references 25 and 33). These are subsequently transported via the transporter of antigenic peptides into the lumen of the endoplasmic reticulum (ER), where they bind to newly synthesized MHC-I molecules. Such MHC-I peptide complexes are trafficked to the cell surface, whereupon they are recognized by T-cell receptors present on CTL precursors. This leads to CTL activation and subsequent CTL-mediated lysis of peptide-presenting cells.

Given the importance of CTLs in clearing the host of infected cells, there is great interest in the development of new vaccination strategies that are capable of inducing effective CTL responses. However, for vaccines composed of soluble protein antigens, immunization usually results in antigen uptake into an exogenous processing pathway that leads to peptide fragments being loaded onto MHC-II rather than MHC-I molecules (11, 23). Thus, in order for soluble antigens to induce MHC-I-restricted CTL responses, antigens need to access intracellular compartments where they can enter the endogenous class I processing and presentation pathway.

Bacterial protein toxins are molecules that combine unique cell-binding properties with efficient cytosolic delivery properties (5). They would therefore appear to be ideally suited for the delivery of antigenic proteins and peptides in the class I presentation pathway, provided that detoxification without apparent loss of delivery capability can be achieved. Indeed, toxoid derivatives of the adenylate cyclase toxin of Bordetella pertussis (30), pertussis toxin (6), anthrax toxin (2, 10), and Shiga toxin B subunit (13) have been investigated as potential vehicles for delivery of peptides or proteins into the class I presentation pathway. The capacities of the nontoxic GM1-binding B subunits of Escherichia coli heat-labile toxin (EtxB) or cholera toxin (CtxB) to deliver antigens into the class I pathway have thus far not been investigated. However, researchers have recently shown that EtxB is capable of delivering peptides into specific intracellular compartments (18). In particular, when a 27-mer peptide derived from the C terminus of the DNA polymerase (Pol) of herpes simplex virus type 1 (HSV-1) was genetically fused to the C terminus of EtxB, it was found that the fusion protein entered cells and that the peptide was liberated from EtxB and translocated into the nuclear compartment. While structural features present in the Pol peptide were speculated to be involved in facilitating both its liberation from EtxB and its translocation from endosomal compartments, their contribution to peptide delivery remained undefined. Here, we have investigated (i) whether EtxB can be used as a vehicle for the delivery of exogenous peptides into the class I presentation pathway, (ii) whether EtxB-mediated peptide delivery is dependent on its capacity to bind to GM1 receptors, and (iii) whether incorporation of elements of the Pol peptide adjacent to the class I epitope would improve the efficiency of peptide delivery.

---

* Corresponding author. Mailing address: Department of Pathology & Microbiology, University of Bristol, School of Medical Sciences, University Walk, Bristol BS8 1TD, United Kingdom. Phone: 44-117-9287538. Fax: 44-117-9300543. E-mail: t.r.hirst@bristol.ac.uk.

TABLE 1. Peptides used in this study

Peptide	Sequence	Mass (Da)
8-mer	SIINFEKL	945
9-mer	CSIINFEKL	1,048
16-mer	CEKLAGFGSIINFEKL	1,751
19-mer	CAVGAGATAEESIINFEKL	1,905
19-mer^{OVA}	CDEVSGLEQLESIINFEKL	2,198
26-mer	CEKLAGFGAVGAGATAEESIINFEKL	2,608
26-mer$^{EE \rightarrow QQ}$	CEKLAGFGAVGAGATAQQSIINFEKL	2,606
26-mer$^{V \rightarrow R}$	CEKLAGFGARGAGATAEESIINFEKL	2,665
31-mer	CEKLAGFGAVGAGATAEESIINFEKLTEWTS	3,212
9-mer^{NP}	ASNENMETM	1,008
10-mer^{NP}	CASNENMETM	1,111
20-mer^{NP}	CAVGAGATAEEASNENMETM	1,968

MATERIALS AND METHODS

Production and characterization of EtxB and EtxB conjugates. Recombinant EtxB was expressed in a nontoxigenic marine vibrio, *Vibrio* sp. strain 60, and purified using hydrophobic interaction and ion-exchange chromatography as reported earlier (1). A non-GM1-binding mutant of EtxB, EtxB(G33D), has been described previously (21) and was expressed and purified as described above. Purified preparations of EtxB and EtxB(G33D) were depleted of lipopolysaccharide using Detoxi-Gel columns (Pierce, Rockford, Ill.) and contained ≤50 endotoxin units per mg of protein, as determined in a *Limulus* amoebocyte lysate assay (BioWhittaker, Walkersville, Md.). Peptides were synthesized by solid-phase synthesis at the peptide synthesis unit of the Department of Biochemistry, University of Bristol, Bristol, United Kingdom, by G. Bloomberg. The peptides were purified by reverse-phase high-performance liquid chromatography, and their molecular masses were confirmed by mass spectrometry. The peptides synthesized contained well-characterized H-2^b-restricted MHC-I epitopes from either chicken egg ovalbumin (OVA), SIINFEKL (28), or influenza nucleoprotein (NP), ASNENMETM (27). The amino acid sequences and molecular weights of the peptides (in daltons) used in this study are listed in Table 1. For conjugation of peptides to EtxB, the chemical bifunctional crosslinker N-(gamma-maleimido-butyryl-oxy) succinimide (GMBS) (Pierce) was used. EtxB was first reacted with GMBS in a 1:4 molar ratio for 1 h at room temperature. Subsequently, excess GMBS was removed by gel filtration on a Sephadex G-25 column (Pharmacia, Uppsala, Sweden). Fractions containing EtxB-GMBS were pooled and reacted with peptide at a 1:2 molar ratio for 2 h at room temperature. Each peptide contained an N-terminal cysteine to allow direct reaction with the maleimide group in the GMBS molecule. After the conjugation reaction, unreacted GMBS groups were quenched by the addition of 2-mercaptoethanol (Sigma, Poole, United Kingdom) to a final concentration of 50 mM and incubation at room temperature for 30 min. Finally, EtxB conjugates were separated from excess peptide on a Sephadex G-50 column (Pharmacia). With all peptides, an EtxB pentamer/peptide ratio of approximately 1:5 was achieved, as determined by gel filtration on a Superdex 200 column connected to a SMART system (both from Pharmacia), using molecular weight standards. EtxB(G33D) peptide conjugates were generated under exactly the same conditions described above, and similar EtxB(G33D) pentamer/peptide ratios were obtained. Conjugates were analyzed either boiled or unboiled on sodium dodecyl sulfate (SDS)-polyacrylamide gels followed by staining with Coomassie brilliant blue R-250. The reactivity of conjugates with an EtxB pentamer-specific monoclonal antibody (MAb) (118-8; kindly provided by E. Lundgren and H. Persson, Department of Molecular Cell Biology, University of Umea, Sweden) was examined by Western blotting, and the GM1-binding properties of EtxB and of EtxB and EtxB(G33D) conjugates were assessed in a GM1 sandwich enzyme-linked immunosorbent assay (ELISA) essentially as previously described (1). The reactivity of conjugated peptides containing the SIINFEKL motif was assessed in a similar fashion using a SIINFEKL-specific polyclonal antiserum (a gift from Y. Reiss, Department of Biochemistry, Tel Aviv University, Tel Aviv, Israel).

Cell lines and culture conditions. JAWSII, an immortalized C57BL/6 bone marrow-derived dendritic cell line, was purchased from the American Type Culture Collection (Manassas, Va.) and cultured in RP10 medium (RPMI 1640 containing Glutamax-1, 100 μg of penicillin-streptomycin/ml, and 10% fetal bovine serum [FBS] [all from GIBCO BRL, Paisley, United Kingdom]) supplemented with 2 ng of recombinant mouse granulocyte-macrophage colony-stim-

ulating factor (Sigma)/ml at 37°C in a humidified CO_2 incubator. The T-cell hybridomas RF33.70 and RF36.84 (24, 26), recognizing the OVA-derived SIINFEKL peptide or the NP-derived ASNENMETM peptide in the context of H-2^b, were a kind gift from K. L. Rock (University of Massachusetts Medical Center) and were cultured as described above in RP10 medium containing 20 mM HEPES, 1 mM nonessential amino acids, 25 μM indomethacin, 0.25 μg of amphotericin B (fungizone-1)/ml (all from GIBCO), and 50 μM 2-mercaptoethanol.

Antigen presentation assays. Peptide presentation in MHC-I was examined by monitoring interleukin-2 (IL-2) release by the RF33.70 or RF36.84 T-cell hybridoma (24, 26). JAWSII dendritic cells were seeded in 96-well plates at 2 × 10^5/ml and cultured overnight. The cells were then incubated with duplicate test samples at various concentrations and for various time intervals. In all experiments, equivalent amounts of either free or conjugated peptide were used. After incubation with antigen, the cells were fixed with 1% (wt/vol) paraformaldehyde in phosphate-buffered saline (PBS) for 10 min at room temperature, washed five times with medium, and incubated overnight with RF33.70 or RF36.84 T-cell hybridomas (5 × 10^5 cells/ml). Treatment of JAWSII cells with free 8-mer SIINFEKL or 9-mer^{NP} ASNENMETM peptide was used as a positive control, while PBS was used as a negative control. After overnight incubation, presentation-induced IL-2 secretion was determined using a commercially available IL-2 ELISA kit (Pharmingen, San Diego, Calif.). IL-2 levels are given as mean units per milliliter ± standard error of the mean (SEM). The data presented are representative of at least three independent experiments.

An alternative fluorescence-activated cell sorter (FACS)-based method for direct assessment of antigen presentation by JAWSII cells, involving the use of the 25D1.16 MAb directed against the MHC-I–SIINFEKL complex (22) (kindly donated by C. Reis e Sousa, Imperial Cancer Research Fund, London, United Kingdom, and R. N. Germain, National Institute of Allergy and Infectious Disease, National Institutes of Health, Bethesda, Md.) was also used to assess EtxB-mediated class I presentation. In brief, 2 × 10^6 to 4 × 10^6 JAWSII cells were treated with antigen at the equivalent concentration of 100 nM peptide for 2 h in a 25-cm^2 tissue culture flask. The cells were then trypsinized, centrifuged (5 min; 145 × g), washed with PBS-FBS-azide (PBS containing 5% FBS and 0.02% sodium azide), and incubated with 25D1.16 MAb (1:200; 30 min; 4°C). Subsequently, the cells were washed with PBS-azide and incubated with a fluorescein isothiocyanate (FITC)-labeled goat antibody specific for mouse immunoglobulin G (DAKO, Ely, United Kingdom) (1:500; 30 min; 4°C). Finally, the cells were washed with FACS flow (Becton Dickinson, San Jose, Calif.) and analyzed by flow cytometry (FACScan; Becton Dickinson). SIINFEKL peptide-treated and untreated cells were used as controls.

The inhibitory effects of bafilomycin A1 (BafA1), brefeldin A (BFA) (both from Sigma), and epoxomicin (Calbiochem, Nottingham, United Kingdom) on EtxB-mediated epitope delivery were also studied. In such experiments, JAWSII cells were pretreated with inhibitors for 1 h at various concentrations and subsequently incubated with EtxB conjugates or EtxB and peptide alone or admixed for 2 h and processed as described above.

Confocal microscopy. For microscopic analysis, JAWSII cells were first grown on sterile coverslips coated with rat collagen type II (Sigma) for 48 h. Subsequently, the cells were treated for various periods of time with EtxB conjugates, fixed with 4% (vol/vol) paraformaldehyde in PBS for 10 min, and then permeabilized by incubation in 4% paraformaldehyde containing 0.5% Triton X-100 (Sigma) for 15 min. After repeated washing with PBS, the cells were incubated

with either MAb 25D1.16, specific for the MHC-I–SIINFEKL complex (1:200), or an EtxB-specific polyclonal rabbit antiserum (1:500) (kindly provided by M. Pizza, IRIS, Siena, Italy) diluted in PBS-bovine serum albumin (PBS containing 3% bovine serum albumin [fraction V; Sigma]) for 1 h at room temperature. The cells were then washed with PBS and incubated with FITC- or tetramethyl rhodamine isothiocyanate-labeled secondary antibodies directed against either mouse or rabbit immunoglobulin G (1:100) (Jackson Immuno Research Laboratories, West Grove, Pa.). In some experiments, fixed cells were pretreated with rhodamine-labeled wheat germ agglutinin (WGA; Sigma) to visualize plasma and Golgi membranes. The washed coverslips were then mounted on glass examination slides spotted with Mowiol containing 2.5% 1,4-diazabicyclo[2.2.2] octane antifading and 4′,6-diamidino-2-phenylindole dihydrochloride (DAPI) (1 mg/ml) for nuclear staining (all from Sigma) and then examined using a DH1RBE inverted confocal microscope (Leica, Buffalo, N.Y.) at the Medical Research Council Cell Imaging Facility of the Department of Biochemistry, University of Bristol.

RESULTS

Epitope attachment to EtxB. To investigate whether EtxB could be used as a vehicle for the delivery of peptides into the class I presentation pathway, we initially designed two peptides, a 9-mer and a 26-mer peptide, both containing the well-characterized class I epitope (SIINFEKL) of OVA. The 9-mer peptide comprised the SIINFEKL epitope and an N-terminal cysteine to allow conjugation to EtxB (Table 1). The design of the 26-mer peptide was based on a previous study, in which it was shown that a 27-mer derived from the Pol of HSV-1, when fused to the C terminus of EtxB, was efficiently delivered into eukaryotic cells (18). Since the Pol peptide contained a number of features speculated to be involved in peptide liberation and endosomal translocation, namely, a putative cathepsin D cleavage site (EKL↓AG↓F) and a loop segment of hydrophobic and charged amino acids (AGFGAVGAGATAEE), these elements were incorporated adjacent to the SIINFEKL epitope in order to investigate whether they would exert an effect on the efficiency of peptide delivery. Thus, a 26-mer synthetic peptide was designed containing an N-terminal cysteine residue suitable for chemical conjugation, the putative cleavage site and loop segment from the Pol peptide, and the SIINFEKL epitope (Table 1).

The 9-mer and 26-mer peptides were chemically conjugated to EtxB using the bifunctional cross-linker GMBS as described in Materials and Methods. The peptides were also conjugated to a well-characterized mutant of EtxB, EtxB(G33D), which retains the structural and biophysical characteristics of native EtxB but lacks affinity for GM1 (20, 21). The resultant conjugates retained the characteristic stability properties of EtxB, migrating as a pentameric high-molecular-weight species on SDS-polyacrylamide gels if kept unheated prior to analysis (Fig. 1A, lanes 1, 3, 5, and 7) and dissociating into monomers when boiled (Fig. 1A, lanes 2, 4, 6, and 8). The unheated conjugates had an electrophoretic mobility that was slower and had a more diffuse appearance than that of the native EtxB pentamer, suggestive of attachment of several peptides per pentamer (Fig. 1A; compare lane 9 with lanes 1, 3, 5, and 7). Upon boiling, monomeric conjugate species with one, two, or more conjugated peptides per EtxB monomer could be clearly distinguished in the EtxB–26-mer and EtxB(G33D)–26-mer conjugates (Fig. 1A, lanes 6 and 8). In the case of the EtxB–9-mer and EtxB(G33D)–9-mer conjugates containing one, two, or more peptides, the monomeric conjugate species were clustered with similar electrophoretic mobilities (Fig. 1A, lanes 2
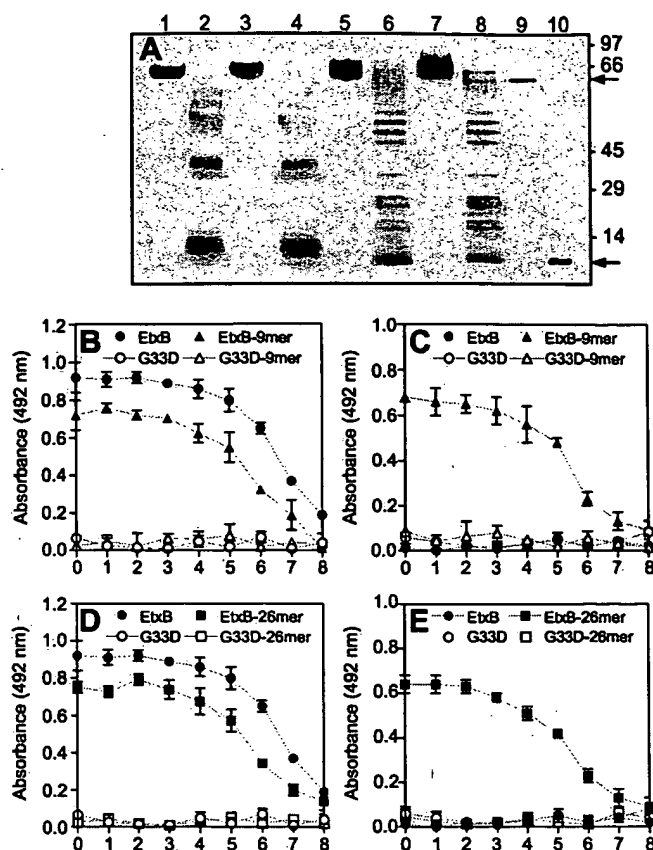

FIG. 1. Production and characterization of EtxB– and EtxB(G33D)–9-mer and –26-mer conjugates. (A) SDS-PAGE analysis of EtxB– and EtxB(G33D)–9-mer and –26-mer conjugates. Lanes: 1, EtxB–9-mer, unheated; 2, EtxB–9-mer boiled; 3, EtxB(G33D)–9-mer, unheated; 4, EtxB(G33D)–9-mer, boiled; 5, EtxB–26-mer, unheated; 6, EtxB–26-mer, boiled; 7, EtxB(G33D)–26-mer, unheated; 8, EtxB(G33D)–26-mer, boiled; 9, EtxB, unheated; 10, EtxB, boiled. Molecular mass standards in kilodaltons and the EtxB monomer and pentamer (arrows) are indicated. (B and D) Detection of EtxB– and EtxB(G33D)–9-mer and –26-mer conjugates in GM1 ELISA using a MAb specific for EtxB (118-8). (C and E) Detection of EtxB– and EtxB(G33D)–9-mer and –26-mer conjugates in GM1 ELISA using a SIINFEKL-specific polyclonal antiserum. Absorbances are plotted against the dilution factor and are given as means ± SEM.

and 4), presumably due to the lower molecular weight of the conjugated peptide. In GM1-binding ELISAs, the EtxB–9-mer and –26-mer conjugates could be readily detected by MAb 118-8, specific for the EtxB pentamer, confirming that the coupling procedure had not interfered with the capacity of the EtxB moiety of the conjugates to bind to GM1 (Fig. 1B and D). By contrast, the EtxB(G33D) conjugates were not detectable in the GM1 ELISA, reflecting the inability of the EtxB(G33D) mutant to bind to GM1 (Fig. 1B and D). The use of a SIINFEKL-specific antiserum demonstrated that the EtxB–9-mer and EtxB–26-mer conjugates display the epitope when the conjugates are bound to GM1 (Fig. 1C and E). Western blot analysis using MAb 118-8 detected both native EtxB and the EtxB and EtxB(G33D) conjugates, while use of the SIINFEKL-specific antiserum detected both the pentameric and monomeric species of the conjugates (data not shown). For all conjugates, the peptide/EtxB pentamer ratio, estimated

by gel filtration chromatography, together with the conjugate concentration, was used to determine the apparent concentration of peptide in the conjugate as described in Materials and Methods. On average, with each peptide, an EtxB pentamer/ peptide ratio of approximately 1:5 was achieved.

EtxB conjugates deliver SIINFEKL peptide into the MHC-I presentation pathway in a dose- and GM1-binding-dependent fashion. The capacities of the EtxB– and EtxB(G33D)–9-mer and –26-mer conjugates to deliver the OVA-derived SIINFEKL epitope into MHC-I were investigated in antigen presentation assays using JAWSII cells as antigen-presenting cells and IL-2 release by the SIINFEKL-specific RF33.70 T-cell hybridoma as a read-out for antigen presentation. In these assays, the free 8-mer SIINFEKL peptide was used as a positive control. This peptide is able to access the MHC-I peptide-binding groove directly, by competing for binding with peptides present in already-displayed MHC-I complexes. Figure 2A shows that the free 9-mer CSIINFEKL peptide also stimulated class I presentation, indicating that, like the 8-mer, the 9-mer peptide is capable of loading directly onto MHC-I molecules present on the cell surface. When the 9-mer was conjugated to EtxB and the resultant conjugate was tested at concentrations ranging from 1 pM to 100 nM peptide equivalents, it was found that the SIINFEKL epitope was delivered in a dose-dependent fashion (Fig. 2A). However, the observed extent of epitope presentation was not as great as that achieved with equivalent amounts of free 8-mer or 9-mer peptide (Fig. 2A). Importantly, treatment of JAWSII cells with equivalent concentrations of the EtxB(G33D)–9-mer conjugate failed to result in epitope presentation, indicating that delivery is dependent on GM1 binding. By comparison, the EtxB–26-mer conjugate was much more efficient at delivering the SIINFEKL epitope than the corresponding EtxB–9-mer conjugate (Fig. 2B). Moreover, delivery of the SIINFEKL epitope by the EtxB–26-mer conjugate was dose dependent and reached maximal levels at concentrations of 10 nM peptide equivalents, similar to that observed when using the free 8-mer SIINFEKL peptide (Fig. 2B). Importantly, no presentation occurred when either the free 26-mer peptide or the EtxB(G33D)–26-mer conjugate was tested, indicating that conjugation to a functional, GM1-binding EtxB moiety is essential for the 26-mer to be delivered into the class I pathway. The striking difference in the extent of SIINFEKL presentation mediated by the EtxB–9-mer and EtxB–26-mer conjugates implies that N-terminal Pol-derived segments within the 26-mer conjugate are exerting an influence on the efficiency of epitope presentation.

For a more direct assessment of antigen presentation, a FACS-based assay involving the use of MAb 25D1.16, specific for MHC-I-SIINFEKL complexes, was employed. The results, obtained at 100 nM peptide equivalents, were in complete agreement with the data obtained in antigen presentation assays as described above (Fig. 2C). Accordingly, the EtxB–26-mer conjugate and free 8-mer SIINFEKL peptide induced clear and similar shifts, while EtxB–9-mer induced a modest shift in fluorescence. The free 8-mer and 9-mer peptides displayed very similar shifts, while 26-mer peptide alone, admixed with EtxB, or conjugated to EtxB(G33D) failed to induce a shift in fluorescence (data not shown). The observed enhancement of antigen presentation was not due to EtxB-induced upregulation of MHC-I expression, as FACS analysis using
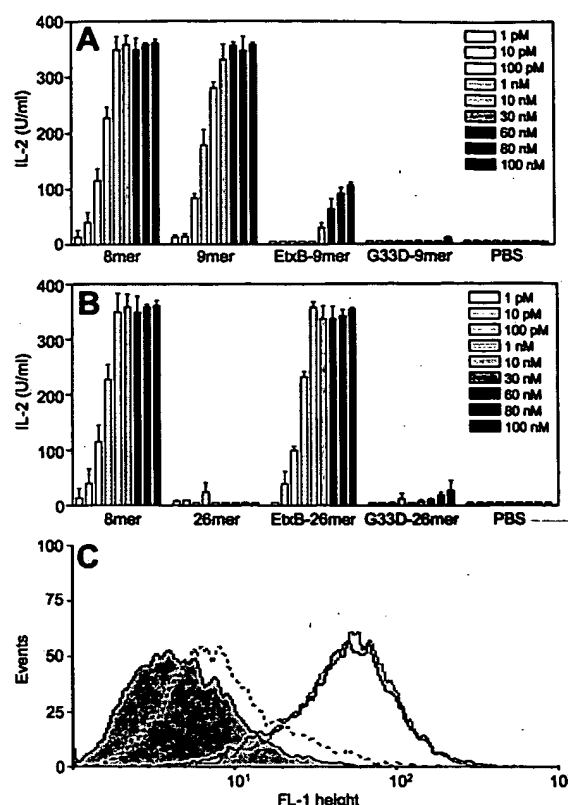

FIG. 2. EtxB conjugates deliver SIINFEKL epitopes into the MHC-I pathway in a dose- and GM1-binding-dependent fashion. (A and B) EtxB-induced antigen presentation as assessed by analysis of IL-2 release by RF33.70 T-cell hybridoma. JAWSII cells were incubated with peptide alone or EtxB- or EtxB(G33D)-peptide conjugates at the indicated equimolar concentrations of peptide for 2 h. The cells were then fixed with 1% paraformaldehyde and incubated overnight with RF33.70 cells; 8-mer peptide and PBS were used as the positive and negative control, respectively. Duplicate samples were tested, and the data are given as means ± SEM. (A) 9-mer peptide and EtxB– and EtxB(G33D)–9-mer conjugates. (B) 26-mer peptide and EtxB– and EtxB(G33D)–26-mer conjugates. (C) EtxB-induced antigen presentation as assessed by FACS analysis using MAb 25D1.16, specific for MHC-I-SIINFEKL complexes. JAWSII cells were treated with 100 nM 8-mer peptide (grey curve), EtxB–9-mer conjugate (dashed curve), EtxB–26-mer conjugate (solid curve), or PBS (filled curve) for 2 h and then sequentially incubated with 25D1.16 MAb and a FITC-labeled secondary antibody. Fluorescence was assessed by flow cytometric analysis.

FITC-labeled MHC-I-specific antibodies did not reveal a significant increase in cell fluorescence (data not shown). Thus, the observed IL-2 release was the result of the appearance of MHC-I-SIINFEKL complexes on the cell surface and subsequent recognition and IL-2 production by the RF33.70 T-cell hybridoma.

The Pol loop segment is responsible for the increase in the efficiency of EtxB-mediated epitope delivery. In an attempt to identify which of the Pol peptide-derived structural elements within the 26-mer peptide were responsible for facilitating more efficient epitope delivery, two truncated peptides, namely, a 16-mer and a 19-mer peptide, were designed (Table 1). Compared to the 26-mer peptide, the 16-mer peptide lacked the Pol loop segment, while the 19-mer peptide lacked the putative cathepsin cleavage site. The 16-mer and 19-mer peptides were conjugated to EtxB as described above, and the
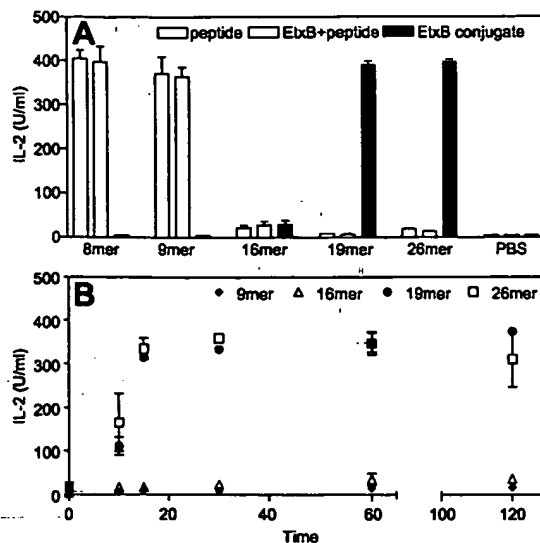
FIG. 3. The Pol loop segment enhances the efficiency of EtxB-mediated peptide delivery. (A) Effect of peptide truncation on EtxB-mediated epitope delivery. JAWSII cells were incubated with the indicated peptides alone or peptides admixed with or conjugated to EtxB at the equivalent concentration of 10 nM peptide for 2 h. The cells were then fixed with paraformaldehyde, and antigen presentation was assessed by determining antigen presentation-induced IL-2 release by RF33.70 T cell hybridoma. (B) Kinetics of antigen presentation upon treatment of JAWSII cells with EtxB–9-mer, –16-mer, –19-mer, or –26-mer conjugate. JAWSII cells were incubated for 0, 10, 15, 30, 60, or 120 min and fixed with paraformaldehyde, and antigen presentation was assessed as described above. Duplicate samples were tested, and data are given as means ± SEM.

abilities of the resultant conjugates to bind to GM1 were confirmed by GM1 sandwich ELISA (data not shown). Figure 3A shows that, at 10 nM peptide equivalents, the free 16-mer, 19-mer, and 26-mer peptides could not load directly onto MHC-I. When the EtxB–9-mer and EtxB–16-mer were tested under these conditions, neither conjugate was able to deliver sufficient SIINFEKL epitope to stimulate IL-2 release by the RF33.70 T-cell hybridoma, indicating that the inclusion of the putative cathepsin D cleavage site is not responsible for the enhanced epitope delivery observed with the EtxB–26-mer. By contrast, conjugation to EtxB of the 19-mer, which contains the Pol loop segment, resulted in high-level peptide delivery, comparable to the maximal loading achieved with free 8-mer SIINFEKL peptide (Fig. 3A). We therefore conclude that incorporation of the Pol loop segment adjacent to the class I epitope causes a marked increase in the extent of EtxB-mediated epitope presentation.

To assess the kinetics of appearance of MHC-I–SIINFEKL complexes on the cell surface upon treatment with EtxB–9-mer, –16-mer, –19-mer, and –26-mer conjugates, cells were fixed at various time points after incubation with the EtxB conjugates. After 0 min of incubation with the conjugates, no peptide presentation was evident. Remarkably, after 15 min, maximal presentation levels had already been attained by the EtxB–19-mer and –26-mer conjugates, which displayed very similar kinetics (Fig 3B). In agreement with the findings described above, no significant levels of presentation were observed with the EtxB–9-mer and –16-mer conjugates, even after 120 min.
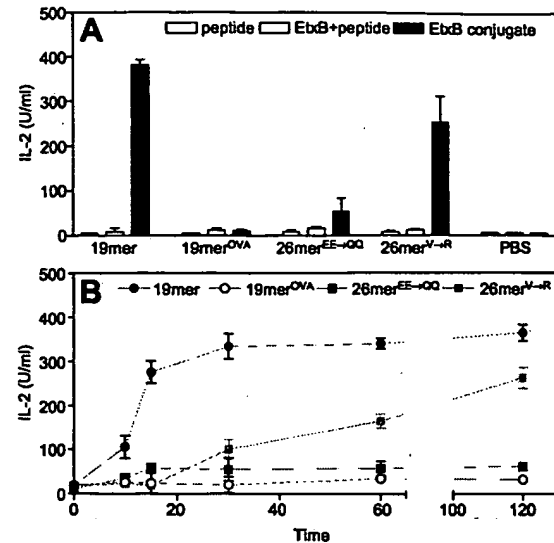

FIG. 4. Mutation or replacement of the Pol segment reduces efficiency or inhibits EtxB-mediated epitope delivery. (A) Effect of amino acid substitution or Pol segment replacement on the extent of epitope delivery. (B) Kinetics of antigen presentation upon treatment of JAWSII cells with EtxB–19-mer, –19-mer^{OVA}, –26-mer$^{EE \rightarrow QQ}$, –26-mer$^{V \rightarrow R}$, or –31-mer conjugate. For details, see the legend to Fig. 3. Duplicate samples were tested, and the data are given as means ± SEM.

To further investigate whether the intrinsic properties of the Pol loop segment contributed to peptide delivery, three additional peptides were designed (Table 1). A 26-mer$^{EE \rightarrow QQ}$ and a 26-mer$^{V \rightarrow R}$ peptide were designed to assess the effects of targeted mutations in the Pol loop segment on delivery. These peptides contained either two Glu-to-Gln substitutions, which alter both the overall charge of the peptide and the potential cleavage site N-terminal to the SIINFEKL epitope, or a single Val-to-Arg substitution, which should disrupt the relative hydrophobicity of the Pol loop segment (Table 1). In addition, a further 19-mer peptide, termed 19-mer^{OVA}, was prepared in which the 10-amino-acid Pol loop segment was replaced by the 10 amino acids that normally precede the SIINFEKL epitope in native OVA. This peptide permitted us to investigate if the observed increase in epitope delivery was due to the intrinsic properties of the Pol loop segment or simply due to peptide length. The three peptides were conjugated to EtxB as described above, and the abilities of the resultant conjugates to bind to GM1 were confirmed by GM1 sandwich ELISA (data not shown).

When these peptides were tested alone or admixed with EtxB at 10 nM peptide equivalents, none of them were efficiently presented. However, upon conjugation, the EtxB–19-mer^{OVA}, –26-mer$^{EE \rightarrow QQ}$, and –26-mer$^{V \rightarrow R}$ conjugates displayed markedly altered epitope delivery characteristics compared with EtxB–19-mer (Fig 4A). The EtxB–19-mer^{OVA} and –26-mer$^{EE \rightarrow QQ}$ conjugates were found to almost completely lack the ability to stimulate epitope presentation, and the EtxB–26-mer$^{V \rightarrow R}$ conjugate displayed a reduction in the extent of epitope presentation (Fig. 4A). Furthermore, the V→R substitution resulted in a marked alteration in the kinetics of SIINFEKL epitope delivery, with no presentation evident in the first 15 min and presentation still rising at 120

min (Fig. 4B). We conclude, therefore, that the Pol loop segment possesses an intrinsic ability to efficiently deliver peptides and that the enhanced extent of epitope presentation observed with the original EtxB–19-mer and –26-mer conjugates is not simply due to the length of the peptide preceding the SIINFEKL epitope.

Endosomal acidification and an intact Golgi are required for EtxB-mediated epitope delivery. The trafficking pathway by which EtxB mediates the delivery of conjugated peptides into the MHC-I pathway was investigated using BafA1, an inhibitor of the V-ATPase responsible for acidification of organelles of the endocytic pathway (3), and BFA, a Golgi-disrupting drug and inhibitor of vesicle-mediated secretion (16). Treatment of JAWSII cells for 60 min with BafA1 or BFA, prior to addition of the EtxB–19-mer, –26-mer, and –26-mer$^{V \to R}$ conjugates, led to complete inhibition of EtxB-mediated epitope delivery, as assessed by both the IL-2 release assay and FACS detection of MHC-I-SIINFEKL complexes. Since the results obtained with all of these conjugates were identical, only the data using the EtxB–19-mer are shown (Fig. 5B, C, F, and G). Importantly, treatment of JAWSII cells with BafA1 or BFA did not inhibit the direct loading and presentation of the free 8-mer peptide (Fig. 5B-C). Also, when ammonium chloride or monensin, an Na^+-ionophor inhibitor of endosomal acidification, was tested, EtxB-mediated epitope delivery was prevented while presentation of the free 8-mer peptide was unaffected (data not shown). In other studies, inhibitors of acid proteases, metalloaminopeptidases, and serine and cysteine proteases (pepstatin, bestatin, and leupeptin, respectively) were found not to have a significant effect on EtxB-mediated epitope presentation (data not shown). However, the metalloprotease inhibitor 1,10-phenanthroline was found to inhibit EtxB-induced antigen presentation (data not shown). Taken together, these findings suggest that EtxB-mediated peptide presentation depends upon (i) conjugate entry into acidic endosomes; (ii) peptide cleavage, possibly by a metalloprotease; and (iii) a functionally intact Golgi network and secretory pathway.

Proteasome involvement in EtxB-mediated epitope presentation. To assess the possible requirement for proteasome-mediated processing of peptides delivered by EtxB, we designed an additional peptide, namely, a 31-mer. The design of this peptide was based on studies in which it was shown that proteasome cleavage of OVA creates the proper C terminus of the SIINFEKL epitope whereas distinct peptidases in the cytosol or ER generate the appropriate N terminus from extended peptides (7, 8). Consequently, since all of the peptides we had tested contained the SIINFEKL epitope at their C termini, it is highly unlikely that the pathway of delivery of these peptides would depend on proteasome-mediated cleavage. We therefore extended the 26-mer peptide at the C terminus with an additional five amino acids derived from the OVA sequence, thus creating an internal SIINFEKL epitope (Table 1), and tested the effects of BafA1, BFA, and a number of well-characterized proteasome inhibitors on peptide delivery.

Incubation of JAWSII cells with the EtxB–31-mer resulted in the efficient presentation of the SIINFEKL epitope, as assessed by the IL-2 release assay and by FACS (Fig. 5A and E). As observed with the EtxB–19-mer conjugate, prior treatment with BafA1 or BFA prevented EtxB–31-mer-mediated epitope
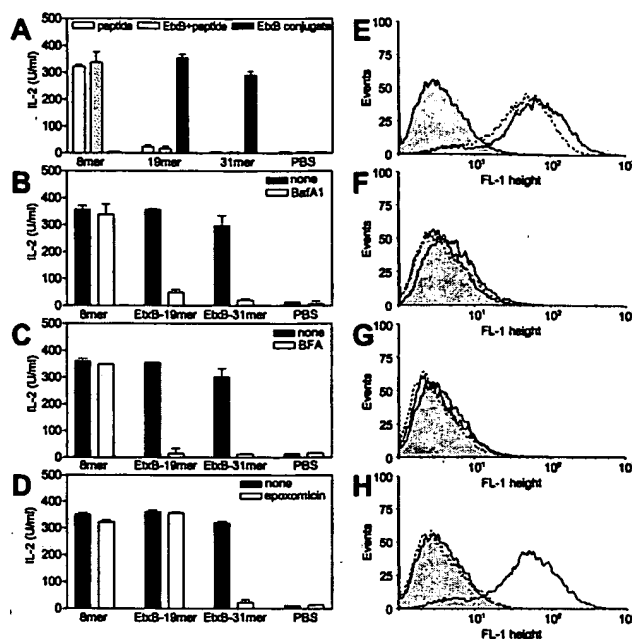

FIG. 5. Effects of inhibitors on EtxB-induced antigen presentation. The effects of BafA1, BFA, and epoxomicin on delivery of 19-mer and 31-mer peptides were assessed by both IL-2 release assays (A to D) and FACS analysis using the 25D1.16 antibody (E to H). PBS and the 8-mer peptide were used as positive and negative controls, respectively. IL-2 release data are given as means ± SEM. In panels E to H, EtxB–19-mer (solid curve), EtxB–31-mer (dashed curve), and PBS (filled curve) are shown. For details, see the legend to Fig. 2. (A and E) Antigen presentation upon treatment with 19-mer or 31-mer peptide alone, admixed with EtxB, or conjugated with EtxB in the absence of inhibitors. (B and F) Effect of BafA1 (200 nM). (C and G) Effect of BFA (10 μM). (D and H) Effect of epoxomicin (10 μM).

presentation (Fig. 5B, C, F, and G). In agreement with the notion that the proteasome does not generate the N terminus of the SIINFEKL epitope, preincubation of JAWSII cells with epoxomicin, a specific proteasome inhibitor (19), did not inhibit epitope presentation when the cells were treated with EtxB–19-mer or free 8-mer (Fig. 5D and H). Likewise, lactacysin or MG132, two additional inhibitors of proteasome activity, failed to prevent EtxB-mediated or free-epitope presentation (data not shown). Similar results were obtained when all of the other EtxB peptide conjugates were tested in the presence of epoxomicin, lactacysin, or MG132 (data not shown). However, in contrast to the behavior of the conjugates described above, epitope delivery by the EtxB–31-mer was completely inhibited by the addition of epoxomicin (Fig. 5D and H). Similar inhibition was observed when lactocystin and MG132 were used (data not shown). This demonstrates that proteasome-mediated cleavage of the 31-mer peptide is necessary for it to enter the class I presentation pathway.

To further visualize the trafficking pathway of the EtxB conjugates and to determine the localization of MHC-I complexes, cells were treated with EtxB–19-mer or EtxB–31-mer and probed with antibodies directed against EtxB or MHC-I-SIINFEKL and then examined by confocal microscopy. After 1 min of incubation with the conjugates, the EtxB moiety could be clearly seen at the cell surface and there was no evidence of detectable MHC-I-SIINFEKL complexes (Fig.

6A, images e to h). After 120 min, both EtxB–19-mer and –31-mer were almost completely internalized, and perinuclear staining was evident with both anti-EtxB and anti-MHC-I–SIINFEKL antibodies, with considerable colocalization (Fig. 6A, images i to l).

This perinuclear staining was suggestive of localization of both EtxB and the MHC-I–SIINFEKL complexes in the ER or Golgi network, consistent with both the trafficking pathway of EtxB (14) and the normal cellular location of newly synthesized MHC-I molecules. In order to identify the cellular localization of the MHC-I–SIINFEKL complexes more accurately, fixed cells were treated with rhodamine-labeled WGA, specific for N-acetyl-β-D-acetylglucosamine present in Golgi-ER and plasma membranes (31), followed by anti-MHC-I–SIINFEKL and secondary antibodies (Fig. 6B). It was found that WGA and MHC-I–SIINFEKL complexes colocalized, confirming that these complexes were present in the Golgi (Fig. 6B, images a to d). Moreover, when cells were preincubated with epoxomicin to inhibit proteasome activity, no staining with MHC-I–SIINFEKL-specific antibodies was obtained when the cells were treated with EtxB–31-mer (Fig. 6B, images d and h), whereas normal colocalization of WGA and MHC-I–SIINFEKL complexes was observed when cells were treated with the EtxB–19-mer (Fig. 6B, images c and g). In addition, no detectable MHC-I–SIINFEKL complexes were observed when cells were pretreated with BafA1 or BFA prior to addition of the EtxB–19-mer or EtxB–31-mer conjugate (data not shown). The above-mentioned findings on the effects of the trafficking and proteasome inhibitors are in full agreement with the results obtained in the antigen presentation assays and indicate that peptides are delivered into the endogenous antigen processing and presentation pathway.

EtxB-mediated delivery of a class I epitope from influenza NP is also enhanced by the Pol loop segment. To establish if conjugation of Pol loop segment-containing peptides to EtxB represents a generic approach for enhanced delivery of class I epitopes into the endogenous pathway, two additional peptides containing a well-characterized H-2^b-restricted epitope from influenza NP were designed. A 10-mer peptide, 10-mer^{NP}, comprising the NP-derived ASNENMETM epitope and an N-terminal cysteine for conjugation to EtxB, and a 20-mer peptide, 20-mer^{NP}, comprising the ASNENMETM epitope, an N-terminal cysteine residue, and the 10-amino-acid Pol loop segment, were synthesized (Table 1). The 10-mer^{NP} and 20-mer^{NP} peptides were conjugated to EtxB as described above, and the abilities of the resultant conjugates to bind to GM1 were confirmed by GM1 sandwich ELISA (data not shown). Similarly, peptides were conjugated to EtxB(G33D), and the conjugates were found to lack GM1-binding activity (data not shown).

The capacities of the EtxB– and EtxB(G33D)–10-mer^{NP} and –20-mer^{NP} conjugates to deliver the NP-derived ASNENMETM epitope into MHC-I were investigated in antigen presentation assays using JAWSII cells as antigen-presenting cells and IL-2 release by the RF36.84 T-cell hybridoma as a read-out for antigen presentation. The results, shown in Fig. 7, were in complete agreement with those obtained using the peptides containing the SIINFEKL epitope. Accordingly, both the 9-mer^{NP} and 10-mer^{NP} peptide were found to be capable of displacing peptides bound to cell surface MHC-I molecules, resulting in maximal
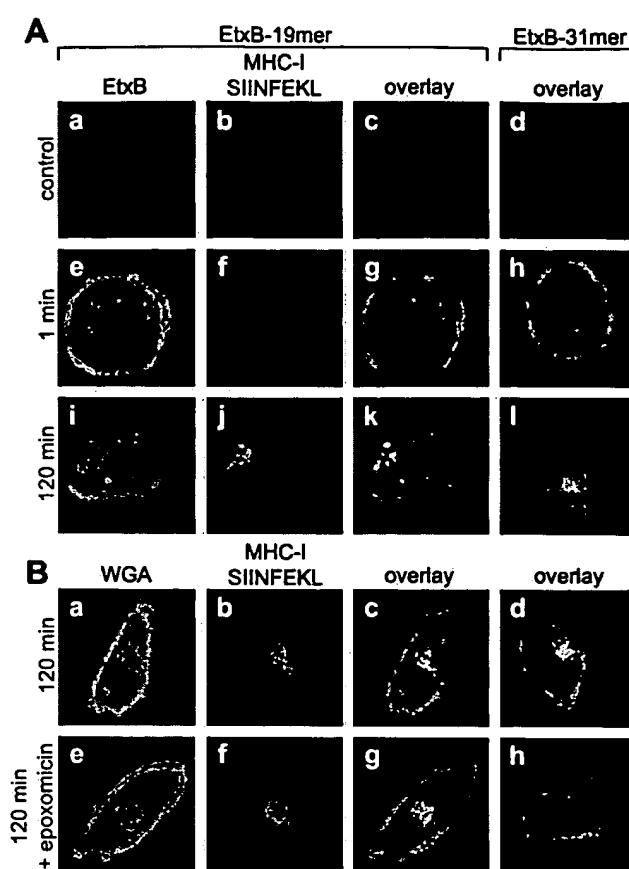

FIG. 6. MHC-I–SIINFEKL complexes are located in the Golgi compartment. (A) Confocal microscopic analysis of the cellular localization of EtxB and MHC-I–SIINFEKL complexes upon treatment of JAWSII cells with EtxB–19-mer and EtxB–31-mer. JAWSII cells were incubated for 1 min (images e to h) or 2 h with either EtxB–19-mer or EtxB–31-mer conjugate (images i to l) or PBS (images a to d). After treatment, the cells were fixed with paraformaldehyde and then stained with a polyclonal rabbit antiserum specific for EtxB and a MAb specific for MHC-I–SIINFEKL-complexes (25D1.16), followed by FITC- or rhodamine-labelled secondary antibodies as described in Materials and Methods. Cell nuclei were stained with DAPI (blue). For EtxB–31-mer, only the overlay is shown. (B) Colocalization of MHC-I–SIINFEKL complexes and Golgi membranes. Cells were treated as described above and incubated with rhodamine-labeled WGA, 25D1.16 MAb, and secondary antibodies (images a to d). The effect of the proteasome inhibitor epoxomicin (10 μM) on formation of MHC-I–SIINFEKL complexes is also shown (images e to h).

stimulation of epitope presentation. When the 10-mer^{NP} peptide was conjugated to EtxB and the resultant conjugate was tested at concentrations ranging from 1 to 100 nM peptide equivalents, it was found that significant ASNENMETM epitope presentation was obtained only at 100 nM peptide equivalents (Fig. 7A). Similar to earlier observations, the extent of epitope presentation was not as great as that achieved with equivalent amounts of free 9-mer^{NP} or 10-mer^{NP} peptide but was dependent on GM1 binding, as treatment of JAWSII cells with the EtxB(G33D)–10-mer^{NP} conjugate at 100 nM peptide equivalents failed to result in epitope presentation (Fig. 7A). Finally, compared to treatment of JAWSII cells with the EtxB–10-mer^{NP} conjugate, treatment with the EtxB–20-mer^{NP} conjugate resulted in much higher levels of ASNENMETM epitope presentation, indicating that inclusion of the Pol loop segment facilitated more efficient delivery of
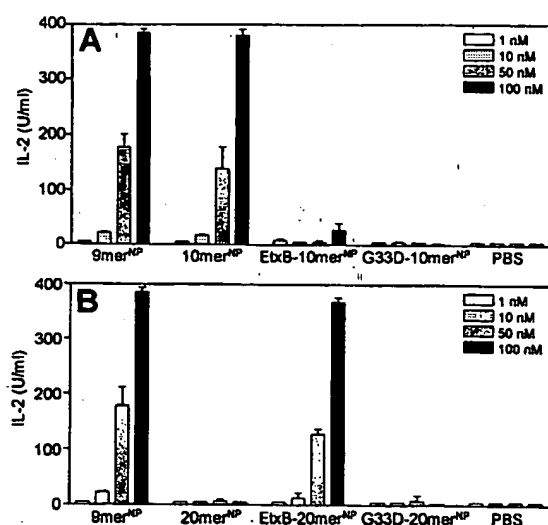
FIG. 7. The Pol loop segment enhances EtxB-mediated delivery of an influenza NP-derived class I epitope. (A and B) EtxB-induced antigen presentation as assessed by analysis of IL-2 release by RF36.84 T-cell hybridoma. JAWSII cells were incubated with peptide alone or EtxB- or EtxB(G33D)-peptide conjugates at the indicated equimolar concentrations of peptide for 2 h. The cells were then fixed with 1% paraformaldehyde and incubated overnight with RF36.84 cells; the 9-mer^{NP} peptide and PBS were used as the positive and negative control, respectively. Duplicate samples were tested, and the data are given as means ± SEM. (A) 10-mer^{NP} peptide and EtxB- and EtxB (G33D)-10-mer^{NP} conjugates. (B) 20-mer^{NP} peptide and EtxB- and EtxB(G33D)-20-mer^{NP} conjugates.

the NP-derived peptide (Fig. 7B). Importantly, no presentation occurred when either the free 20-mer^{NP} peptide or the EtxB(G33D)-20-mer^{NP} conjugate was tested, indicating that conjugation to a functional, GM1-binding EtxB moiety is essential for the 20-mer^{NP} to be delivered into the class I pathway. We therefore conclude that conjugation of peptides to EtxB facilitates their entry into the cell via a GM1-binding-dependent pathway and that the efficiency of EtxB-mediated delivery can be strikingly enhanced by the inclusion of the Pol loop segment in the conjugated peptide, leading to highly efficient delivery of the epitope into the endogenous class I antigen processing and presentation pathway.

DISCUSSION

Bacterial A-B protein toxins are composed of structurally and functionally distinct enzymatically active A and receptor-binding B subunits or domains, of which the A domain requires enzymatic cleavage and entry into the target cell cytosol in order for it to exert its toxic enzymatic effects (for a review, see reference 5). Given the intrinsic capacities of these toxins to deliver their toxic A subunits into cells, several investigators have attempted to exploit A-B toxins for the delivery of heterologous antigens into the endogenous class I pathway. Most of these studies have focused on the development of recombinant constructs comprising heterologous peptide or protein antigens fused to the toxin A subunits. Such constructs have been shown to be capable of stimulating MHC-I-restricted presentation of the heterologous antigen (2, 6, 30). The use of

the toxin B subunits of bacterial toxins as delivery vehicles has not been widely evaluated because, in contrast to the A subunits, the toxin B subunits are not thought to enter the cell cytosol. However, Lee et al. showed that fusion of a peptide epitope to the B subunit of Shiga toxin resulted in presentation of the epitope in the context of MHC-I (13). Here, we report the systematic evaluation of the use of the receptor-binding B subunit of E. coli heat-labile toxin as a vehicle for the delivery of peptide epitopes into the class I pathway. We chose to adopt a versatile chemical conjugation strategy rather than a genetic strategy for attaching peptides to EtxB in order to facilitate the rapid preparation of conjugates containing different peptides. We show for the first time that EtxB can be used for the intracellular delivery of the well-characterized SIINFEKL class I epitope from OVA and that EtxB-mediated delivery is dependent on its ability to bind to GM1 receptors on the target cell. However, conjugation of the SIINKEKL epitope alone to EtxB, as exemplified by the EtxB-9-mer conjugate, resulted in inefficient presentation relative to direct loading with the free 8-mer SIINFEKL epitope.

In an attempt to overcome this, we sought to take advantage of our previous observation that a 27-mer peptide derived from the C terminus of the Pol peptide of HSV-1 was efficiently delivered into intracellular compartments when fused to EtxB, a finding that suggested that the Pol peptide may contain a number of features which facilitate both liberation from EtxB and translocation from endosomal compartments. These included a putative cathepsin D cleavage site and a loop segment of hydrophobic and charged amino acids. We therefore decided to investigate whether incorporation of these elements adjacent to the SIINFEKL epitope would improve the efficiency of EtxB-mediated peptide delivery into the class I pathway. We found that the inclusion of elements of the Pol peptide in the conjugated peptides contributed to the extent and efficiency of epitope presentation. In this respect, such EtxB-Pol peptide-SIINFEKL conjugates were capable of achieving levels of presentation comparable to those resulting from direct loading by the free SIINFEKL peptide. We were able to map the region of the Pol peptide necessary for efficient delivery to a 10-amino-acid region corresponding to the Pol loop segment. This segment is part of a 36-amino-acid hairpin-like structure, consisting of two helical regions interrupted by a flexible loop region that contains two glutamate residues (4, 9). The Pol segment used in the present study contains the two glutamates and the flexible region composed of hydrophobic and nonpolar amino acids and shows a degree of similarity with fusion peptides from viral glycoproteins (29). Therefore, one explanation for the improved delivery of the SIINFEKL epitope by peptides containing the Pol loop segment may be that this segment has an intrinsic propensity to penetrate lipid bilayers. Furthermore, it is known that for pH-dependent translocation of diphtheria toxin, protonation of acidic residues in helical hairpins permits insertion of hydrophobic domains into lipid bilayers, and mutation of such residues in diphtheria toxin is known to result in a reduction in toxicity (12). Thus, liberation from EtxB, followed by protonation of the glutamates and then translocation across a vesicular membrane into the cytosol, should permit highly efficient entry into the endogenous class I presentation pathway.

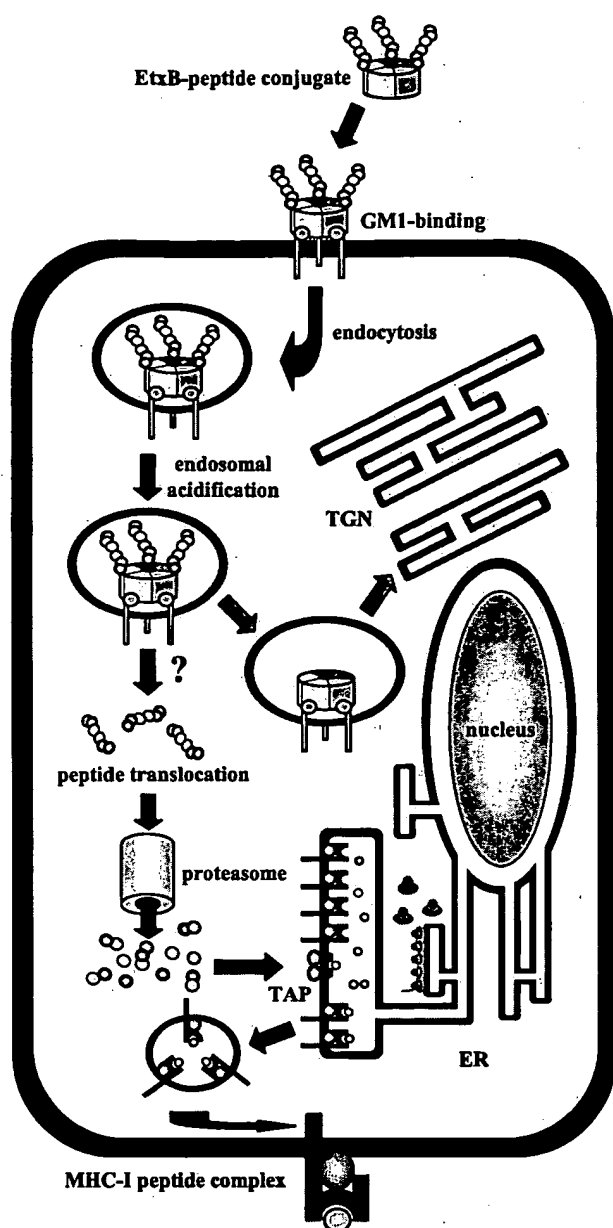In support of this hypothesis, replacement of the 10-amino-

FIG. 8. Schematic representation of the pathway of EtxB-mediated delivery of class I epitopes. GM1 binding by the EtxB-peptide conjugate mediates uptake into smooth endocytic vesicles. Upon endosomal acidification, the peptide is cleaved from the conjugate and translocated into the cytosolic compartment, while EtxB traffics to the trans-Golgi network (TGN). Depending on the exact peptide sequence, the peptide is processed by the proteasome and, following transport into the lumen of the ER by the transporter of antigenic peptides (TAP), binds to empty MHC-I molecules. Stable MHC-I–peptide complexes are then transported to the cell surface.

acid Pol loop segment with the 10 amino acids that precede SIINFEKL in native OVA completely abolished the enhancement of epitope presentation observed with the EtxB–19-mer conjugate. Furthermore, conjugation to EtxB of a 26-mer$^{EE \rightarrow QQ}$ peptide, in which the two Glu residues present in the native 26-mer peptide are replaced by Gln residues, or a 26-mer$^{V \rightarrow R}$ peptide, in which the stretch of nonpolar and hydrophobic amino acid residues in the Pol loop segment is

interrupted by an Arg residue, resulted in a marked decrease in the efficiency of epitope delivery, possibly due to decreased translocation efficiency. Moreover, the finding that BafA1, ammonium chloride, and monensin inhibited EtxB-mediated epitope presentation indicates that entry into an acidic endosome is essential. Given that the trafficking and toxicity of cholera toxin is refractory to chaotropic agents (15), this would imply that entry into an acidic environment is required for efficient epitope delivery rather than for trafficking of the carrier. Consequently, an acidic environment could enable protonation of the Pol loop glutamate residues for subsequent translocation.

It is also possible that entry into acidic endosomes is necessary for peptide liberation from EtxB as a result of the activities of acid-dependent proteases, such as cathepsins. However, when EtxB-mediated presentation of the 26-mer peptide was assessed in the presence of pepstatin, an inhibitor of acid proteases, it had no effect on the extent of SIINFEKL presentation (data not shown). In addition, there was no difference in the extent of epitope presentation mediated by EtxB–19-mer and EtxB–26-mer conjugates, the first of which lacks the putative cathepsin D cleavage site. As indicated above, only the metalloprotease inhibitor 1,10-phenanthroline was found to inhibit EtxB-induced antigen presentation, suggesting that a metalloprotease may be involved in liberation and/or processing of the EtxB-conjugated peptides. Given the finding that the proteasome can participate in the pathway of EtxB-mediated epitope presentation, it would imply that conjugated peptides are liberated from EtxB and translocated into the cytosol for proteasome processing.

Consequently, it is hypothesized, as depicted in Fig. 8, that EtxB-mediated delivery of peptides into the endogenous class I presentation pathway involves three distinct steps: (i) binding of the EtxB moiety to GM1, which mediates uptake of peptide conjugates into the endosomal pathway; (ii) liberation of the attached peptide, possibly by a metalloprotease; and (iii) translocation of the peptide from an acidic endosome into the cytosolic compartment.

The potential of using the combined targeting and translocating functions of EtxB and the Pol loop segment, respectively, as a generic delivery system for class I epitopes is demonstrated by our results using an epitope derived from influenza virus NP. Here again, the extent of loading of the class I epitope onto MHC-I by the EtxB–20-mer^{NP} conjugate was as efficient as direct loading of surface MHC-I molecules with free 9-mer^{NP} ASNENMETM peptide. The importance of the Pol loop segment in mediating translocation into the class I pathway is highlighted by the finding that the EtxB–10-mer^{NP} conjugate was unable to facilitate loading of MHC-I. The combined abilities, therefore, of EtxB and the Pol-loop segment to efficiently deliver class I-restricted epitopes into the endogenous MHC-I pathway should open up new opportunities for the design of vaccines able to stimulate CTLs. Experiments investigating the potential of such constructs to trigger CTL responses are under way.

REFERENCES

1. Amin, T., and T. R. Hirst. 1994. Purification of the B-subunit oligomer of *Escherichia coli* heat-labile enterotoxin by heterologous expression and secretion in a marine *Vibrio*. Protein Expr. Purif. 5:198–204.
2. Ballard, J. D., R. J. Collier, and M. N. Starnbach. 1996. Anthrax toxin-mediated delivery of a cytotoxic T-cell epitope *in vivo*. Proc. Natl. Acad. Sci. USA 93:12531–12534.
3. Bowman, E. J., A. Siebers, and K. Altendorf. 1988. Bafilomycins: a class of inhibitors of membrane ATPases from microorganisms, animal cells, and plant cells. Proc. Natl. Acad. Sci. USA 85:7972–7976.
4. Bridges, K. G., Q. Hua, M. R. Brigham-Burke, J. D. Martin, P. Hensley, C. E. Dahl, P. Digard, M. A. Weiss, and, D. M. Coen. 2000. Secondary structure and structure-activity relationships of peptides corresponding to the subunit interface of herpes simplex virus DNA polymerase. J. Biol. Chem. 275:472–478.
5. Burnette, W. N. 1994. AB(5) ADP-ribosylating toxins. Comparative anatomy and physiology. Structure 2:151–158.
6. Carbonetti, N. H., T. J. Irish, C. H. Chen, C. B. O'Connell, G. A. Hadley, U. McNamara, R. G. Tuskan, and G. K. Lewis. 1999. Intracellular delivery of a cytolytic T-lymphocyte epitope peptide by pertussis toxin to major histocompatibility complex class I without involvement of the cytosolic class I antigen processing pathway. Infect. Immun. 67:602–607.
7. Cascio, P., C. Hilton, A. F. Kisselev, K. L. Rock, and A. L. Goldberg. 2001. 26S proteasomes and immunoproteasomes produce mainly N-extended versions of an antigenic peptide. EMBO J. 20:2357–2366.
8. Craiu, A., T. Akopian, A. Goldberg, and K. L. Rock. 1997. Two distinct proteolytic processes in the generation of a major histocompatibility complex class I-presented peptide. Proc. Natl. Acad. Sci. USA 94:10850–10855.
9. Digard, P., K. P. Williams, P. Hensley, I. S. Brooks, C. E. Dahl, and D. M. Coen. 1995. Specific inhibition of herpes simplex virus DNA polymerase by helical peptides corresponding to the subunit interface. Proc. Natl. Acad. Sci. USA 92:1456–1460.
10. Goletz, T. J., K. R. Klimpel, N. Arora, S. H. Leppla, J. M. Keith, and J. A. Berzofsky. 1997. Targeting HIV proteins to the major histocompatibility complex class I processing pathway with a novel gp120-anthrax toxin fusion protein. Proc. Natl. Acad. Sci. USA 94:12059–12064.
11. Harding, C. V. 1996. Class II antigen processing: analysis of compartments and functions. Crit. Rev. Immunol. 16:13–29.
12. Kaul, P., J. Silverman, W. H. Shen, S. R. Blanke, P. D. Huynh, A. Finkelstein, and R. J. Collier. 1996. Roles of Glu 349 and Asp 352 in membrane insertion and translocation by diphtheria toxin. Protein Sci. 5:687–692.
13. Lee, R. S., E. Tartour, P. van der Bruggen, V. Vantomme, I. Joyeux, B. Goud, W. H. Fridman, and L. Johannes. 1998. Major histocompatibility complex class I presentation of exogenous soluble tumor antigen fused to the B-fragment of Shiga toxin. Eur. J. Immunol. 28:2726–2737.
14. Lencer, W. I., C. Delp, M. R. Neutra, and J. L. Madara. 1992. Mechanism of cholera toxin action on a polarized human intestinal epithelial cell line: role of vesicular traffic. J. Cell Biol. 117:1197–1209.
15. Lencer, W. I., G. Strohmeier, S. Moe, S. L. Carlson, C. T. Constable, and J. L. Madara. 1995. Signal transduction by cholera toxin: processing in vesicular compartments does not require acidification. Am. J. Physiol. 32: G548–G557.
16. Lippincott-Schwartz, J., L. C. Yuan, J. S. Bonifacino, and R. D. Klausner. 1989. Rapid redistribution of Golgi proteins into the ER in cells treated with brefeldin A: evidence for membrane cycling from Golgi to ER. Cell 56:801–813.
17. Long, E. O., and S. Jacobsen. 1989. Pathways of viral antigen processing and presentation to CTL: defined by mode of virus entry? Immunol. Today 10:45–48.
18. Loregian, A., E. Papini, B. Satin, H. S. Marsden, T. R. Hirst, and G. Palu. 1999. Intranuclear delivery of an antiviral peptide mediated by the B subunit of *Escherichia coli* heat-labile enterotoxin. Proc. Natl. Acad. Sci. USA 96: 5221–5226.
19. Meng, L., R. Mohan, B. H. Kwok, M. Elofsson, N. Sin, and C. M. Crews. 1999. Epoxomicin, a potent and selective proteasome inhibitor, exhibits *in vivo* anti-inflammatory activity. Proc. Natl. Acad. Sci. USA 96:10403–10408.
20. Merritt, E. A., S. Sarfaty, M. G. Jobling, T. Chang, R. K. Holmes, T. R. Hirst, and W. G. J. Hol. 1997. Structural studies of receptor binding by cholera toxin mutants. Protein Sci. 6:1516–1528.
21. Nashar, T. O., H. M. Webb, S. Eaglestone, N. A. Williams, and T. R. Hirst. 1996. Potent immunogenicity of the B subunits of *Escherichia coli* heat-labile enterotoxin: receptor binding is essential and induces differential modulation of lymphocyte subsets. Proc. Natl. Acad. Sci. USA 93:226–230.
22. Porgador, A., J. W. Yewdell, Y. Deng, J. W. Bennink, and R. N. Germain. 1997. Localization, quantitation, and in situ detection of specific peptide-MHC class I complexes using a monoclonal antibody. Immunity 6:715–726.
23. Raychaudhuri, S., and K. L. Rock. 1998. Fully mobilizing host defense: building better vaccines. Nat. Biotechnol. 16:1025–1031.
24. Rock, K. L., S. Gamble, L. Rothstein, and B. Benacerraf. 1991. Reassociation with beta 2-microglobulin is necessary for Db class I major histocompatibility complex binding of an exogenous influenza peptide. Proc. Natl. Acad. Sci. USA 88:301–304.
25. Rock, K. L., and A. L. Goldberg. 1999. Degradation of cell proteins and the generation of MHC class I-presented peptides. Annu. Rev. Immunol. 17: 739–779.
26. Rock, K. L., L. Rothstein, and S. Gamble. 1990. Generation of class I MHC-restricted T-T hybridomas. J. Immunol. 145:804–811.
27. Rotzschke, O., K. Falk, K. Deres, H. Schild, M. Norda, J. Metzger, G. Jung, and H. G. Rammensee. 1990. Isolation and analysis of naturally processed viral peptides as recognized by cytotoxic T cells. Nature 348:252–254.
28. Rotzschke, O., K. Falk, S. Stevanovic, G. Jung, P. Walden, and H. G. Rammensee. 1991. Exact prediction of a natural T cell epitope. Eur. J. Immunol. 21:2891–2894.
29. Samuel, O., and Y. Shai. 2001. Participation of two fusion peptides in measles virus-induced membrane fusion: emerging similarity with other paramyxoviruses. Biochemistry 40:1340–1349.
30. Sebo, P., C. Fayolle, O. d'Andria, D. Ladant, C. Leclerc, and A. Ullmann. 1995. Cell-invasive activity of epitope-tagged adenylate cyclase of *Bordetella pertussis* allows in vitro presentation of a foreign epitope to CD8+ cytotoxic T cells. Infect. Immun. 63:3851–3857.
31. Tartakoff, A. M., and P. Vassalli. 1983. Lectin-binding sites as markers of Golgi subcompartments: proximal-to-distal maturation of oligosaccharides. J. Cell Biol. 97:1243–1248.
32. Townsend, A., and H. Bodmer. 1989. Antigen recognition by class I-restricted T lymphocytes. Annu. Rev. Immunol. 7:601–624.
33. Yewdell, J. W., and J. R. Bennink. 2001. Cut and trim: generating MHC class I peptide ligands. Curr. Opin. Immunol. 13:13–18.

Editor: J. T. Barbieri

Gas Chromatography/Mass Spectrometry (GC/MS)

Description

The Gas Chromatography/Mass Spectrometry (GC/MS) instrument separates chemical mixtures (the GC component) and identifies the components at a molecular level (the MS component). It is one of the most accurate tools for analyzing environmental samples. The GC works on the principle that a mixture will separate into individual substances when heated. The heated gases are carried through a column with an inert gas (such as helium). As the separated substances emerge from the column opening, they flow into the MS. Mass spectrometry identifies compounds by the mass of the analyte molecule. A "library" of known mass spectra, coverng several thousand compounds, is stored on a computer. Mass spectrometry is considered the only definitive analytical detector.

Limitations and Concerns

Sample analysis is often time consuming. Newly developed portable GC/MS models may offset this concern.

Applicability

GC/MS is a technique that can be used to separate <u>volatile</u> <u>organic</u> compounds <u>(VOCs)</u> and <u>pesticides</u>. However other uses of GC or MS, combined with other separation and analytical techniques, have been developed for <u>radionuclides</u>, explosive compounds (<u>Royal Demolition Explosive (RDX)</u> and <u>Trinitrotoluene (TCE)</u>), and metals. Some of these are described below.

A type of spectrometry can also be used to continuously monitor incinerator emissions, in place of a standard method that collects samples from a gas stream for laboratory analysis. That standard method has a relatively long turn around time, and it does not provide information that catastrophic releases have occurred or that there is a system failure. With <u>real-time</u>, continuous monitoring, all releases are monitored, and if there is a system breakdown, the system can be turned off and/or the nearby community can be notified.

Technology Development Status

The first general application of molecular mass spectrometry occurred in the early 1940s in the petroleum industry for quantitative analysis of <u>hydrocarbon</u> mixtures in catalytic crackers. Recently, manufacturers of GC/MS instruments have significantly reduced their overall size and increased durability. This allows what was once a laboratory bench-top instrument to perform field analysis.

Web Links

http://caag.state.ca.us/bfs/toxlab/gcms.htm

http://www.chem.vt.edu/chem-ed/sep/gc/gc.html

http://www.clu-in.org/download/techdrct/tdmpa_gc-ms_report.pdf

http://fate.clu-in.org/gc.asp?techtypeid=44

http://fate.clu-in.org/mspec.asp?techtypeid=47

Other Resources and Demonstrations

See http://www.clu-in.org/download/techdrct/tdmpa_gc-ms_report.pdf for "Innovations in Site Characterization—Technology Evaluation: Real-Time VOC Analysis Using a Field Portable GC/MS" (EPA 542-R-01-011). This report describes the use of a field GC/MS to measure trichloroethylene on a real-time basis.

See http://www.epsci.ameslab.gov/etd/technologies/projects/icpms/icpms.html for a description of inductively coupled plasma-mass spectrometry (ICP-MS), a technique developed at Ames Laboratory in the 1970s. It is a tool that is very sensitive and selective for multi-element analysis. This method needs only very small samples, from a nanoliter to a microliter in volume. Reportedly, it can analyze radioactive samples with little or no containment considerations.

See http://www.epsci.ameslab.gov/etd/technologies/projects/fiberoptic/index.html for a description of Interferometric Spectrometry. Incorporating high-resolution optics with a well-established spectroscopy technique, Ames Lab researchers have developed a compact instrument for rapid, on-site detection of elements that are traditionally difficult to identify in the field.

See http://apps.em.doe.gov/ost/pubs/itsrs/itsr1564.pdf for a description of using spectrometry as a component of a Continuous Emissions Monitor (CEM). It analyzes, and measures the light produced when off-gas emissions from the thermal treatment of mixed waste. Its principal application at Department of Energy (DOE) sites is monitoring the volatile metal, mercury (Hg), two semi-volatile metals, cadmium (Cd) and lead (Pb), and three low-volatile metals, arsenic (As), beryllium (Be), and chromium (Cr). The U. S. Environmental Protection Agency has classified these metals as hazardous air pollutants (HAPs). DOE incinerators that treat mixed waste also have to monitor any emissions of alpha-emitting materials, including uranium (U) and plutonium (Pu). Currently, DOE uses filters to control particulate emissions and uses high volume air samplers and laboratory analysis of the filters from those samplers to monitor emissions.

See http://apps.em.doe.gov/ost/pubs/itsrs/itsr69.pdf for a report describing Direct Sampling Ion Trap Mass Spectrometry (DSITMS). This technology is used to determine the presence of volatile organic compounds (VOCs) and semi-volatile organic compounds (SVOCs) in groundwater and soil, and in gaseous remediation process streams at hazardous waste sites. The system utilizes a commercially available ion trap mass spectrometer. With some modifications, the mass spectrometer is made field transportable.

For a list of other technologies that contain these properties click the **'SEARCH'** button.

○ (AND) Match all words ◉ (OR) Match any words	○ (AND) Match all words ◉ (OR) Match any words	○ (AND) Match all words ◉ (OR) Match any words

Contaminant	Media	Technology
☐ Fuel	☑ Off-gas	☑ Analytical/ACM
☑ Organics/VOC	☑ Ground Water	☐ In-Situ Treatment
☑ Organics/SVOC	☑ Surface Water / Sed.	☐ Removal
☑ Pest/Herbicides	☑ Soil	☐ Treatment/Destruct.
☑ Metals	☑ Landfill Materials	☐ Containment
☑ Radionuclides	☐ Bldg. Surfaces	
☑ Explosives-UXO		
☐ Not Specific		
NEW SEARCH	SEARCH	RESET CHART

Go back to the... **TECH CHART** | **TECH LIST** | **ABOUT PAGE** | **MAKE COMMENTS**

DISCLAIMER

STATUS: The preceding technology description and links were last updated 10/2002.
If you believe any of the information is out of date, please let us know at cpeo@cpeo.org.